ASSESSMENT REPORT

March, 2023

AIRBORNE MAGNETIC SURVEY and TIME-DOMAIN ELECTROMAGNETIC GROUND SURVEY (2022)

SINCLAIR - GOLDEN LARCH – TAP CLAIMS

(Tenures 1052363, 1055795, 1055865, 1062227, 1069925, 1072425, 1072426, 1074009, 1089278, 1089375, 1093153, 1093154, 1093155)

ST. MARY RIVER REGION (N.T.S. 082F09)

EAST KOOTENAY – PURCELL RANGE

FORT STEELE MINING DIVISION

Ownership of claims:
Paul Ransom
9452 Clearview Road
Cranbrook, BC, V1C 7E2

Edward (Ted) Sanders
P.O. Box 154,
Fernie, BC, V0B 1M0

Operator:
Amaroq Gold Corp.
1705-488 Helmcken Street,
Vancouver, BC, V6B 6E4

Report by: E. Sanders

BRITISH COLUMBIA
The Best Place on Earth

Ministry of Energy, Mines & Petroleum Resources
Mining & Minerals Division
BC Geological Survey

Assessment Report
Title Page and Summary

TYPE OF REPORT [type of survey(s)]: Technical [Geophysical] **TOTAL COST:** $ 165,553.73

AUTHOR(S): Edward (Ted) Sanders **SIGNATURE(S):** E. Ted Sanders

NOTICE OF WORK PERMIT NUMBER(S)/DATE(S): **YEAR OF WORK:** 2022

STATEMENT OF WORK - CASH PAYMENTS EVENT NUMBER(S)/DATE(S): 5961233 (Dec 14, 2022)

PROPERTY NAME: Pakk / Mt. Evans

CLAIM NAME(S) (on which the work was done): 1052363, 1055795, 1055865, 1062227, 1069925, 1072425, 1072426, 1074009, 1089278, 1089375, 1093151, 1093153, 1093154, 1093155, 1093157

COMMODITIES SOUGHT: Precious and Base Metals

MINERAL INVENTORY MINFILE NUMBER(S), IF KNOWN:

MINING DIVISION: Ft. Steele **NTS/BCGS:** 082F059

LATITUDE: 49 ° 34 ' 42.5 " **LONGITUDE:** -116 ° 17 ' 15.6 " **(at centre of work)**

OWNER(S):
1) Edward (Ted) Sanders
2) Paul Ransom

MAILING ADDRESS:
P.O. Box 154, Fernie, BC, V0B 1M0
9452 Clearview Rd., Cranbrook, BC V1C 7E2

OPERATOR(S) [who paid for the work]:
1) Amaroq Gold Corp.
2)

MAILING ADDRESS:
1705-488 Helmcken Street, Vancouver, BC V6B 6E4

PROPERTY GEOLOGY KEYWORDS (lithology, age, stratigraphy, structure, alteration, mineralization, size and attitude):
Aldridge, Sullivan Horizon, LMC, Quartzite, Pyrrhotite, Sedex, Siliciclastic Turbidite Sequence

REFERENCES TO PREVIOUS ASSESSMENT WORK AND ASSESSMENT REPORT NUMBERS: 4235, 12825, 23622, 25976, 26693, 27916, 28424, 32911, 37220, 37937, 37952, 39837

Next Page

TYPE OF WORK IN THIS REPORT	EXTENT OF WORK (IN METRIC UNITS)	ON WHICH CLAIMS	PROJECT COSTS APPORTIONED (incl. support)
GEOLOGICAL (scale, area)			
Ground, mapping			
Photo interpretation			
GEOPHYSICAL (line-kilometres)			
Ground			
Magnetic			
Electromagnetic	Volterra TDEM Survey (9.55 km)	as listed above less 1093153 & 1093154	$ 125,672.79
Induced Polarization			
Radiometric			
Seismic			
Other			
Airborne	Magnetometer Survey (303 km)	as listed above	$ 38680.94
GEOCHEMICAL (number of samples analysed for...)			
Soil			
Silt			
Rock			
Other			
DRILLING (total metres; number of holes, size)			
Core			
Non-core			
RELATED TECHNICAL			
Sampling/assaying			
Petrographic			
Mineralographic			
Metallurgic			
PROSPECTING (scale, area)			
PREPARATORY / PHYSICAL			
Line/grid (kilometres)			
Topographic/Photogrammetric (scale, area)			
Legal surveys (scale, area)			
Road, local access (kilometres)/trail			
Trench (metres)			
Underground dev. (metres)			
Other	Writing Report		$ 1,200.00
		TOTAL COST:	$ 165,553.73

TABLE OF CONTENTS page

LIST OF FIGURES page

Introduction

In January 2022, two additional Sinclair claims were staked on forfeited tenures. This completed staking of mineral claims over a prospective airborne (1995) Mag anomaly in an area having geoscience character favourable for mineralization at depth as outlined in the History section of AR 39837. In February 2022 the Sinclair – Golden Larch claims were optioned by Amaroq Gold Corp. In March 2022 an airborne Magnetic survey was flown over the property. The Aeromag survey confirmed the previously noted Mag anomaly of interest and a subsequent ground Time-Domain Electromagnetic survey was conducted in July. This report provides descriptions and maps of the two surveys as well as interpretive observations and conclusions based on the new geophysical information.

Location and Access

The Sinclair-Golden Larch property is located 25 km WSW of Kimberley, BC. The location map below (Figure 1) shows local communities, Kimberley, and Cranbrook. Roads and access to the Sinclair and Golden Larch Claims are described below.

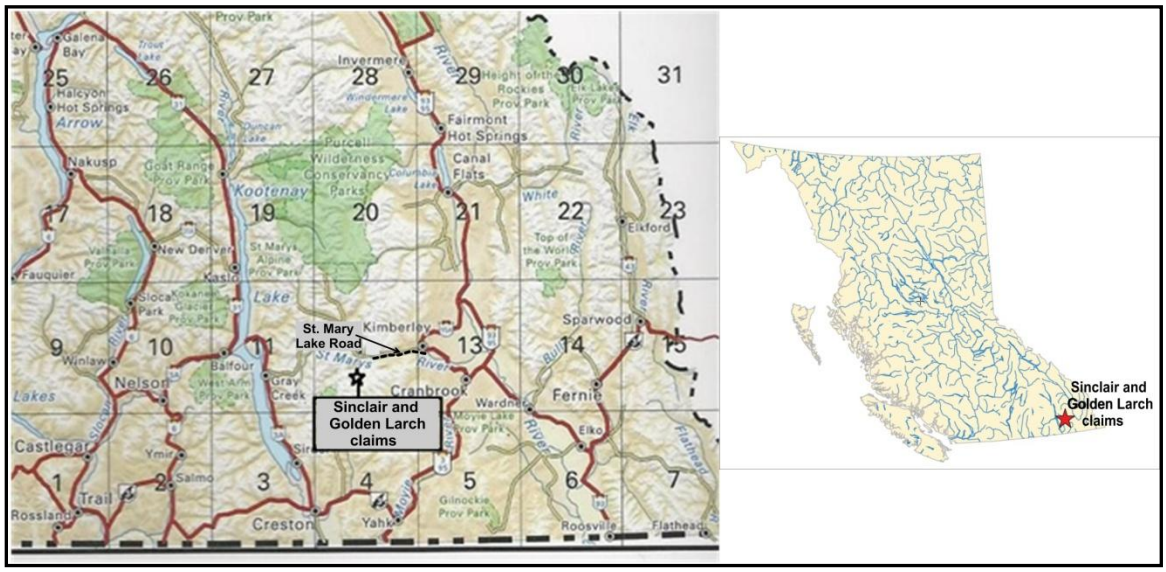

Figure 1 Location Map

Directions to the property:

1. Take St. Mary road 10 km west from Kimberley (starts immediately north of Marysville suburb).
2. Cross St. Mary River at east end of St. Mary Lake.
3. Proceed to Hellroaring Creek FSR, second junction to the right after crossing St. Mary River bridge.
4. At 1 km on Hellroaring FSR take junction west, the Meachen FSR.
5. The east part of the Sinclair-Golden Larch claims is accessed by a road to the south along Sinclair Creek, 700m past the 34 km marker. FSRs provide access southwest to about 38 km on Meachen Creek FSR and south along Fiddler Creek.
6. Hazard FSR branches to the north at the 35 km Marker on Meachen FSR and provides bridge access to portions of the claims north of Meachen Creek.

Claims

The Sinclair and Golden Larch claims are shaded in green on the MTO map (Figure 2). The TAP claims shaded in yellow were staked on Feb 9, 2022 subsequent to commencement of the option agreement, and obtained on behalf of Amaroq Gold Corp. Claims filed for assessment herein include all of the Sinclair – Golden Larch claims and three of the TAP claims (1093153, 1093154, 1093155) as indicated on the Statement of Work and MTO Exploration and Development page for event 5961233 (Appendix 1).

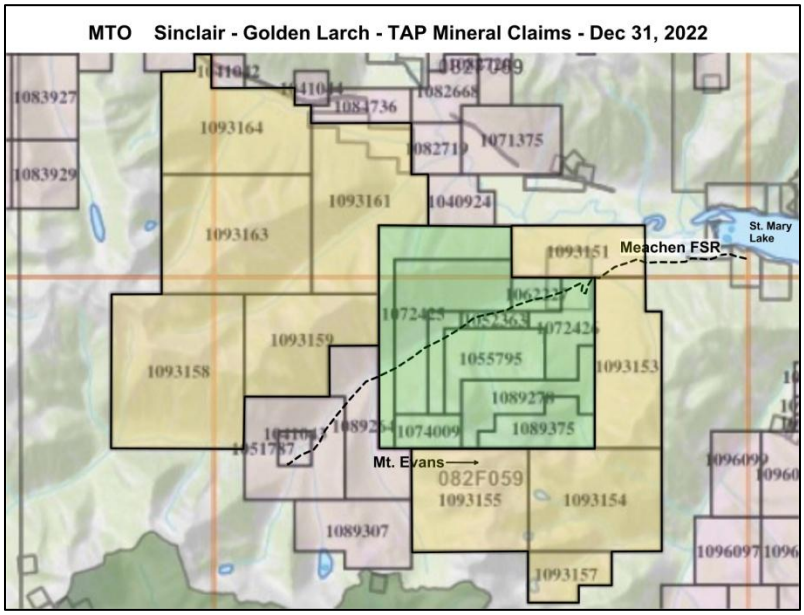

Figure 2 Mineral Titles Map Sinclair-GoldenLarch-TAP Mineral Claims

Regional Geology

A regional geology map is shown in Figure 3 below that is part of a 1:250,000 compilation map (Hoy, T., Price, R., Legun, A., et al., 1995). Rocks of the Mesoproterozoic Purcell Supergroup form a conformable sequence that dominates this part of southeastern BC. Lowest rocks of the Purcell Supergroup include the Fort Steele and Aldridge Formations. The Fort Steele Fm. is only exposed east of the Rocky Mountain Trench in the Hughes Range (i.e. north of the St Mary - Boulder Creek Fault). A transitional sequence assigned to the Aldridge Fm. rests conformably between Fort Steele and regional style Aldridge strata there. The Fort Steele Formation accumulated as quartz sands and siliciclastic muds deposited in sub aerial to shallow water fluvial to deltaic environments (Hoy, 1993). The transitional sequence represents a transgressive period of increasing water depth as rift development advanced and the interpreted depositional environment changed from shelf to basinal. In the Purcell Mountains the Aldridge Formation is over 5 kilometres thick of deep-water siliciclastic sediments primarily of turbidite origin (Bishop et al., 1970). The lower section of Aldridge in the Purcells is reasonably assumed time equivalent to the Fort Steele plus the lower portion of the overlying transitional sequence of Aldridge sediments. Seismic studies suggest the Aldridge Formation in the Purcells is about 12 kilometres below (Middle Aldridge) surface in the Moyie area, about 25 kilometres SE of Mt Evans (Cook et al., 1995).

A very significant rock of non-turbidite origin occurs throughout the Aldridge Formation called Carbonaceous Wacke Laminite (CWL). A few centimetres of CWL is commonly found between every turbidite in some sequences; in other sequences where not present between turbidites, CWL is assumed to have either been eroded or that turbidite deposition was so rapid it did not have time to accumulate. When or where turbidite input was low or restricted, a few centimetres to up to tens of metres of CWL dominant strata accumulated. For example, the top of the Lower Aldridge Formation in the Kimberley area is a 20 metre interval of CWL. In the immediate mine area this 20 metres of CWL bifurcates around and interfingers with the 200 metres of sulphide and unique sedimentary rocks intimately associated with the Sullivan ore body (Ransom et al., 2000).

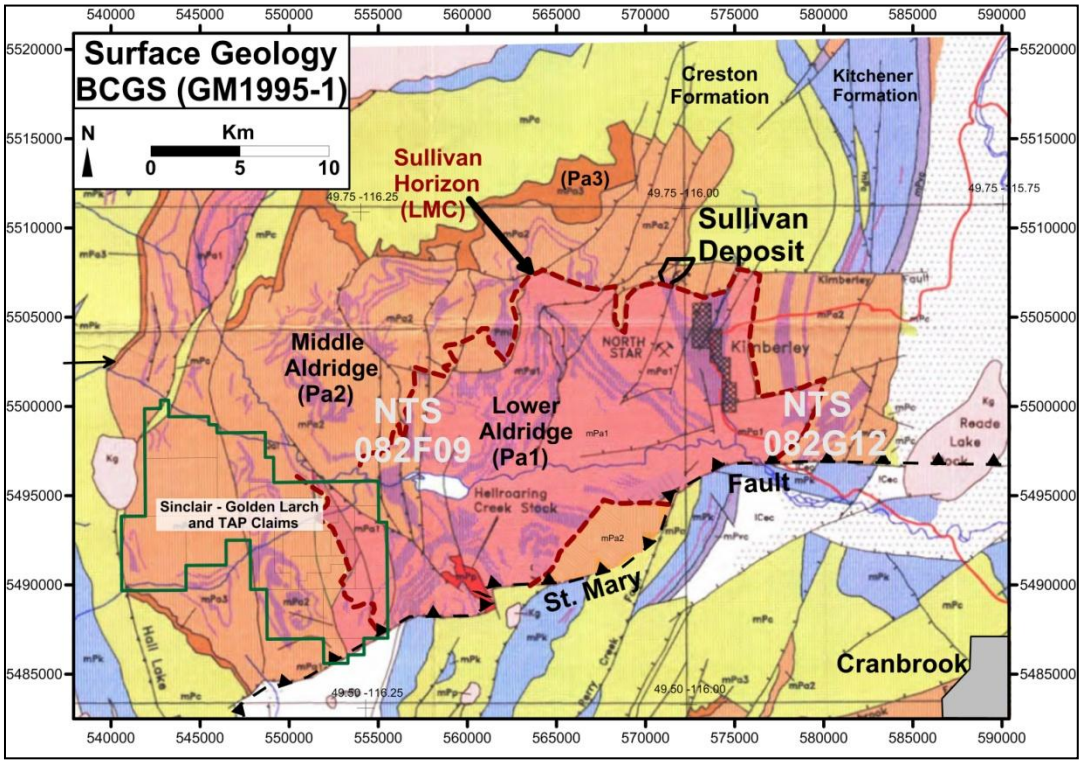

Figure 3 Regional Geology Showing Claims Location.

A further significant variant of CWL is light and dark grey bar-code-like laminated intervals. Units of these laminites form markers that provide precise stratigraphic control of the 1500 to 2000 metre stratigraphic interval above the Sullivan ore horizon. Individual markers from 10 cm to 10 metres thick were named by Cominco geologists. Aldridge markers have been correlated from field locations as much as 300 kilometres apart. Marker and turbidite sequences bifurcate, and detailed study aids understanding of basin sedimentology, mapping and can be used to place limits on fault displacement. These markers are important for exploration planning as they provide an estimate of depth to the Sullivan ore horizon, one of the prime exploration model targets. This information is used to guide geophysics planning and interpretation and well as planning and monitoring progress of drill holes. Core intersections of all Cominco marker standards are archived at the GSC ISPG repository in Calgary.

Above the Aldridge is the Creston Formation, deposited as muds, silts and sands in a shallow aqueous to emergent environment, parts of which have been interpreted as shallow marine to lacustrine and other parts as alluvial fans.

Mesoproterozoic tabular gabbro sills and dikes known as “Moyie Sills” or “Moyie Intrusions” intrude Aldridge (and rarely Creston) strata and are only slightly younger than the rocks they intrude.

Kitchener Formation strata succeed the Creston Formation are carbonate-rich silts and muds deposited in a shallow marine environment. Above the Kitchener Formation is the Van Creek Formation (included in or with the Kitchener as Siyeh in early studies) dominated by siltstones that accumulated in a shallow water environment and was followed by the Nicol Creek Formation, a thin but very widespread flood basalt lava and associated volcaniclastic sediments. Sub-volcanic sills to Nicol Creek Fm lavas are common in the Kitchener Formation.

The Nicol Creek volcanics mark the top of the lower Purcell Supergroup. Approximate age of deposition of the Lower Purcell Supergroup is constrained from before the 1475 Ma age of the Sullivan orebody at the top of the Lower Aldridge Formation (Slack et al., 2020) and extrusion of the Nicol Creek Formation lavas at 1443 MA (Evans et al., 2000).

The upper Purcell Supergroup comprises Dutch Creek and Mount Nelson Formations in the Purcell Mountains, and stratigraphic equivalents in the Rockies, and consist primarily of units that were deposited as sands, silts, muds and carbonates in a mud flat-shoreline and adjacent basinal environments.

The Purcell supergroup was folded, metamorphosed and the Lower Aldridge Formation was intruded by granite during the East Kootenay orogeny that lasted from 1360 to 1330 (McMechan et al., 1982; Lydon, 2000; Pattison et al, 2013, McFarlane 2015).

The Windermere Supergroup deposited on an unconformity from 900 to 800 MA following the Goat River orogeny (McMechan et al., 1982). In turn subsequent uplift and erosion resulted in an unconformity upon which lower Paleozoic sediments were deposited, the Lower Cambrian Cranbrook Formation conglomerates and sandstones and upper Lower Cambrian Eager Formation argillite, siltstone and carbonate.

Sedimentation and erosion cycles continued through the Phanerozoic. Late Mesozoic to early Cenozoic compression produced large fold structures in the Purcell and Rocky Mountains. Syenite to monzonite plugs and stocks of Cretaceous age intruded along and locked some of the longer-lived faults. Peripheral to these intrusions are coeval and possibly younger minor thin syenite sills and dikes. Mid Cenozoic extension resulted in tilting (Bally et. al. 1966) and rotation (Ransom et. al. 2017) of large fault blocks and development of several narrow basins at the north end of the Basin and Range Province. The major Rocky Mountain Trench is one of these basins and numerous fault blocks display "basin and range" topography locally. Alluvial deposition continues to this day.

Local Geology

The most recent published 1:50,000 scale geology map of sheet 82F09 is GSC Open File 6308 (Brown, et al., 2011) that overlaps BC Geological Survey map (Hoy, et al., 2004). This map shows most marker localities that had been identified by Cominco field crews. The Sullivan ore body and the Stemwinder and North Star massive sulphide deposits are significant mineral occurrences on this map, 25 kilometres northeast of Sinclair - Golden Larch claims. Rocks on the Sinclair - Golden Larch claims are entirely Lower and Middle Aldridge Formation strata and gabbro intrusions. Maps at 1:10000 and 1:5,000 scales (Appendix 3 and 4 in AR 39837) are compilations primarily of earlier GSC and Cominco work, Black Bull (Anderson et.al. 1999) mapping, and new work by author P.W. Ransom for the claims. These maps show some notable differences from the GSC map used for mapping in previous assessment reports (AR 37220, 37937) for this prospect. Interpretive work for this year's work utilizes an updated 1:20,000 scale geology map for Mt. Evans.

History

The Sinclair - Golden Larch claims flank west, south and north portions of Mt. Evans. Several adits were driven on copper sulphide in quartz veins in gabbro W of Mt. Evans, last extensively explored in 1972 (Lenard) and 1984 (Margrum and Crowe). Cominco carried out regional mapping and ground electromagnetic surveys in the Mt. Evans area during the 1970s to mid 1990s. This work targeted Sullivan Horizon, the stratum that hosts the giant SEDEX Sullivan deposit 25 km to the NE. Cominco drilled several conductors without success. In 2000 Chapleau deepened Cominco hole R95-1, renamed it P00-15, and intersected Sullivan Horizon several hundred metres below the geophysical conductor targeted by Cominco, and below that a substantial thickness of pebble fragmental (Soloviev, 2001). Pebble fragmental is a unique rock similar to the mud volcano complex in the footwall of Sullivan. In 2004 Hastings drilled 1758 metres in P04-01E about 1.7 km southwest of P00-15 with similar results and significant sparse laminations of Pb-Zn-Fe sulphides (Anderson, 2005, Kennedy et al., 2015). E. Sanders (2015) carried out a review of geophysics in the area with a revised interpretation of aeromagnetic surveying that indicates a large-dimensioned anomaly with the characteristics of a buried Sullivan-like deposit in the vicinity of the Sinclair and Golden Larch claims. Ground gravity and magnetic survey data were subsequently acquired (Sanders, 2018, 2019) as well as soil geochemistry samples (Ransom, 2018, 2021).

Information learned from Paul Ransom has led to some significant changes regarding local geology. One change is that the Sinclair Fault of unknown dip and variable trend on GSC OF 6308 map (Brown et al.,) has not been verified in the field. However, a steep west side down normal fault called Evans Fault has been mapped. This fault trends along Evans Creek and the western edge of the Mag anomaly of interest (Mag AOI).

Favourable geoscience data for the prospect are described in the History section of AR 39837. These data include having Sullivan Horizon at drillable depth, airborne Magnetic and EM anomalies of interest, and a RGS stream sediment geochemistry sample in Evans Creek hosting relatively high levels of base metal and pathfinder elements. UTEM conductors (Cominco, 1994) were also noted in the north basin of Mt. Evans where Sullivan Horizon is estimated at 700-1000m below surface in some locations.

In 2017 a gravity survey was conducted on the Meachen FSR (Sanders, 2018) and the processed data was merged with the data from Geoscience BC - East Kootenay Gravity Database (Sanders, 2013). A second gravity survey was conducted in 2021 (AR 39837) to access secondary logging roads and do a hiked traverse of the upper basin hosting the Mag anomaly of interest. That survey provided additional data to enable a more definitive interpretation and the residualization of a 0.3 mGal gravity anomaly that roughly coincides with the location of the Mag AOI described in prior assessment reports.

In 2020 geological mapping and soil and rock geochemistry sampling (AR 39837) was done at the site where a 90 nT Mag anomaly was detected in a 2018 ground Mag survey (AR 37937). The anomaly suggested a near-surface source but resides on a steep talus slope. There is also an associated conductive anomaly here as seen on the St. Mary 56KHz EM map (Figure 11, AR 37937). Soil geochemistry samples at the Mag anomaly indicated the typical threshold levels of 25 ppm Pb and 100 ppm Zn were exceeded in most of the 12 samples. This may represent weak Sullivan-type mineralization from a diatreme or may be related to a thin gabbro sill a few tens of metres below surface here.

New Work

The 2022 work included acquisition of two new geophysical surveys. In March a high-resolution airborne Magnetic survey was flown over the Sinclair, Golden Larch, and TAP claims. In July a Volterra TDEM ground survey was conducted along traversed lines over the central west half of the 2022 Aeromag survey area.

Objectives

1. It is known that the 1995 airborne Mag survey had challenges towing two sensors in the rugged terrain of this area. The new Aeromag survey was intended to clean up problem areas found in the older Mag data and to confirm the broad low amplitude magnetic anomaly referred to as the Mag AOI in prior reports.
2. The new Aeromag survey confirmed a similar broad, possibly deep-sourced, magnetic anomaly corresponding to the previous Mag AOI. The Volterra ground EM survey was subsequently conducted to measure levels of conductivity associated with the Mag AOI and adjacent ground up to 2 km either side of the Evans Fault.

2022 Aeromag Survey

On March 5 and 6 an Aeromag Survey was conducted on the Mt. Evans property claims for Amaroq Gold Corp. This is the only known airborne survey flown over the North Evans Basin since the BCGS/GSC 1995 St. Mary Mag/EM Survey. The Aeromag survey, by Precision GeoSurveys (Langley, BC), was conducted to better delineate the magnetic area of interest (Mag AOI) in the North Evans Basin as well as the surrounding Sinclair-GL-TAP claims. The 2022 survey flight lines were directed N-S with 200m line spacing whereas the 1995 survey was flown E-W at 400m spacing.

Survey Personnel:	**Position**
Harmen Keyser, P.Geo.	Helicopter pilot
Bruce Larsen	Helicopter co-pilot and geophysical operator
Michael Marriot, B.Sc.	Geophysical technician
Jenny Poon, B.Sc., P.Geo.	Geophysicist – data processor and reporting (off-site)
Shawn Walker, M.Sc., P.Geo.	Geophysicist – data processor and mapping (off-site)

Flight lines were flown on a heading of 179°/359° and tie lines were flown at 2000m spacing on a heading of 089°/269°. The contour-draped survey averaged 50m height above ground level in terrain which ranged from 1000m-2700m ASL over the full survey which roughly covered a 7 km x 10 km area.

Precision GeoSurveys delivered a (.csv) file containing the field data as well as grids and images of the Mag and Radiometric (not covered in this report) data. The full survey logistics report is included in Appendix 3. A zipped file containing the raw Mag data, 50m Geosoft/Surfer binary grids for Total Mag Intensity (TMI), Residual Mag Intensity (RMI-with IGRF removed), and Reduced-To-Pole (RTP), as well as Radiometric grids and pdf images is included with this submission. Figures 4 - 7 are images of the contractor's survey layout and the three Mag maps listed above, respectively.

The International Geomagnetic Reference Field (IGRF) model is the empirical representation of Earth's dynamic magnetic field (main core field without external sources) collected and is disseminated from satellite data and magnetic observatories around the world. The IGRF has historically been revised and updated every five years.

The IGRF contains a vertical component that changes inversely with the changing elevation (ASL) of the helicopter and Mag sensor. This free-air gradient adjusts data for the variation in Mag intensity as the distance between the source and sensor changes. It should be noted that the equivalent GSC RTF (IGRF removed) grids for the 1995 St. Mary Aeromag Survey used a fixed elevation IGRF for the entire map area. As a result the TMI maps from 1995 and 2022 are compatible but their Residual Magnetic Intensity grids/maps have had different versions and configurations of the IGRF applied.

Reduced to Magnetic Pole (RTP) data were determined from the leveled Residual Magnetic Intensity (RMI) data. The RTP filter was applied in the Fourier domain and rotates the observed magnetic inclination and declination field to what the field would look like at the north magnetic pole, to allow observation of magnetic trends and patterns independent of magnetic inclination and declination. Reducing the dipolar nature of magnetic anomalies is useful for interpretation because peak RTP magnetic values can be related to the centre of magnetic rock bodies and asymmetries in the RTP imagery closely reflect true dips and plunges. No RTP Mag grids were available for the 1995 survey.

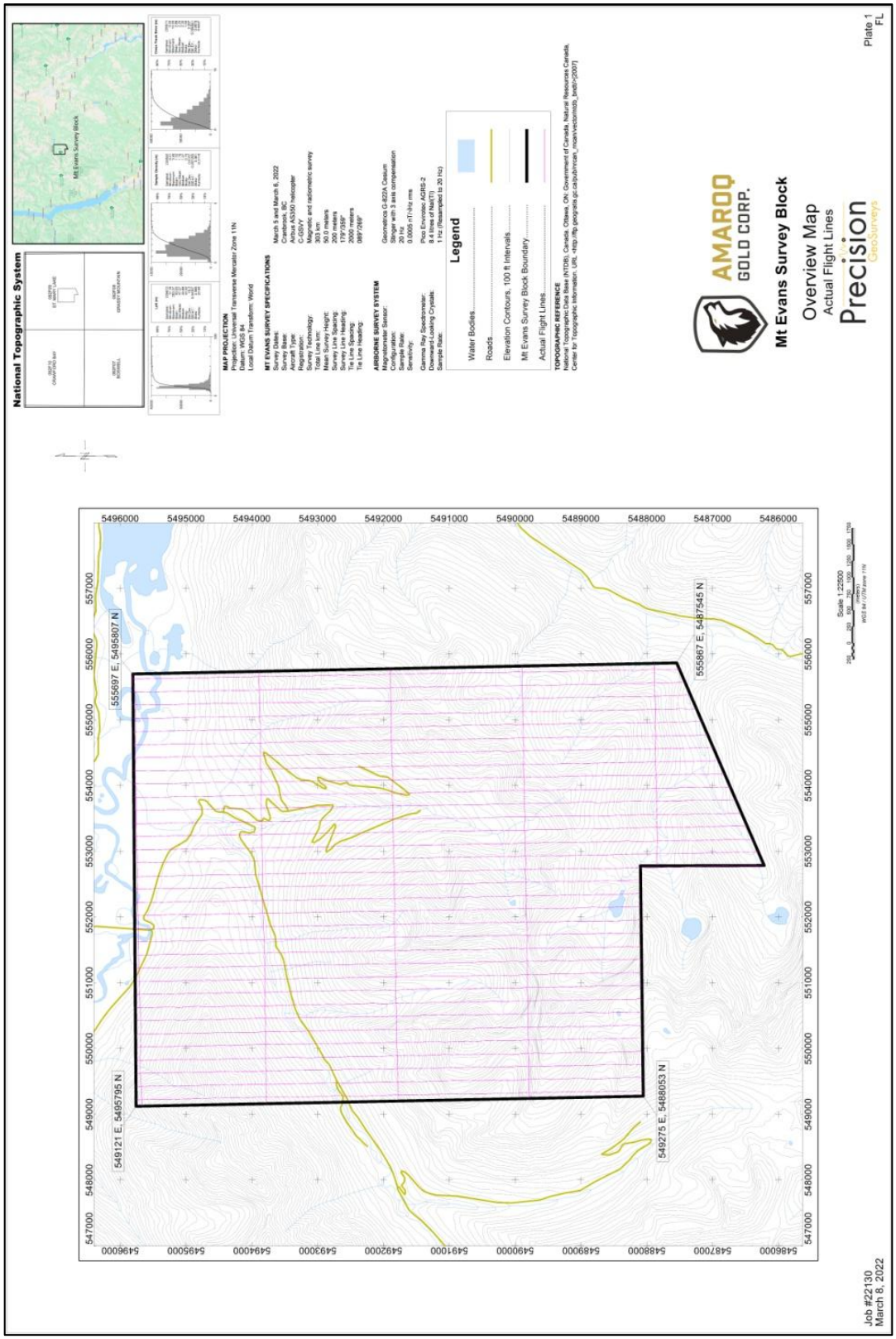

Figure 4 Mt. Evans 2022 - Aeromag Survey Layout

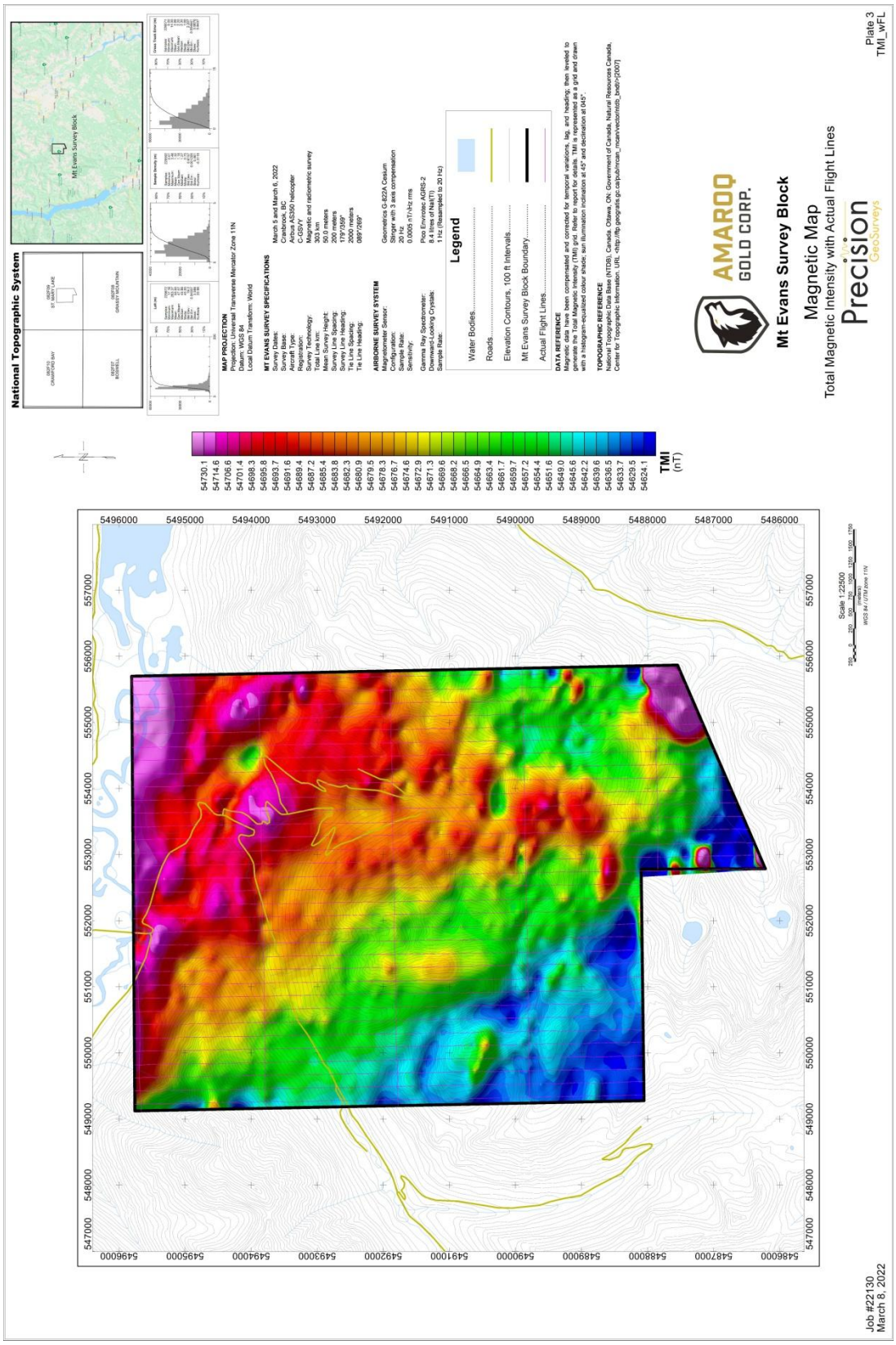

Figure 5 Mt. Evans - Total Magnetic Intensity (TMI)

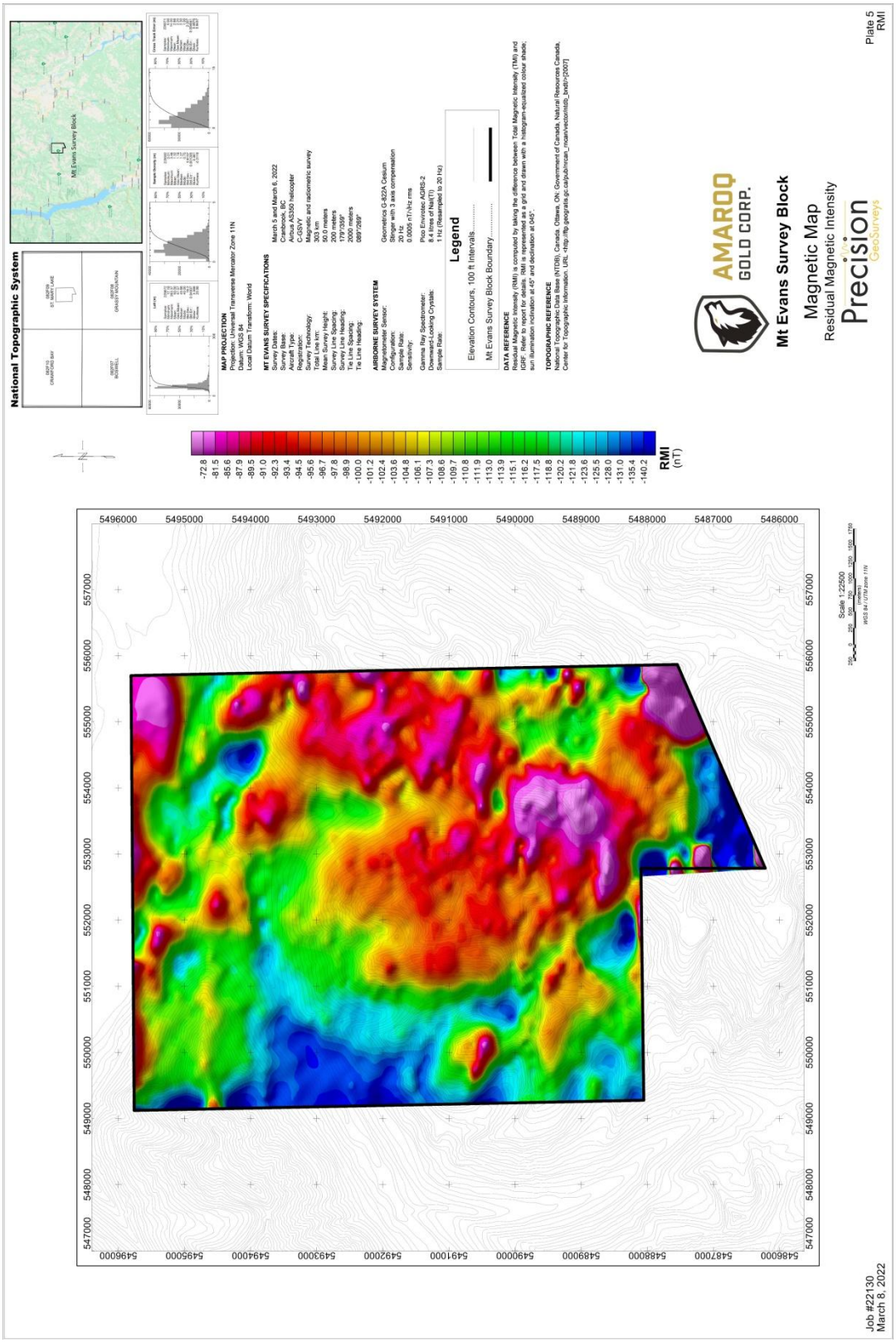

Figure 6 Mt. Evans - Residual Magnetic Intensity (RMI)

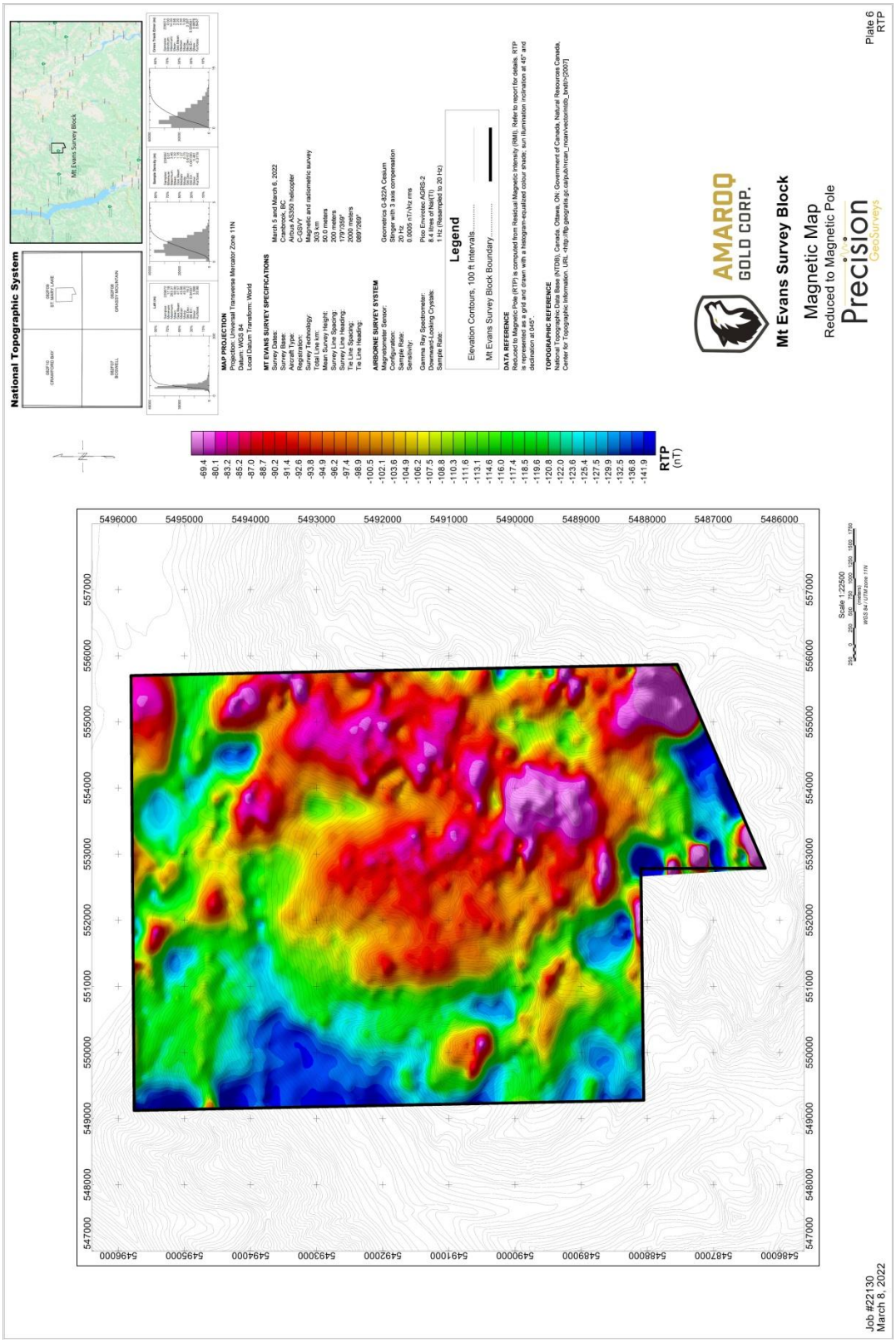

Figure 7 Mt. Evans - Reduced-to-Pole Mag (RTP)

Aeromag Interpretation

Figure 8 is a composite geology map for the Aeromag survey area. The grayish green areas are gabbro (sills) and the yellow indicates Lower Aldridge Footwall Quartzite stratigraphy. The dashed red line marks the Lower-Middle Aldridge Contact (LMC) which closely coincides with the stratigraphic level of Sullivan Horizon hosting the Sullivan Pb-Zn-Ag deposit 25 km to the ENE in the same (St. Mary) tectonic block. In the AOI, Middle Aldridge stratigraphy west of the LMC generally dips WSW 25° to 45°.

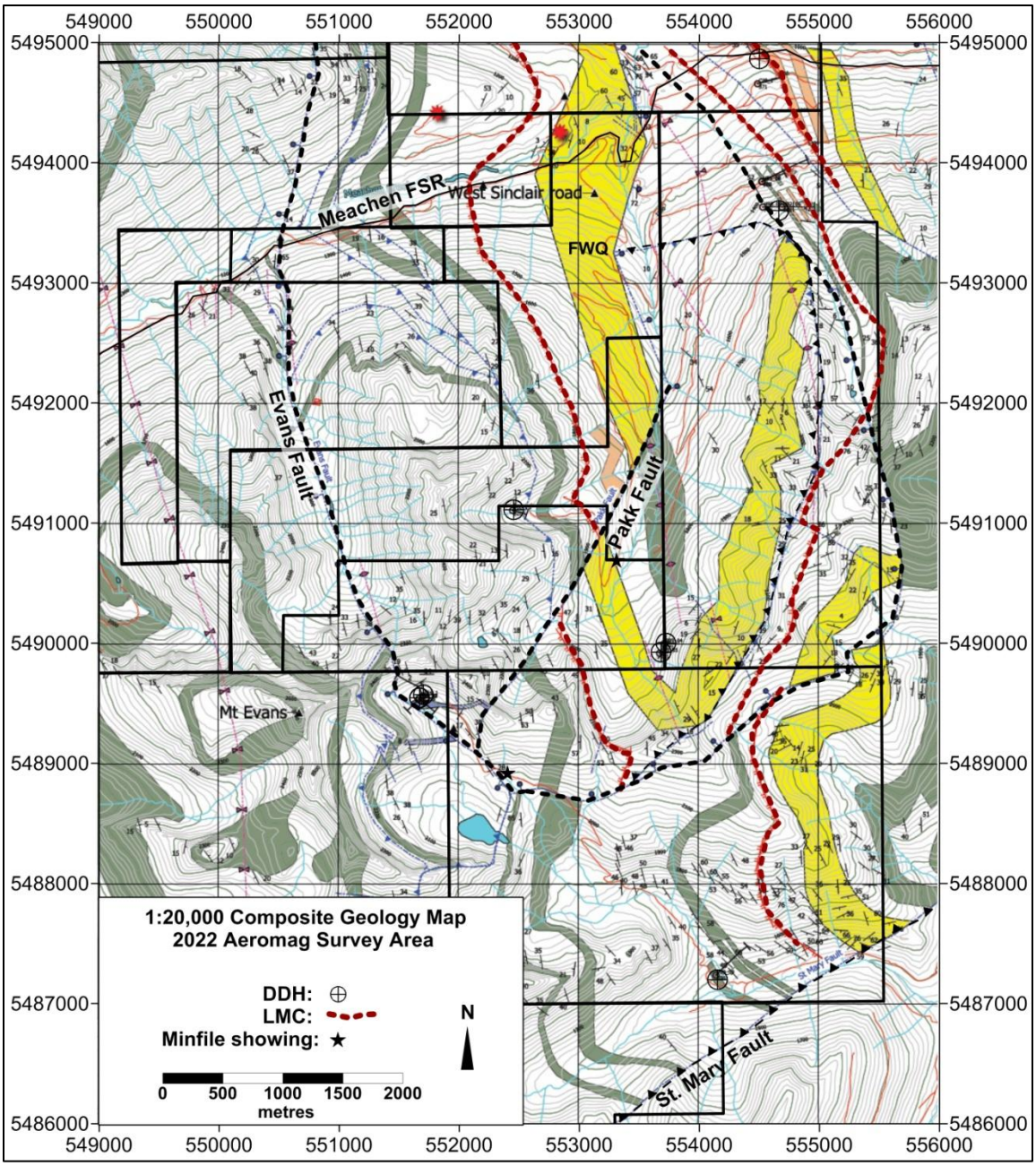

Figure 8 1:20,000 Composite Geology Map for Aeromag Survey Area (P. Ransom)

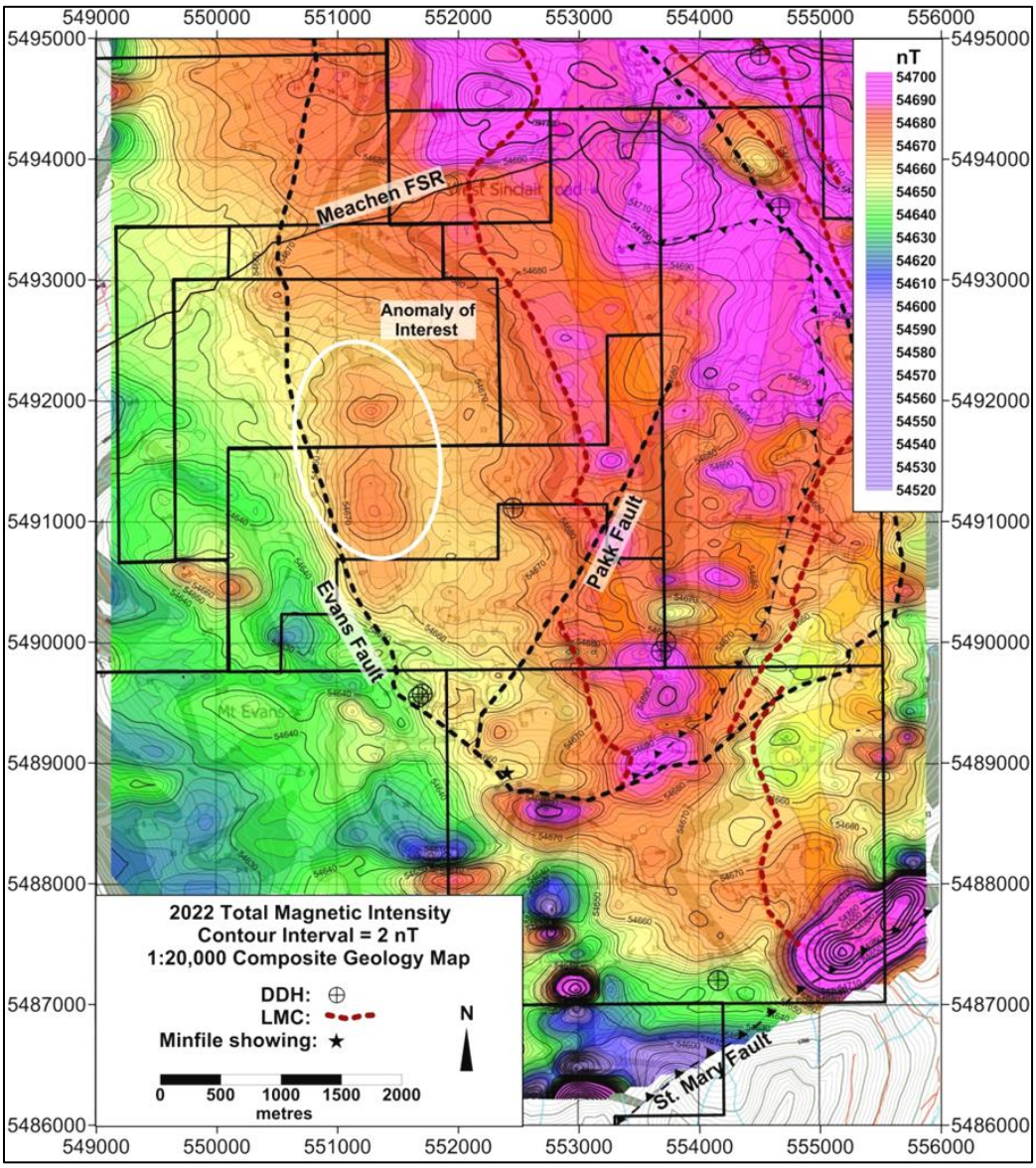

Figure 9 1:20,000 Composite Geology Map with TMI Mag Overlay

The 50m TMI grid/map (Figure 9) indicates an anomalous high within the white ellipse in the Mag AOI similar to the 1995 map. However, this map indicates a narrow Mag saddle that appears to divide the anomaly into an 1100m (N-S) x 700m southern high and a 700m x 700m high to the north. The larger southern TMI high has amplitude of about 15-17 nT (slightly less than the 1995 TMI map). The northern high contains a 20 nT spike anomaly on one flight line suggesting a near-surface source. A half-slope depth estimate using a Mag profile of Line 110 over the spike anomaly suggests the top of source may be 30-35 metres from the Mag sensor therefore possibly at surface. There is still a broad Mag high to the north, east, and west of the spike which, like the south high, could have a deep source. The two Mag highs cover about the same (N-S) dimension as the singular high on the 1995 TMI map but the 2022 TMI map suggests the Mag area of interest may be 200-300m south of previous estimates.

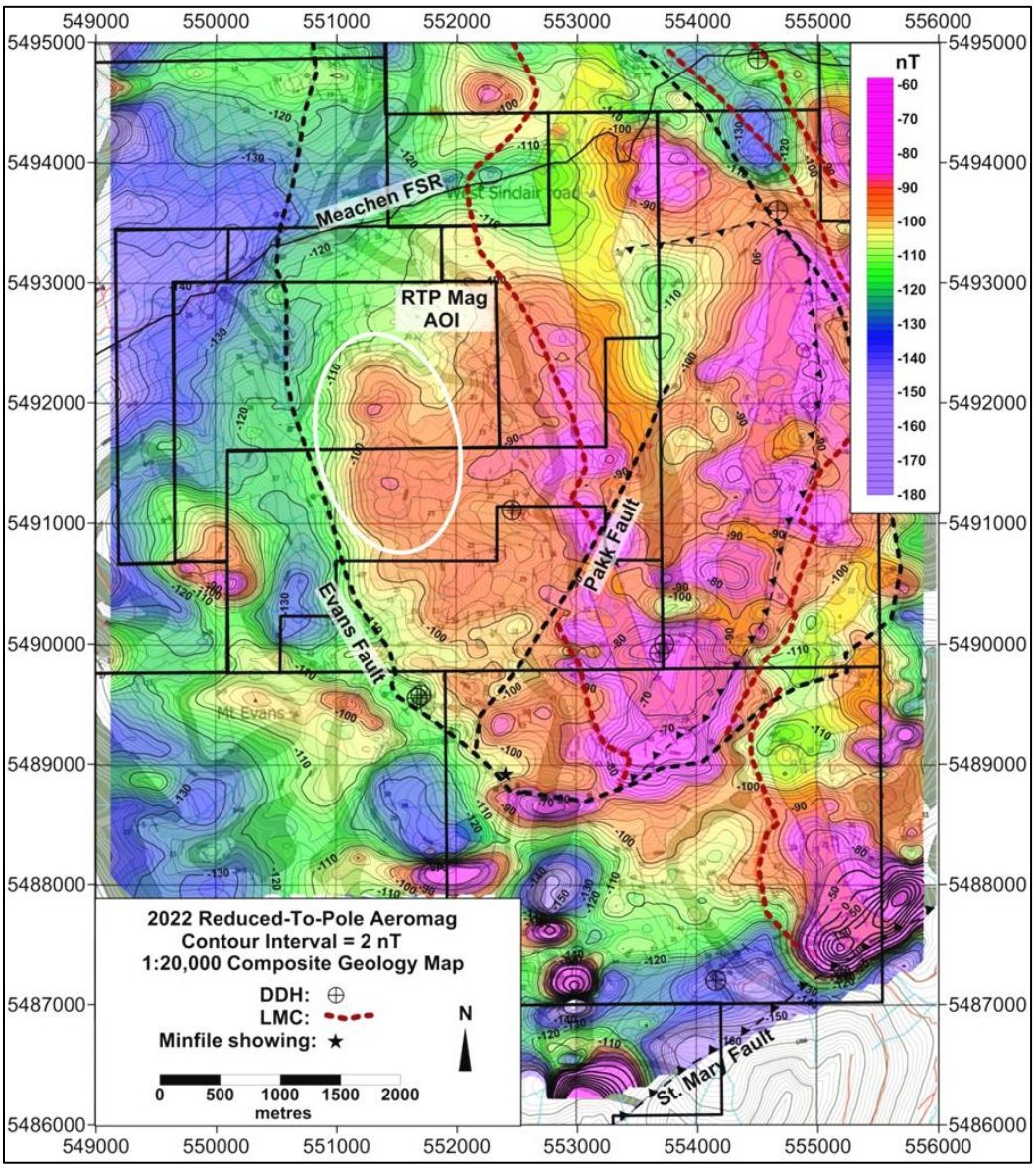

Figure 10 1:20,000 Composite Geology Map with RTP Mag Overlay

Removal of the IGRF shifts the TMI Mag high of interest about 150m east on the RMI map (not shown) due to the higher elevations of the steep west-facing ridge here. The RTP Mag map (Figure 10) derived from the RMI data has shifted the peak of the south Mag high 150-200m to the north. Due to the Reduction-To-Pole transform, peak RTP magnetic values tend to correlate with the centre of buried magnetic sources whereas the source is generally centred beneath the gradient of (dipolar) TMI anomalies.

The gradient at the north end of the RTP Mag AOI appears ~150m farther north than on the TMI map, yet the spike anomaly peak within the N RTP high is only ~50m farther north. This suggests the spike may have a very near-surface source while the broad portion of the N Mag high may still have a deep source. There is a good correlation of RTP Mag highs near Sullivan Time strata where the LMC outcrops east of the Mag AOI.

Figure 11 compares a previous Residual Mag map on the left (from Figure 7 in AR 39837), created from the edited St. Mary RTF data, and the 2022 Mt. Evans Residual RTP Mag map on the right. The inferred Mag AOI (red ellipse) on the left was based on modelling of a dipolar anomaly (low to the north) with the inferred source centered beneath the anomaly's gradient. The red X's and dashed lines are the noted 1994 UTEM conductors and survey lines. The ruby red line at the north end of the Mag AOI marks a zone of conductivity noted on UTEM line 8000. The three UTEM conductors SE of the Mag AOI indicated deeper sources than the conductors within the north half of the AOI.

The 2022 50m RTP grid was re-gridded at 100m in order to use the same filters (400m High Cut & 1500m Low Cut) used to make the 1995 100m Residual grid. Since the 2022 Mag grid/map is only 7 km x 10 km in size, and the median filter used doesn't calculate residual values near the edges of the grid, the new 100m grid was made wider by 2 km to the west and 1 km to the east. Mag data was extrapolated for these areas which were then blanked out by the filter on the 2022 Residual RTP Mag map below right.

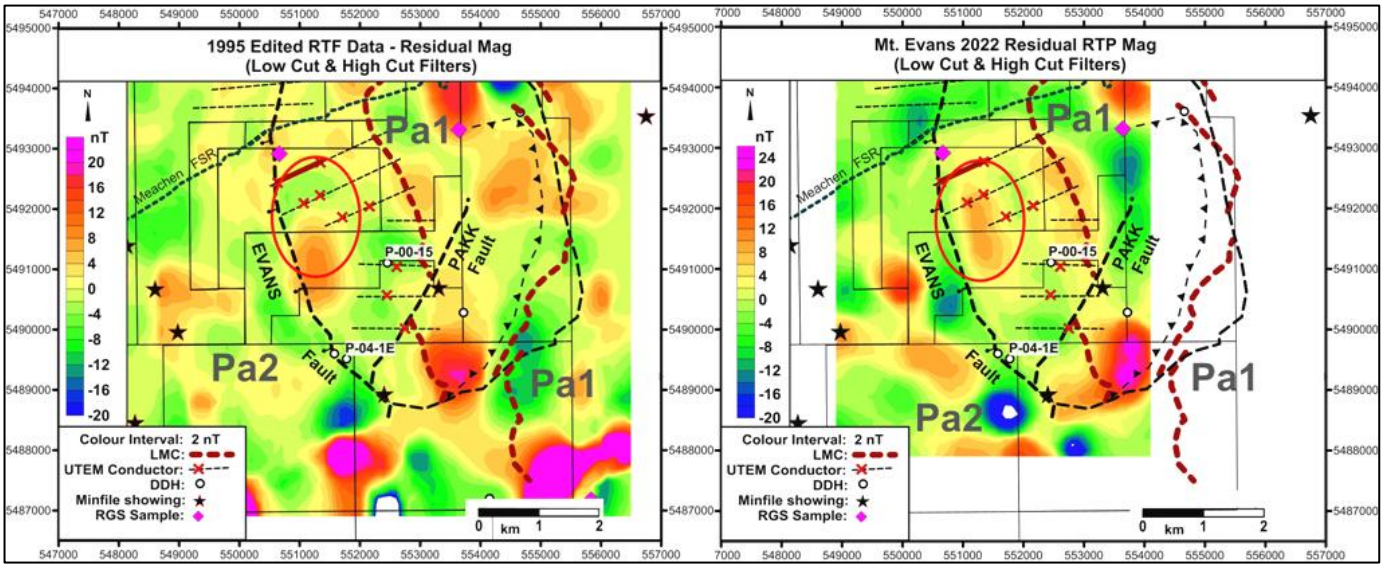

Figure 11 1995 TMI (RTF) Residual Mag 2022 Mt. Evans RTP Residual Mag

The Mag AOI ellipse is in the same location on both maps. The 2022 Residual RTP high appears to correlate very well with the previous 1995 Mag AOI based on a dipolar anomaly. The 2022 Residual RTP high is narrower than on the 1995 map but the north end without the (filtered) spike on this map still has the (larger) dimensional indications of possibly having a deeper source. Considering that stratigraphy here dips 30°- 40° W, the Mag high could still have a Sullivan Horizon source of considerable dimension.

The Evans Fault is a steep, west side down normal fault. The portion of the 1995 St. Mary Residual Mag high west of the Evans Fault (beside the Evans label) suggests the source is deeper as it would be less likely for a shallow Mag source (i.e. gabbro sill) to be near surface on both sides of the fault. The Mt. Evans 2022 RTP Residual high is east of the Evans Fault and hence, could have a near-surface source that drops west of the fault. There may be much steeper W dips in strata immediately east of (normal) Evans Fault.

Pyrrhotite has magnetic susceptibility an order of magnitude lower than magnetite. The Residual RTP high has amplitude about 10 nT which is less than the 12-14 nT anomaly on the 1995 Residual map. Mag modelling suggests that a Sullivan-sized volume of pyrrhotite (top at 250m depth) that creates the 90 nT magnetic anomaly at Sullivan would produce a 10 nT anomaly if buried 800m below surface so the anomaly's amplitude isn't necessarily unfavourable.

The position of the Mt. Evans 2022 Residual Mag high fits with the concept of buried pyrrhotite mineralization at depth east of the fault. However it could also have a gabbro sill source if the gabbro is widespread, close to the surface, and consistent in its elevated magnetite content.

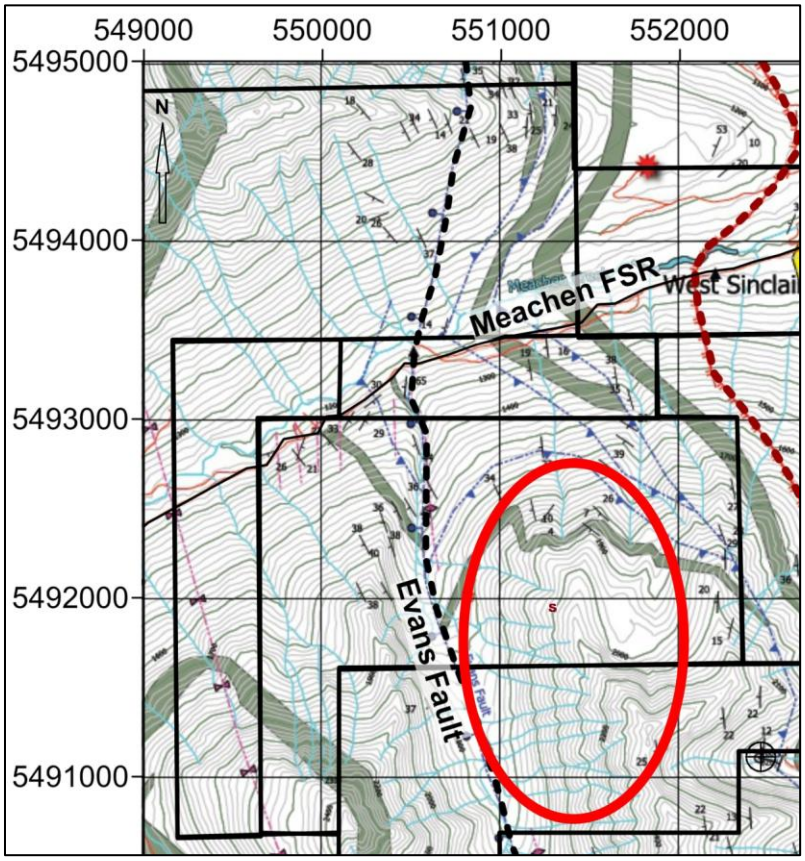

Figure 12 Enlargement of Geology Map (Figure 8) for Mag AOI

Figure 12 shows the thin gabbro sill near the north end of the Mag AOI. The sill's west edge at the Evans Fault is at 1650m ASL and the east edge is at 2000m ASL 1800 metres away. The sill could be the source of the EM and ground Mag anomalies noted in AR 37937 and the Mag spike anomaly ('**s**' on Figure 12) noted in the 2022 survey. The outcrop dips noted on and near the sill do not easily support it as being a possible source of the larger south RTP high which is more than 500m south of the sill outcrop and at higher elevations. Based on local geological mapping, no gabbro sill projects into the vicinity of the mag spike, however there may be a small cross-cutting magnetite-rich gabbro dike or plug or a pyrrhotite vein at that locality.

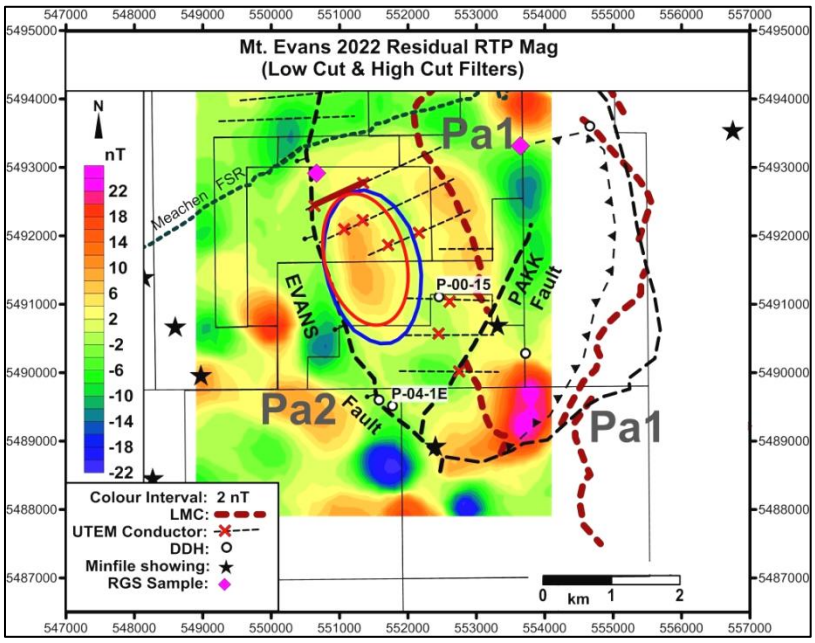

Figure 13 Mt. Evans 2022 Revised Mag AOI

Based on the 2022 RTP Mag data and Residual RTP Mag map, the red ellipse on Figure 13 is a revised, slightly narrower, Mag AOI. The blue ellipse is the digitized extent of the previously mentioned inferred source of a hand-residualized 0.3 mGal gravity anomaly which was created and detailed in AR 39837 after acquisition of new gravity data in 2021. These two independent anomalous potential field anomalies correlate well and could be sourced by a buried ore body at Sullivan Horizon east of the Evans Fault.

Based on the Aeromag results it was decided to continue exploration and proceed with an Electromagnetic survey to test the Mag anomaly and surrounding area for conductivity.

Volterra Time-Domain Electromagnetic Survey

The complete logistics report for the 2022 Volterra TDEM Survey is included in Appendix 4. The following contains excerpts from that report.

Overview

SJ Geophysics Ltd. was contracted by Amaroq Gold Corp. to acquire Volterra Time-Domain Electromagnetic (TDEM) data on the Mt Evans project. The Volterra-TDEM data was acquired with a fixed-loop configuration utilizing one large loop.

The geology in the area is Lower to Middle Aldridge sediments intermixed with long, thin layers of gabbro sills. The mineralization of interests is usually associated with the Middle Lower Aldridge contact. The objective of the Volterra TDEM survey was to image geologic structures that may indicate the possibility of a lead/zinc deposit similar to the Sullivan Mine.

SJ Geophysics Survey Personnel:	**Position**
Justin Hall	Field Technician July 11 – 22, 2022
Kalen Martens	Geophysical office support
Syd (Spike) Visser	Geophysical office support

Due to the rugged terrain throughout the survey area, the field crew needed to have excellent mountaineering skills. TerraLogic Exploration (Cranbrook) was contracted to provide an experienced crew suitable for the survey. Crew safety was a priority.

Field Crew Member	**Role**	**Dates on Site**
Ben Rogers	Field Assistant	July 11 – 16, 2022
Logan Robison	Field Assistant	July 11 – 22, 2022
Megan Howe	Field Assistant	July 11 – 22, 2022
Joel Comely	Field Assistant	July 11 – 22, 2022
Paul Ransom	Client Field Rep.	July 11 – 22, 2022

Survey Grid

The Volterra TDEM surface survey grid consisted of 5 lines and one loop. The survey lines ranged in length from 1.5 km to 3.5 km with a 50 metre station spacing. No line or loop preparations were completed in advance of the survey. The loop setup and the data collection were conducted with the guidance of hand-held GPS units using predetermined points. The planned loop location was modified in the field and placed where the terrain allowed. The lines and stations were surveyed in sections where terrain allowed. Stations were not flagged or marked. The EM survey lines are detailed in Table 1 below. Due to severe terrain, and time/budget constraints, portions of the EM lines were not completed.

Line	Series	Start Station	End Station	Survey Length (m)
1000	N	750	1850	1100
1400	N	900	3100	2200
		3600	4500	900
1800	N	900	1750	850
		2400	2950	550
		3750	4350	600
2200	N	900	1600	700
		2350	2950	600
2600	N	900	2250	1350
		2700	3400	700
				Linear Meters: 9550

Table 1 Mt. Evans TDEM Survey Lines

The EM loop had approximate dimension 3500m x 1800m and was comprised mostly of insulated 14-gauge copper wire. The west edge, along Fiddler FSR, used double strands of braided 12-gauge wire to reduce loop resistance. The loop location was slightly modified from the planned loop due to extreme topography. Final loop length was 10.6 km. The resistance of the loop was close to 80 ohm and was operated at Base Frequency 30.975 Hz. Figure 14 is a plan view of the EM Loop and station locations.

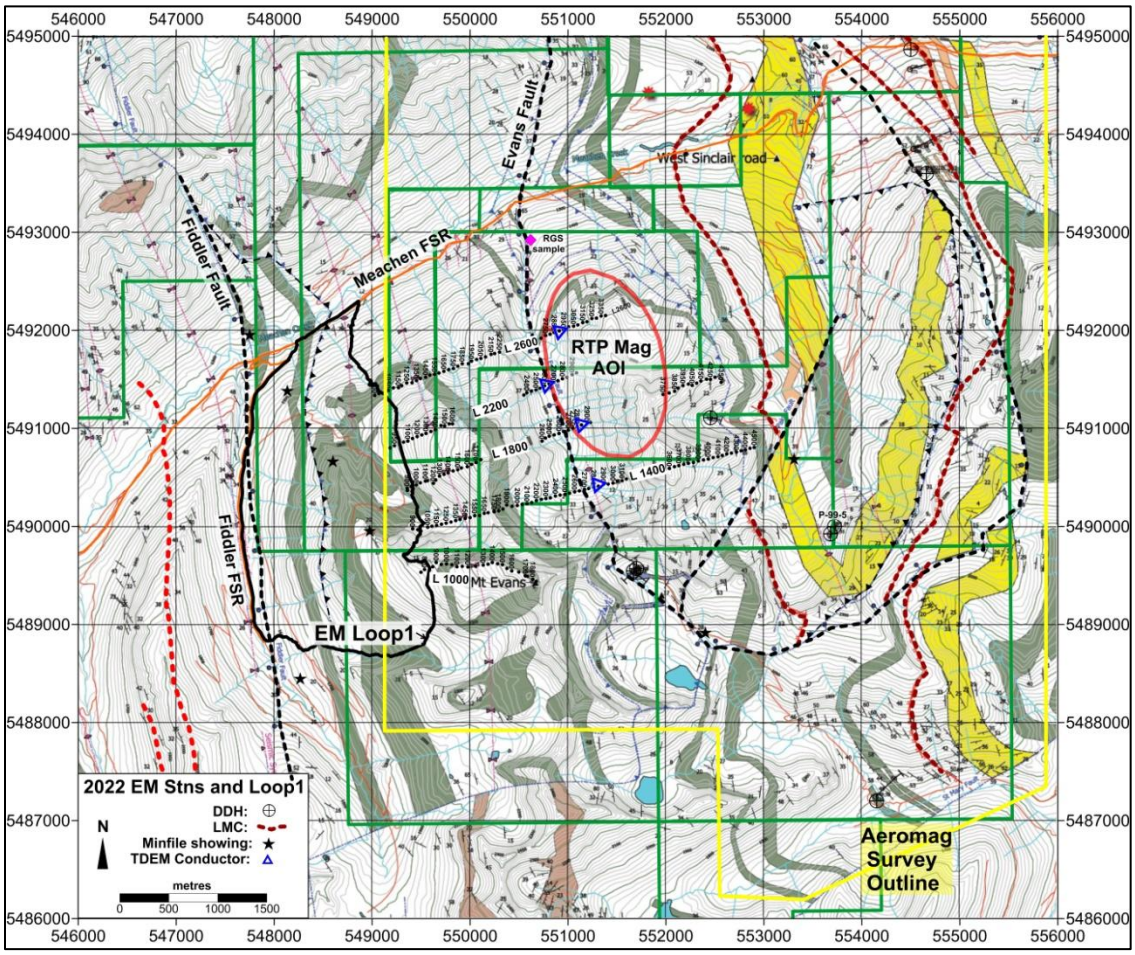

Figure 14 Volterra TDEM Loop and Survey Line Layout

Two transmitter power supplies were connected in series to increase the voltage and the current to about 7 Amps (Peak-to-Peak). The Vertical component EM data acquired was of good quality whereas the Horizontal component was of very poor quality due to orientation errors. The site is a significant distance from anthropogenic sources of noise, allowing for very clean data.

Location data was collected using Garmin handheld GPS units in the WGS 84 UTM Zone 11 N coordinate system. GPS points were acquired at each survey station where an induction magnetometer was set up. For the transmitter loop, GPS points were acquired approximately every 25 m along the loop. Listings of the TDEM station locations and coordinates for Loop1 are provided in Appendix 5 and .csv files in the attached zip file.

TDEM Survey Information

The time domain EM technique energizes the ground with a variable magnetic field known as the primary field. A transmitter sends an alternating electric current through a loop of wire laid on the surface to create the primary field. Each time a variation occurs in the current (e.g. succession of on-time/off-time) and therefore in the primary field, induced voltage causes eddy currents to flow within underground conductors near the loop. Circulating about these currents is another magnetic field termed the "secondary" field. The magnitude and rate of decay of the eddy currents depend on the electrical conductivity and the geometry of the medium. As the secondary field is directly proportional to the eddy currents, recordings of the secondary field can be exploited to infer information about the conductivity structure of the subsurface. In resistive media eddy currents decay rapidly, whereas in conductive media the currents will decay more slowly.

A typical Volterra surface EM system will use sensitive induction magnetometer sensors connected to a data acquisition unit to measure the total magnetic field – the vector sum of the primary and secondary magnetic fields on the surface. The information carried by the secondary magnetic field will be extracted during a processing stage using filtering, modelling and normalization techniques.

The transmitted ("primary") field of a typical TDEM survey induces current flow in the ground below and around the transmitter loop (i.e. in the "half-space") which itself produces a measurable EM field called the secondary field. This current flow has an inherent "inertia" which resists the change in primary field direction (at each step). This inertial effect is called self-inductance: it limits the rate at which current can change. Inductance is only dependent on the shape and size of a conductive path. It takes a certain amount of time for the current to be redirected by the new primary field direction and re-established to full amplitude; this time is called the time (decay) constant. The time constant of a good conductor is greater than that of a poor conductor because the terminal current level is greater whereas the rate of change is limited by the inductance of the current path.

In general the early-time decay channels 5-14 will respond to near-surface conductors with channel profiles crossing over while deeper-sourced conductors generally register as cross-overs or profile disturbances on the late-time channels 2-5.

Volterra TDEM Survey Interpretation

Figures 15 to 19 are the five Volterra TDEM profiles. The blue triangles indicate where SJG staff acknowledged the presence of conductor cross-overs on four of the five lines. The cross-over locations are indicated with blue triangles on lines 1400, 1800, 2200, and 2600 on Figure 14. Three of the four cross-over locations are clearly east of the Evans Fault but all appear on the higher number (early-time) channels representing weaker near-surface conductors. This is similar to the 1994 UTEM conductor source depths noted on Figures 11 and 13 in this area. No late-time conductors on the lower channels were indicated on any of the 2022 Volterra TDEM lines.

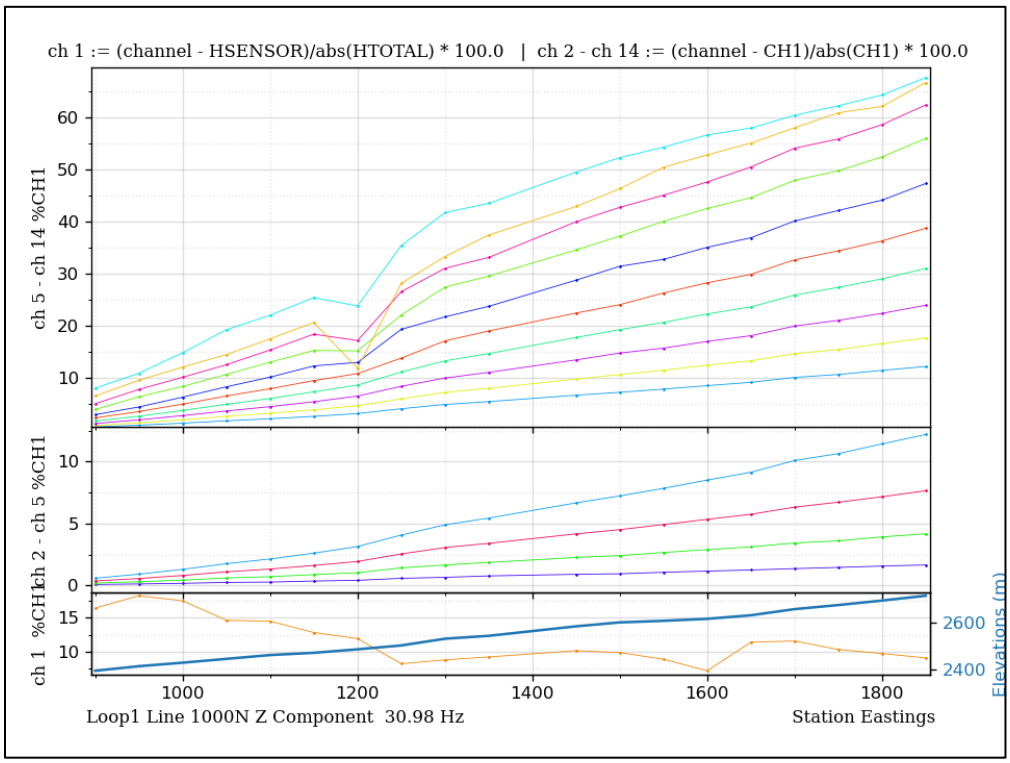

Figure 15 Volterra TDEM Line 1000

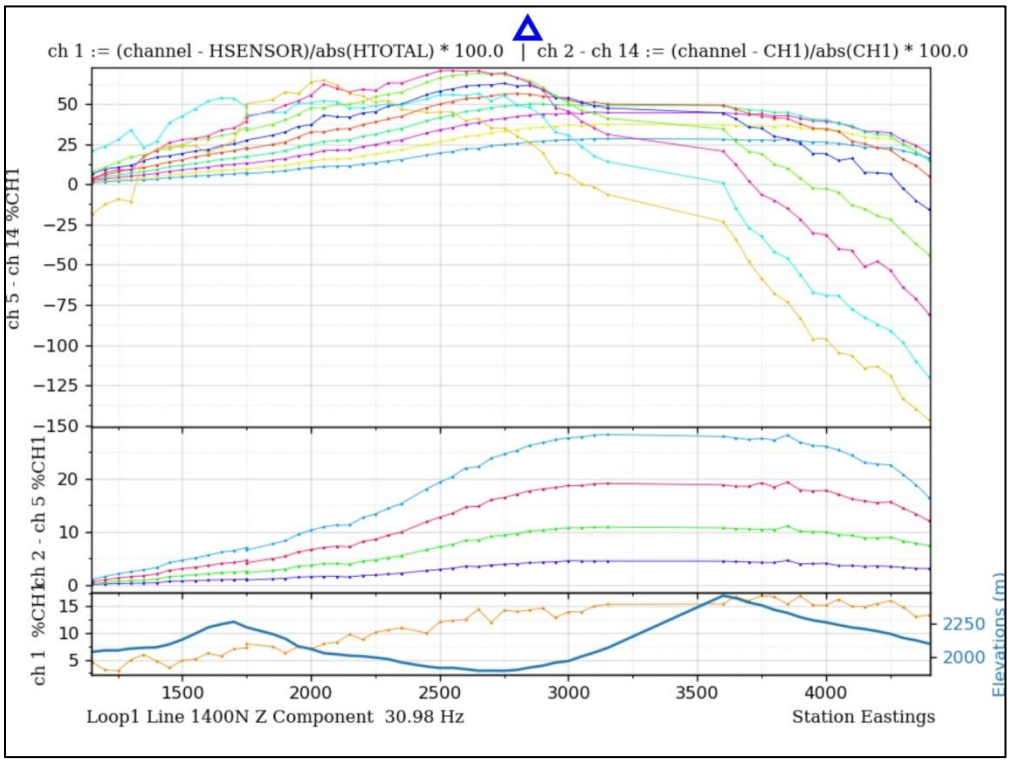

Figure 16 Volterra TDEM Line 1400

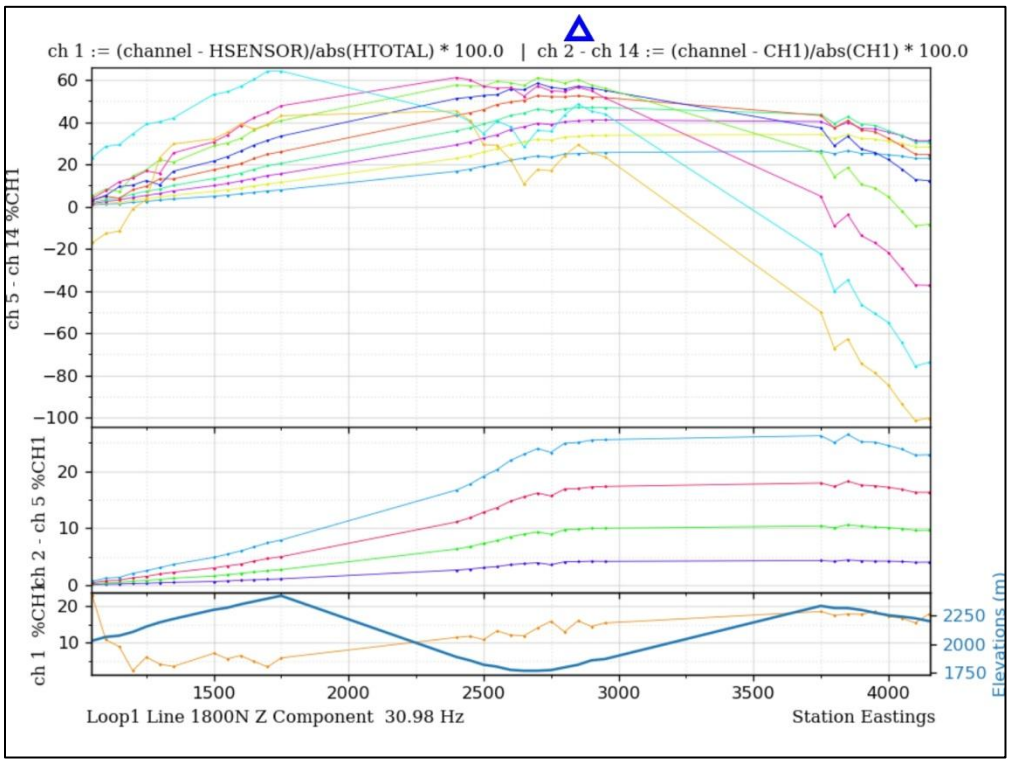

Figure 17 Volterra TDEM Line 1800

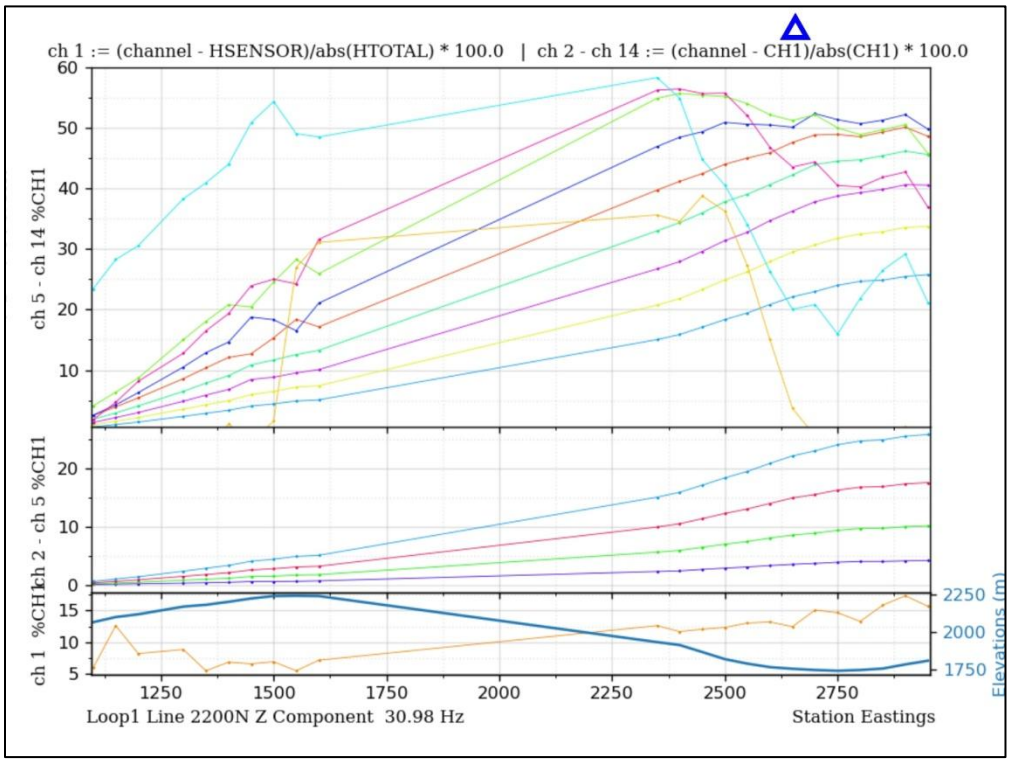

Figure 18 Volterra TDEM Line 2200

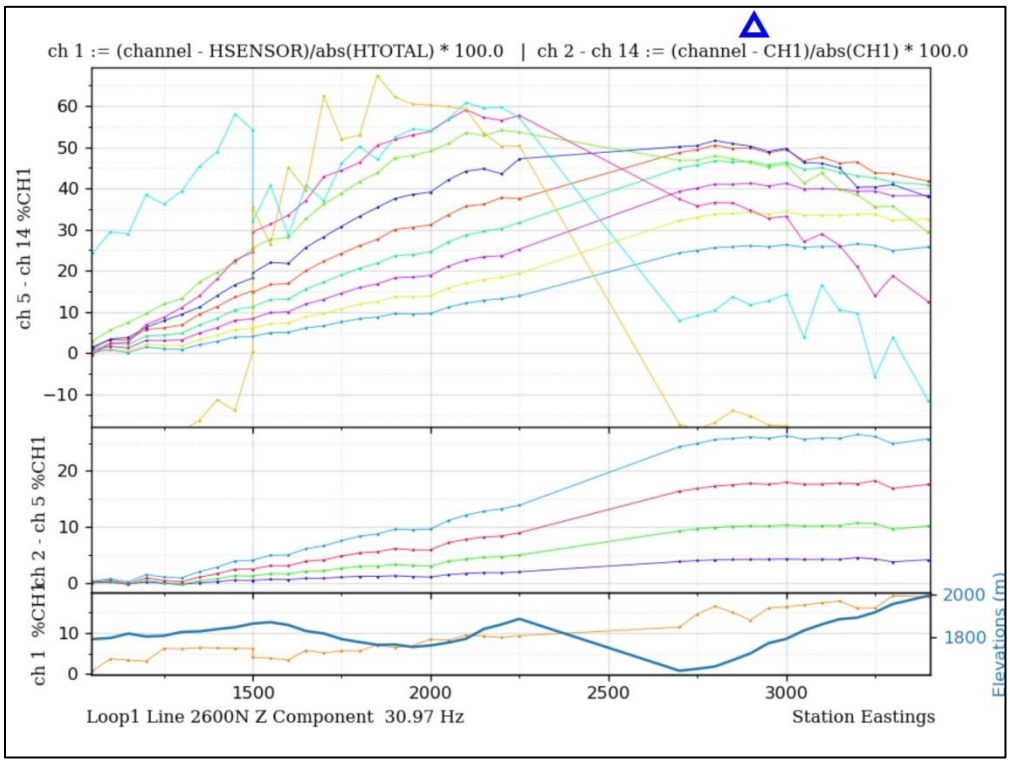

Figure 19 Volterra TDEM Line 2600

Conclusions

The Volterra TDEM survey revealed early-time cross-over responses on the four survey lines that intersected the Evans Fault. These bear a similarity to the shallower conductive responses in this area noted during the 1994 UTEM survey. Because there were no significant late-time channel cross-over responses on the Volterra TDEM line profiles, it is concluded there is no Sullivan size or type of conductor associated with the Magnetic and Gravity anomalies of interest. The source(s) of these and the anomalous RGS stream sediment sample from Evans Creek remain uncertain at this time.

References

Anderson, D and Kennedy, C., 1999, Geological and Prospecting Assessment Report on the Horn Claims, AR 25976.

Anderson, D., 2005, Road Access Work and Diamond Drilling on the PAKK Property, AR 27916.

Anderson, D., 2006, Diamond Drilling on the PAKK Property, AR 28424.

Bally, A.W., Gordy, P.L., and Stewart, G.A., 1966, Structure, Seismic Data and Orogenic Evolution of Southern Canadian Rocky Mountains, Bulletin of Canadian Petroleum Geology, v 14, No. 3.

Bishop, D.T., Morris, H.C. and Edmunds, F.R., 1970, Turbidites and Depositional Features in the Lower Belt-Purcell Supergroup (Abstr.), GSA Abstr. 2. No. 7, 497.

Brown, D. A., MacLeod, R. F., and Wagner, C. L. (compilers) 2011. Geology, St. Mary Lake, British Columbia, Geological Survey of Canada Open File 6308, scale 1:50000.

Cook, F., and Van der Velden, A., 1995, Three-dimensional crustal structure of the Purcell Anticlinorium in the Cordillera of SW Canada, GSA Bulletin, v.107, no 6.

Evans, K.V., Aleinikoff, J.N., Obradovich, J.D., and Fanning, M.C., 2000, SHRIMP U-Pb geochemistry of volcanic rocks, Belt Supergroup, western Montana: evidence for rapid deposition of sedimentary strata; Canadian Journal of Earth Sciences, v. 37, no.9.

Hoy, T., 1993, Geology of the Purcell Supergroup in the Fernie West-Half Map Area, Southeastern British Columbia, British Columbia Ministry of Energy, Mines and Petroleum Resources, Bulletin 84, 157p.

Hoy, T., Price, R., Legun, A., et al, 1995, Purcell Supergroup, Southeastern BC, Geoscience Map 1995-1, British Columbia Geological Survey Branch.

Hoy, T., and Jackman, W., 2004, Geology of the St. Mary Map Sheet 82F/9, Geoscience Map 2004-01, British Columbia Geological Survey.

Jackish, I., Cominco, 1994, Geophysical Report on a UTEM Survey on the Roar Property, AR 23622.

Lenard, N.C., 1972, Geological and Geochemical Study – Jag Group, AR 4235.

Lydon, J.W., 2000, The Geological Environment of the Sullivan Deposit, British Columbia, (ed.) J.W. Lydon, T. Hoy, J.F. Slack and M.E. Knapp, Geological Association of Canada, Mineral Deposits Division, Special Publication No 1.

McFarlane, C.R.M. 2015 A geochronological framework for sedimentation and Mesoproterozoic tectono-magmatic activity in lower Belt–Purcell rocks exposed west of Kimberley, British Columbia Canadian Journal of Earth Sciences v. 52, no.7.

McMechan, M.E. and Price, R.A., 1982, Superimposed low-grade metamorphism in the Mount Fisher area, southeastern British Columbia – implications for the East Kootenay orogeny, Canadian Journal of Earth Sciences, v. 19, no. 3.

Magrum, M.M. and Crowe, G.G., 1984, Geological Report on the Whitefish and Good Hope Claims, AR 12825.

Pattison, D.R.M., Moynihan, D.P., and McFarlane, C.R.M., 2013, Second edition, Field guide to metamorphism and tectonics in the Rocky Mountains, Purcell anticlinorium and Kootenay Arc, southern Alberta and British Columbia, Geological Association of Canada, field guide series, GeoCanada 2010 meeting, Calgary, AB, 153 pp.

Ransom, P.W. And Lydon, J.W., 2000, Geology, Sedimentology, and Evolution of the Sullivan Sub-Basin in The Geological Environment of the Sullivan Deposit, British Columbia, (ed.) J.W. Lydon, T. Hoy, J.F. Slack and M.E. Knapp, Geological Association of Canada, Mineral Deposits Division, Special Publication No 1, p.440-469.

Ransom, P.W., Day, T., and Enkin, R.J., 2017, Paleomagnetic Evidence for Extreme Block Faulting East of the Rocky Mountain Trench near Kimberley, BC , Geoscience BC Report 2017-09.

Ransom, P.W., 2018, Golden Larch 2018 Assessment Report AR 37952

Ransom P., Sanders, E., 2022, Geological Mapping, Geophysical (Gravity) Survey, and Geochemical Soil Sampling on the Sinclair Mineral Claims, AR 39837

Sanders, E., 2013, The Updated East Kootenay Gravity Database (EKGDB) and The 2013 St. Mary Gravity Survey, Geoscience BC Report 2013-23.

Sanders, E., 2018, Geophysical (Gravity) Survey on the Sinclair Mineral Claims, AR 37220

Sanders, E., 2019, Geophysical (Ground Mag) Survey and Geochemical Soil Sampling on the Sinclair Mineral Claims, AR 37937

Slack, J.F., Neymark, L.A., Moscati, R.J., Lowers, H.A., Ransom, P.W. Hauser, R.L. and Adams, D.T., 2020, Origin of Tin Mineralization in the Sullivan Pb-Zn-Ag Deposit, British Columbia: Constraints from Textures, Geochemistry, and LA-ICP-MS U-Pb Geochronology of Cassiterite, Econ. Geol., v. 115, no. 8.

Soloviev, S., 2001, Diamond Drilling Horn/PAKK Property, AR 26693.

Statement of Qualifications

I, Edward (Ted) Sanders, certify that:

- I am an independent prospector, presently residing in Fernie, British Columbia.
- I have been actively prospecting for minerals in British Columbia for 13 years and own mineral claims in southeastern British Columbia.
- I was formerly employed (7 years) as a Geophysical Technician for an Oil & Gas company (Potential Fields Dept.), and have been a Geophysical Consultant for over 20 years.
- I am a graduate of the University of Waterloo (B. Mathematics, 1978).
- I am the creator the East Kootenay Digital Gravity Database (EKGDB), now property of Geoscience BC (data file #2013-23).

APPENDICES

Appendix 1. Exploration and Development Work for event 5961233.

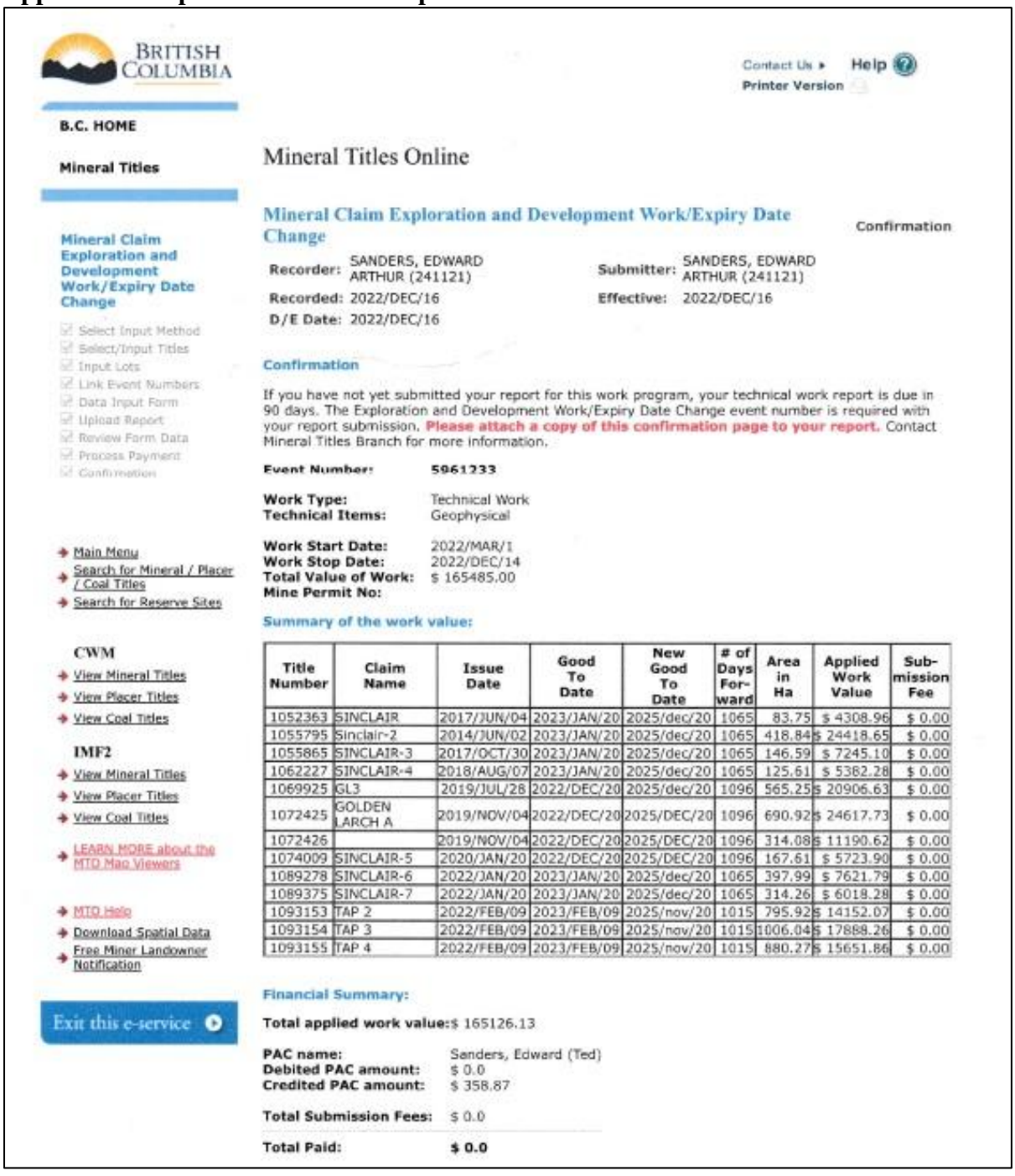

BRITISH COLUMBIA

Contact Us ▸ Help
Printer Version

B.C. HOME

Mineral Titles

Mineral Titles Online

Mineral Claim Exploration and Development Work/Expiry Date Change

Confirmation

Mineral Claim Exploration and Development Work/Expiry Date Change

- Select Input Method
- Select/Input Titles
- Input Lots
- Link Event Numbers
- Data Input Form
- Upload Report
- Review Form Data
- Process Payment
- Confirmation

Recorder: SANDERS, EDWARD ARTHUR (241121)
Submitter: SANDERS, EDWARD ARTHUR (241121)
Recorded: 2022/DEC/16
Effective: 2022/DEC/16
D/E Date: 2022/DEC/16

Confirmation

If you have not yet submitted your report for this work program, your technical work report is due in 90 days. The Exploration and Development Work/Expiry Date Change event number is required with your report submission. **Please attach a copy of this confirmation page to your report.** Contact Mineral Titles Branch for more information.

Event Number: 5961233

Work Type: Technical Work
Technical Items: Geophysical

Work Start Date: 2022/MAR/1
Work Stop Date: 2022/DEC/14
Total Value of Work: $ 165485.00
Mine Permit No:

- Main Menu
- Search for Mineral / Placer / Coal Titles
- Search for Reserve Sites

CWM
- View Mineral Titles
- View Placer Titles
- View Coal Titles

IMF2
- View Mineral Titles
- View Placer Titles
- View Coal Titles

- LEARN MORE about the MTO Map Viewers
- MTO Help
- Download Spatial Data
- Free Miner Landowner Notification

Exit this e-service

Summary of the work value:

Title Number	Claim Name	Issue Date	Good To Date	New Good To Date	# of Days For-ward	Area in Ha	Applied Work Value	Sub-mission Fee
1052363	SINCLAIR	2017/JUN/04	2023/JAN/20	2025/dec/20	1065	83.75	$ 4308.96	$ 0.00
1055795	Sinclair-2	2014/JUN/02	2023/JAN/20	2025/dec/20	1065	418.84	$ 24418.65	$ 0.00
1055865	SINCLAIR-3	2017/OCT/30	2023/JAN/20	2025/dec/20	1065	146.59	$ 7245.10	$ 0.00
1062227	SINCLAIR-4	2018/AUG/07	2023/JAN/20	2025/dec/20	1065	125.61	$ 5382.28	$ 0.00
1069925	GL3	2019/JUL/28	2022/DEC/20	2025/dec/20	1096	565.25	$ 20906.63	$ 0.00
1072425	GOLDEN LARCH A	2019/NOV/04	2022/DEC/20	2025/DEC/20	1096	690.92	$ 24617.73	$ 0.00
1072426		2019/NOV/04	2022/DEC/20	2025/DEC/20	1096	314.08	$ 11190.62	$ 0.00
1074009	SINCLAIR-5	2020/JAN/20	2022/DEC/20	2025/DEC/20	1096	167.61	$ 5723.90	$ 0.00
1089278	SINCLAIR-6	2022/JAN/20	2023/JAN/20	2025/dec/20	1065	397.99	$ 7621.79	$ 0.00
1089375	SINCLAIR-7	2022/JAN/20	2023/JAN/20	2025/dec/20	1065	314.26	$ 6018.28	$ 0.00
1093153	TAP 2	2022/FEB/09	2023/FEB/09	2025/nov/20	1015	795.92	$ 14152.07	$ 0.00
1093154	TAP 3	2022/FEB/09	2023/FEB/09	2025/nov/20	1015	1006.04	$ 17888.26	$ 0.00
1093155	TAP 4	2022/FEB/09	2023/FEB/09	2025/nov/20	1015	880.27	$ 15651.86	$ 0.00

Financial Summary:

Total applied work value: $ 165126.13

PAC name: Sanders, Edward (Ted)
Debited PAC amount: $ 0.0
Credited PAC amount: $ 358.87

Total Submission Fees: $ 0.0

Total Paid: **$ 0.0**

Appendix 2. Cost Statement

Activity	Invoice	Date	Details	Amount
Airborne Magnetometer Survey				
Precision GeoSurveys Inc	22-016	April 18	Aeromag Survey: March 5-6, 2022	$ 35,175.00
TerraLogic Exploration Inc.	3804	March 31	Equipment, fuel delivery, etc.	$ 505.94
Truck, Heli-Staging, Fuel (P.Ransom)		March 5-6	2 days @ $300/day	$ 600.00
Mapping, Interpretation (T. Sanders)			4 days @ $600/day	$ 2,400.00
			Subtotal	$ 38,680.94
Volterra Elecromagnetic Survey				
SJ Geophysics Ltd.	SJ221877	April 4	Security Deposit	$ 15,000.00
SJ Geophysics Ltd.	SJ221928	July 26	Mob, staff, support, Demob	$ 31,562.16
SJ Geophysics Ltd.	SJ221933	August 5	staff, map products	$ 3,801.00
TerraLogic Exploration Inc.	3861	July 6	Survey Crew, Management, Advance	$ 35,000.00
TerraLogic Exploration Inc.	3903	August 31	Disbursements / Final Billing	-$ 529.97
Bighorn Helicopters Inc	2515	July 11	EM Survey Heli-Support	$ 5,953.50
Bighorn Helicopters Inc	2530	July 28	EM Survey Heli-Support	$ 23,751.00
Bighorn Helicopters Inc	2533	July 29	EM Survey Heli-Support	$ 9,935.10
Mapping, Interpretation (T. Sanders)			2 days @ $600/day	$ 1,200.00
			Subtotal	$ 125,672.79
Writing Report (T. Sanders)			2 days @ $600/day	$ 1,200.00
			Total Cost	$ 165,553.73

Appendix 3. Mt. Evans 2022 Aeromag Survey-Logistics Report.

Precision GeoSurveys

AIRBORNE GEOPHYSICAL SURVEY REPORT

Mt. Evans Survey Block

Cranbrook, British Columbia

AMAROQ Gold Corp.

Precision GeoSurveys Inc.

BC Permit to Practice 1002615

www.precisiongeosurveys.com

Hangar 42, Langley Airport

21330 - 56th Ave., Langley, BC

Canada V2Y 0E5

604-484-9402

Jenny Poon, B.Sc., P.Geo.

March 2022

Job# 22130

Table of Contents

List of Figures

List of Tables

List of Appendices

List of Mt. Evans Survey Block Plates

Plate 1: Mt. Evans – Actual Flight Lines (FL)
Plate 2: Mt. Evans – Digital Terrain Model (DTM)
Plate 3: Mt. Evans – Total Magnetic Intensity with Actual Flight Lines (TMI_wFL)
Plate 4: Mt. Evans – Total Magnetic Intensity (TMI)
Plate 5: Mt. Evans – Residual Magnetic Intensity (RMI)
Plate 6: Mt. Evans – Reduced to Magnetic Pole (RTP) of RMI
Plate 7: Mt. Evans – Calculated Horizontal Gradient (CHG) of RMI
Plate 8: Mt. Evans – Calculated Vertical Gradient (CVG) of RMI
Plate 9: Mt. Evans – Analytic Signal (AS) of RMI
Plate 10: Mt. Evans – Potassium - Percentage (%K)
Plate 11: Mt. Evans – Thorium - Equivalent Concentration (eTh)
Plate 12: Mt. Evans – Uranium - Equivalent Concentration (eU)
Plate 13: Mt. Evans – Total Count (TC)
Plate 14: Mt. Evans – Total Count - Exposure Rate (TCexp)
Plate 15: Mt. Evans – Potassium over Thorium Ratio (%K/eTh)
Plate 16: Mt. Evans – Potassium over Uranium Ratio (%K/eU)
Plate 17: Mt. Evans – Uranium over Thorium Ratio (eU/eTh)
Plate 18: Mt. Evans – Uranium over Potassium Ratio (eU/%K)
Plate 19: Mt. Evans – Thorium over Potassium Ratio (eTh/%K)
Plate 20: Mt. Evans – Thorium over Uranium Ratio (eTh/eU)
Plate 21: Mt. Evans – Ternary Image (TI)

1.0 Introduction

This report outlines the geophysical survey operations and data processing procedures taken during a high resolution helicopter-borne magnetic and radiometric survey flown over the Mt. Evans survey block for AMAROQ Gold Corp. The survey block is located in southeastern British Columbia (Figure 1). It was flown on March 5 and March 6, 2022.

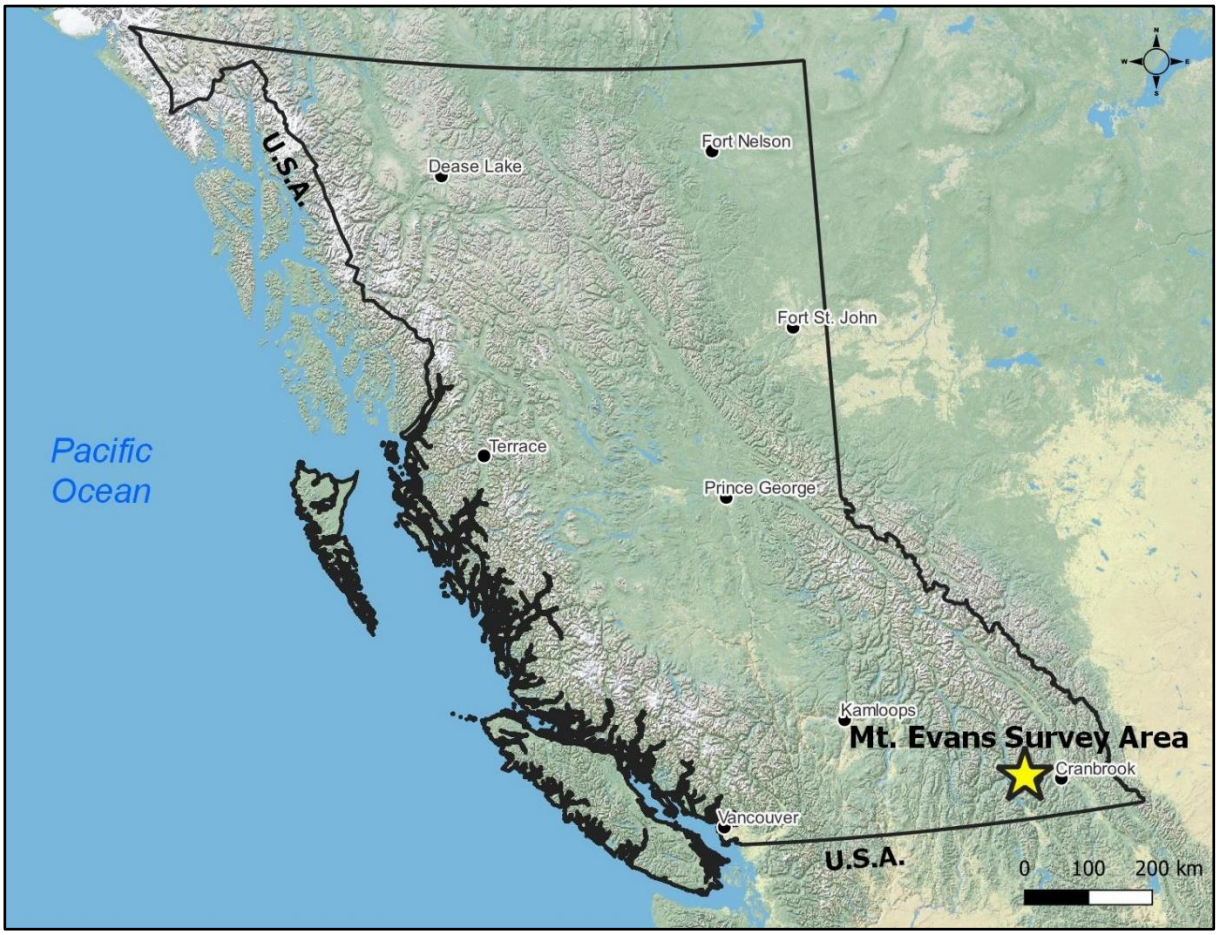

Figure 1: Mt. Evans survey area located in southeastern British Columbia.

1.1 Survey Area

The survey block is centred approximately 40 km west of Cranbrook, British Columbia (Figure 2).

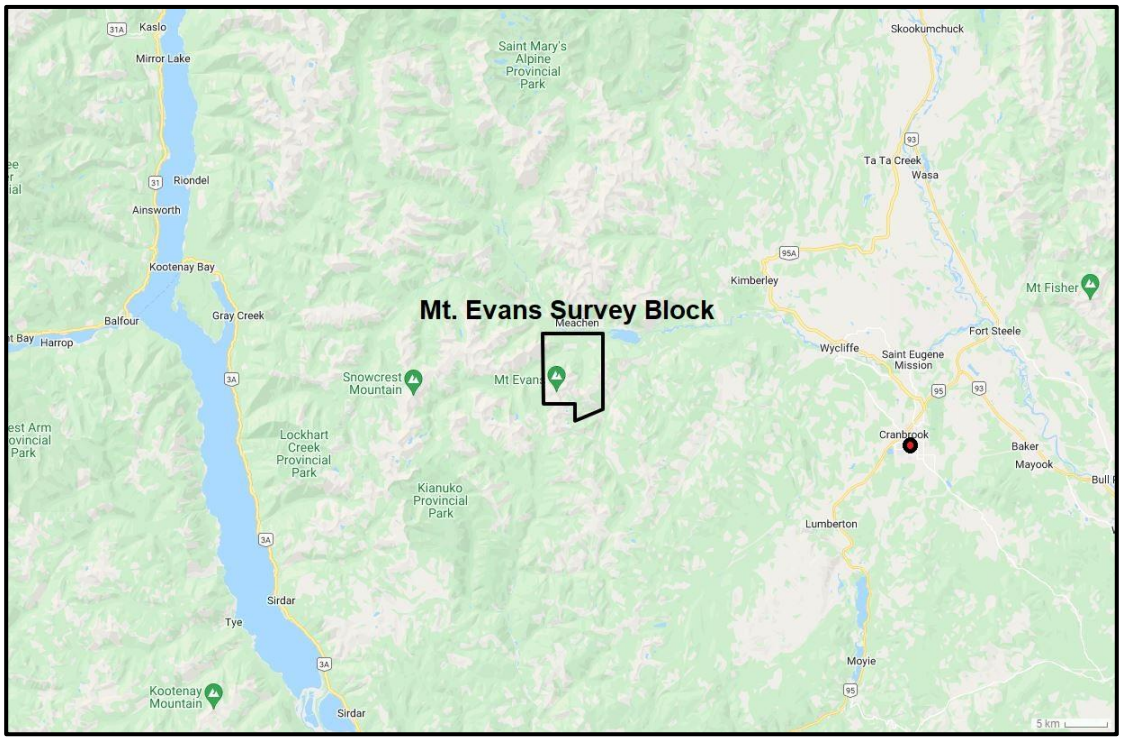

Figure 2: Mt. Evans survey block 40 km west of Cranbrook, British Columbia.

The Mt. Evans survey block was flown at 200 m line spacing on a heading of 179°/359°; tie lines were flown at 2000 m spacing on a heading of 089°/269° (Figures 3 and 4).

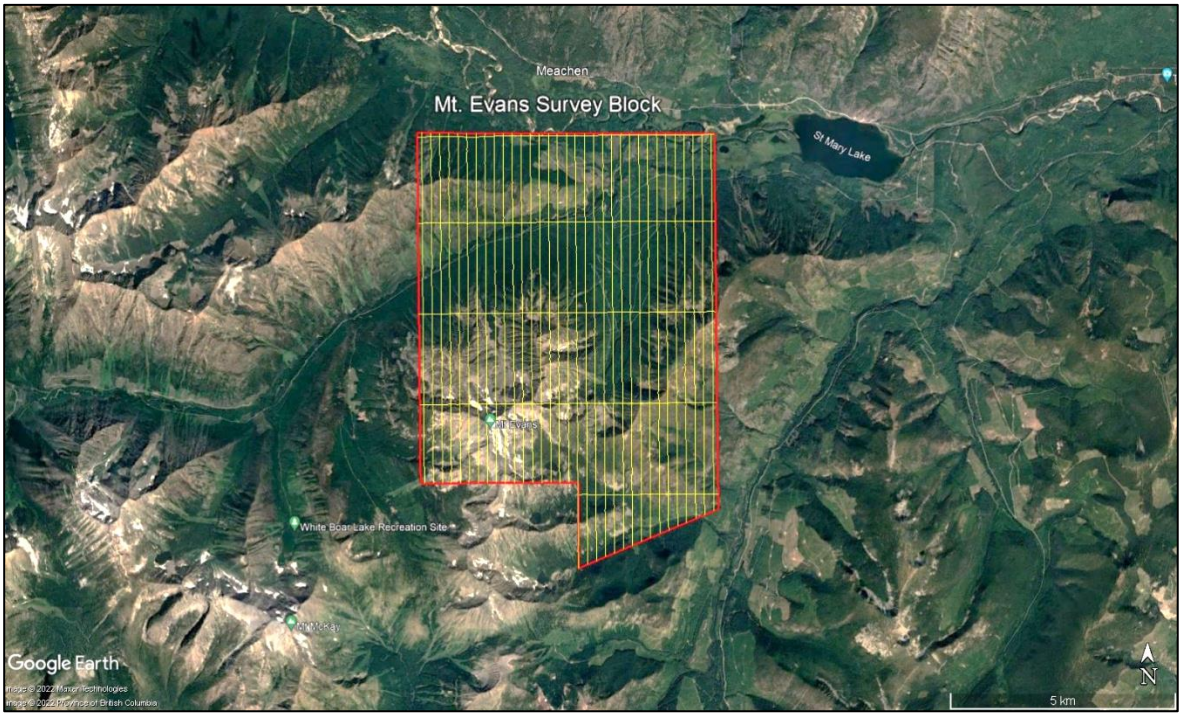

Figure 3: Plan View – Mt. Evans survey block with actual flight lines in yellow and outer survey block boundary in red.

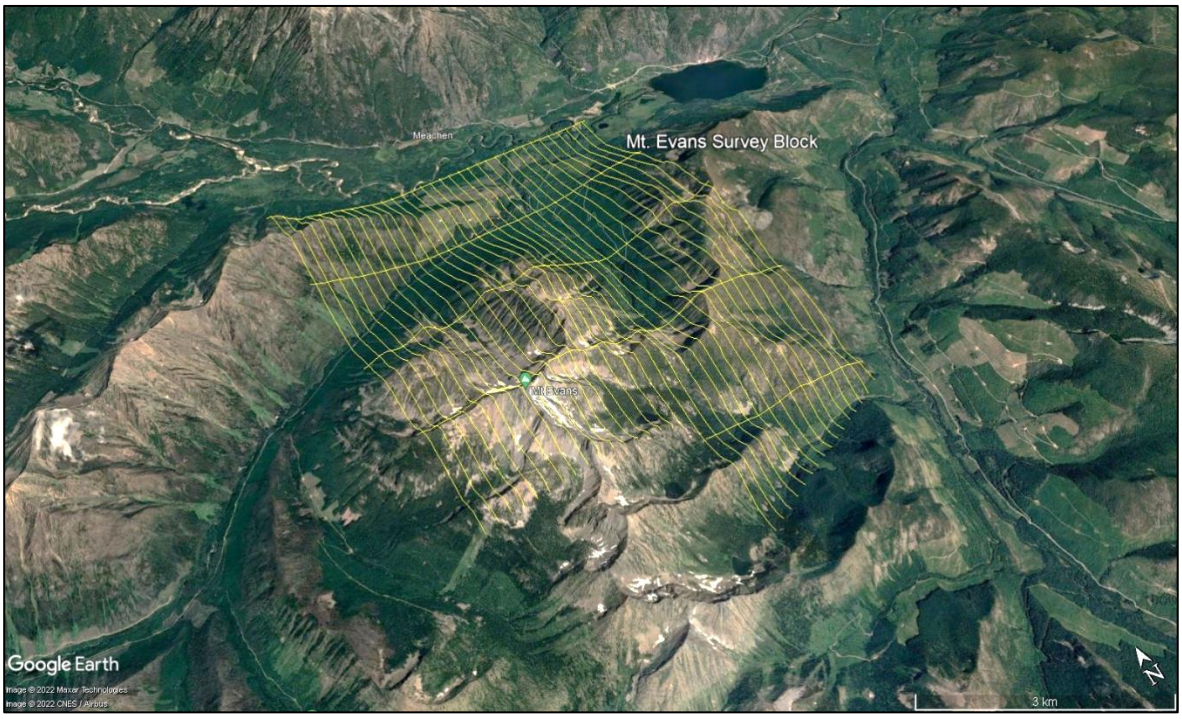

Figure 4: Terrain View – Mt. Evans survey block with actual flight lines in yellow.

1.2 Survey Specifications

The geodetic system used for the geophysical survey was WGS 84 in UTM Zone 11N. A total of 303 line km was flown over an area of 54.4 km^2 (Table 1). This total includes 6 km of data from an additional tie line flown on the north end of the survey block. Polygon coordinates for the Mt. Evans survey block are specified in Appendix A.

Survey Block	Area (km^2)	Line Type	No. of Lines Planned	No. of Lines Completed	Line Spacing (m)	Line Orientation (UTM grid)	Total Planned Line km	Total Actual km Flown
Mt. Evans	54.4	Survey	33	33	200	179°/359°	274	274
		Tie	4	5	2000	089°/269°	23	29
		Total	**37**	**38**			**297**	**303**

Table 1: Survey flight line specifications for Mt. Evans survey block.

2.0 Geophysical Data

Geophysical data are collected in a variety of ways and are used for many purposes including aiding in the determination of geology, mineral deposits, oil and gas deposits, geotechnical investigations, contaminated land sites, and UXO (unexploded ordnance) detection.

For the purposes of this survey, airborne magnetic and radiometric data were collected to serve in geological mapping and exploration for mineral deposits.

2.1 Magnetic Data

Magnetic surveying is the most common airborne geophysical technology used for both mineral and hydrocarbon exploration. Aeromagnetic surveys measure and record the total intensity of the magnetic field at the magnetometer sensor, which is a combination of the desired geomagnetic field as well as influences from the constantly varying solar wind and the aircraft's magnetic field. By subtracting temporal and aircraft magnetic effects, the resulting aeromagnetic maps show the spatial distribution and relative abundance of magnetic minerals - most commonly the iron oxide mineral magnetite - in the upper levels of Earth's crust, which in turn are related to lithology, structure, and alteration of bedrock. Survey specifications, instrumentation, and interpretation procedures depend on the objectives of the survey. Magnetic surveys are typically performed for:

- Geological Mapping - to aid in mapping lithology, structure, and alteration.
- Depth to Basement Mapping - for exploration in sedimentary basins or mineralization associated with the basement surface.

2.2 Radiometric Data

Radiometric surveys are used to determine either the absolute or relative concentrations of the naturally occurring radioelements uranium (U), thorium (Th), and potassium (K) in surface rocks and soils using radioactive emanations. Gamma radiation is utilized due to its greater penetration depth compared with alpha and beta radiation. Radiometric data are useful for mapping lithology, alteration, and structure as well as providing insights into weathering. For example, individual radioelements follow very different pathways of evolution during alteration of rocks, natural radioactivity of igneous rocks generally increases with SiO_2 content, and clay minerals tend to fix the natural radioelements.

Gamma rays are electromagnetic waves with frequencies between 10^{19} and 10^{21} Hz emitted spontaneously from an atomic nucleus during radioactive decay, in packets referred to as photons. The energy E transported by a photon is related to the wavelength λ or frequency ν by the formula:

$$E = h\nu = hc/\lambda$$

where: c is the velocity of light
h is Planck's constant (6.626×10^{-34} joule)

All detectable gamma radiation from Earth materials comes from the natural decay products of three primary radioelements: U, Th, and K. Each individual nuclear species (element) emits gamma rays at one or more specific energies, as shown in Figure 5. Of these elements, only potassium (^{40}K) emits gamma energy directly, at 1.46 MeV. Uranium (^{238}U) and thorium (^{232}Th) emit gamma rays through their respective decay series; ^{214}Bi at 1.76 MeV for uranium and ^{208}Tl

at 2.61 MeV for thorium. Accordingly, the ^{214}Bi and ^{208}Tl measurements are considered equivalents for uranium (eU) and thorium (eTh), as the daughter products will be in equilibrium under most natural conditions.

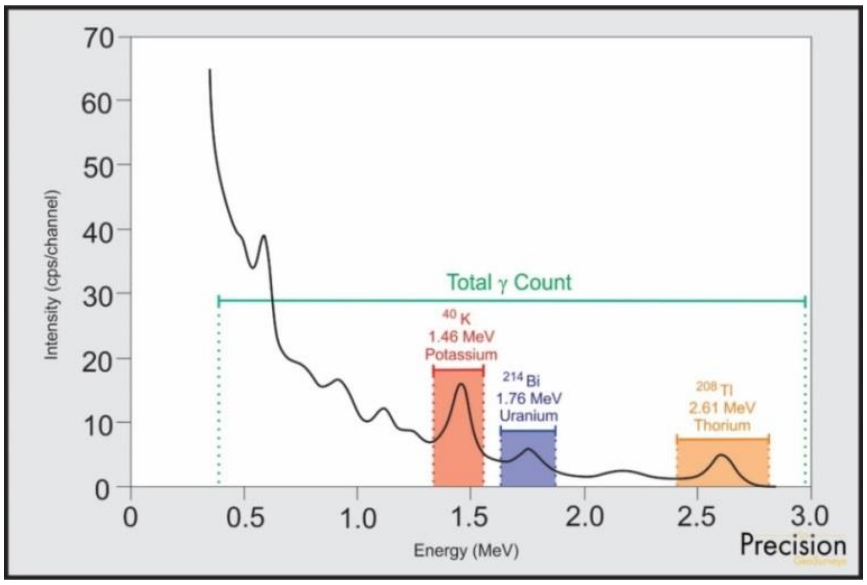

Figure 5: Typical natural gamma spectrum showing the three spectral windows (^{40}K 1.37-1.57 MeV, ^{214}Bi 1.66-1.86 MeV, ^{208}Tl 2.41-2.81 MeV) and total count (0.40-2.81 MeV) window.

Airborne radiometric measurements are strongly influenced by surficial features including soil, water, glaciers, glacial debris, vegetation, and snow. Therefore, variations in measured gamma concentrations and distributions must be carefully evaluated with respect to potential sources of surficial attenuation.

3.0 Aircraft and Equipment

All geophysical and subsidiary equipment were carefully installed on an aircraft by Precision GeoSurveys to collect magnetic and radiometric data.

3.1 Aircraft

Precision GeoSurveys flew the survey using an Airbus AS350 helicopter, registration C-GSVY.

3.2 Geophysical Equipment

The survey aircraft (Figure 6) was equipped with a data acquisition system, GPS navigation system, pilot guidance unit (PGU), laser altimeter, cesium vapor magnetometer, fluxgate magnetometer, gamma ray spectrometer, barometer, and temperature/humidity probe. Magnetic

base stations were used to record temporal magnetic variations. Technical specifications for the geophysical equipment are provided in Appendix B.

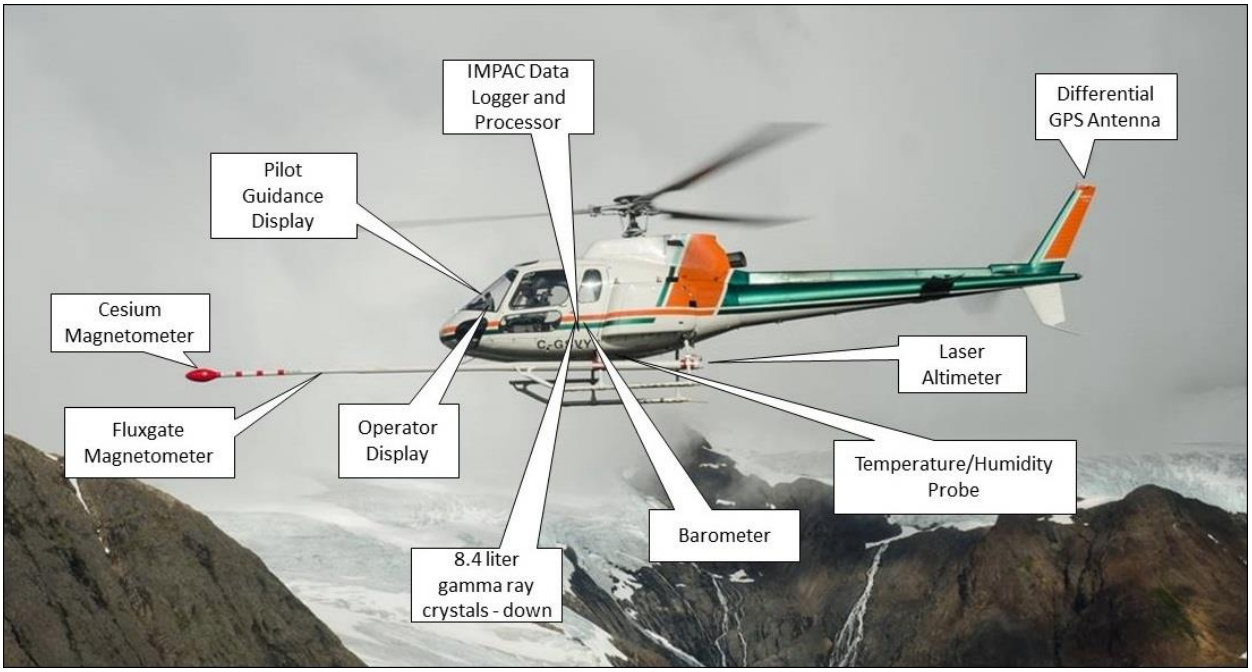

Figure 6: Survey helicopter equipped with a magnetic sensor for magnetic data acquisition and gamma spectrometer.

3.2.1 IMPAC

The Integrated Multi-Parameter Acquisition Console (IMPAC) (Figure 7), manufactured by Nuvia Dynamics Inc. (previously Pico Envirotec Inc.), is the main computer used in integrated data recording, data synchronizing, providing real-time quality control data for the geophysical operator display, and the generation of navigation information for the pilot and operator display systems.

Figure 7: IMPAC data acquisition system.

IMPAC uses the Microsoft Windows operating system and geophysical parameters are based on Nuvia's Airborne Geophysical Information System (AGIS) software. Depending on survey

specifications, information such as magnetic field, electromagnetic response, total gamma count, counts of various radioelements (K, U, Th, etc.), cosmic radiation, barometric pressure, atmospheric humidity, temperature, aircraft attitude, aircraft height, navigation parameters, and GPS status can all be monitored on the AGIS on-board display (Figure 8).

While in flight, the raw magnetic response, magnetic fourth difference, compensated and uncompensated data, radiometric spectra, aircraft position, survey altitude, cross track error, and other parameters are recorded (depending on sensor configuration) and can be viewed by the geophysical operator for immediate QC (quality control). Additional software allows for post or real time magnetic compensation.

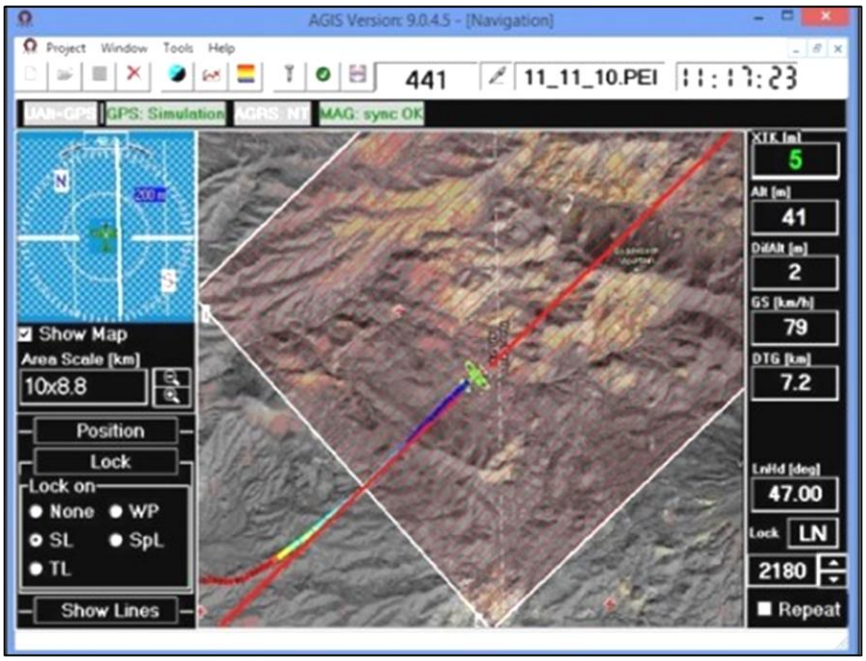

Figure 8: AGIS operator display showing real time flight line recording and navigation parameters. Additional windows display real-time geophysical data to operator.

3.2.2 GPS Navigation System

A Hemisphere R330 GPS receiver (Figure 9) and a Novatel GPS antenna on the tail of the aircraft integrated with the AGIS navigation system and pilot display (PGU) provide accurate navigational information and position control. The R330 GPS receiver supports fast updates at a rate of up to 20 Hz (20 times per second); delivering sub-meter positioning accuracy in three dimensions. It receives GNSS (GPS/GLONASS) L1 and L2 signals.

The receiver supports differential correction methods including L-Band, RTK, SBAS, and Beacon. The R330 employs innovative Hemisphere GPS Eclipse SureTrack technology, which allows it to model the phase on satellites that the airborne unit is currently tracking. With SureTrack

technology, dropouts are reduced and speed of the signal reacquisitions is increased; enhancing accurate positioning when base corrections are not available.

Figure 9: Hemisphere R330 GPS receiver.

3.2.3 Pilot Guidance Unit

Steering and elevation (ground clearance) information is continuously provided to the pilot by the Pilot Guidance Unit (PGU). The graphical display is mounted on top of the aircraft's instrument panel, remotely from the data acquisition system. The PGU is the primary navigation aid (Figure 10) to assist the pilot in keeping the aircraft on the planned flight path, heading, speed, and at the desired ground clearance.

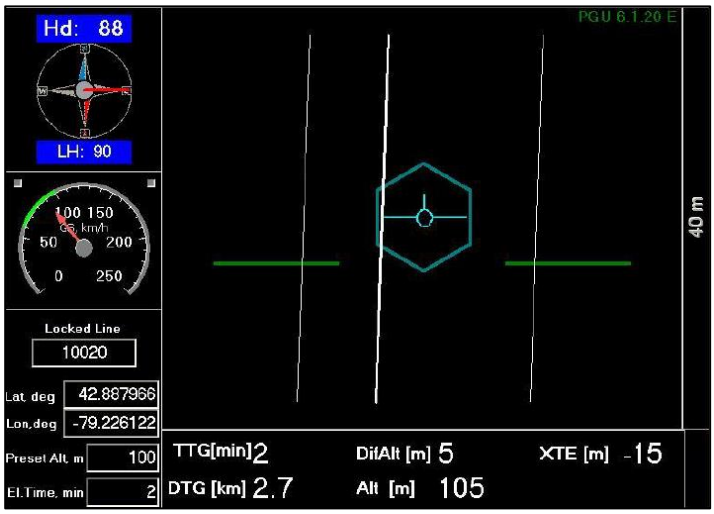

Figure 10: PGU screen displaying navigation information.

PGU information is displayed on a full VGA 600 x 800 pixel 7 inch (17.8 cm) LCD display. The CPU for the PGU is contained in a PC-104 console and uses Microsoft Windows operating system control, with input from the GPS antenna on the aircraft, laser altimeter, and AGIS.

3.2.4 Laser Altimeter

Terrain clearance is measured by an Opti-Logic RS800 Rangefinder laser altimeter (Figure 11) attached to the aft end of the magnetometer boom. The RS800 laser is a time-of-flight sensor that measures distance by a rapidly modulated and collimated laser beam that creates a dot on the target surface. The maximum range of the laser altimeter is 700 m off natural surfaces with accuracy of ±1 m on a 1 x 1 m diffuse target with 50% (±20%) reflectivity. Within the sensor unit, reflected signal light is collected by the lens and focused onto a photodiode. Through serial communications and digital outputs, ground clearance data are transmitted to an RS-232 compatible port and recorded and displayed by the AGIS and PGU at 10 Hz in meters.

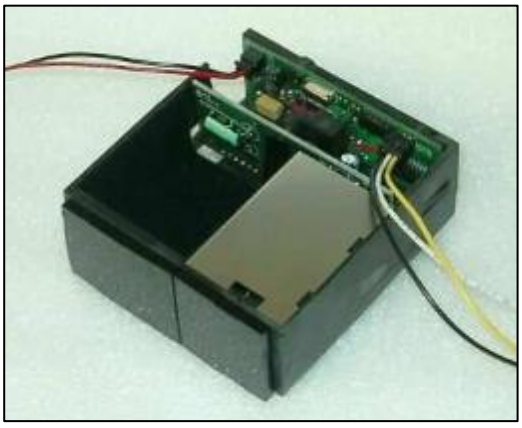

Figure 11: Opti-Logic RS800 Rangefinder laser altimeter.

3.2.5 Magnetometer

The survey was flown with a Geometrics G-822A split-beam cesium vapor magnetometer (Figure 12) mounted on the front of the helicopter in a non-magnetic and non-conductive “stinger” configuration to measure total magnetic intensity. The magnetometer sensor was oriented at 45° to couple with local magnetic field at Mt. Evans survey area.

Figure 12: Geometrics G-822A cesium vapor magnetometer.

3.2.6 Fluxgate Magnetometer

As the survey helicopter flies along a survey line, small attitude changes (pitch, roll, and yaw) are measured by a triaxial fluxgate magnetometer (Figure 13). The fluxgate consists of three magnetic sensors, X, Y, and Z, operating independently and simultaneously. Each sensor has an analog output corresponding to the directional component of the ambient magnetic field along its axis. Response of the sensors is proportional to the cosine of the angle between the applied field and the sensor's sensitive axis.

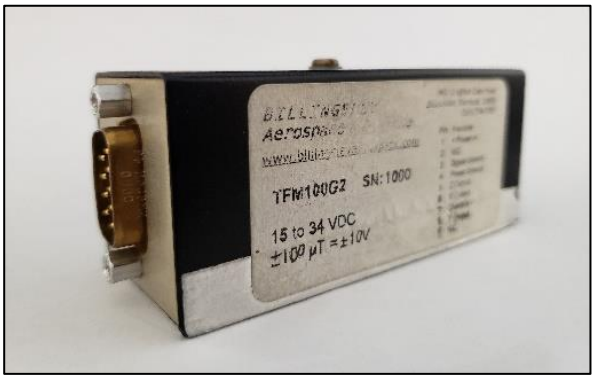

Figure 13: Billingsley TFM100G2 triaxial fluxgate magnetometer.

3.2.7 Magnetic Base Station

Temporal variations of Earth's magnetic field, particularly diurnal, were monitored and recorded by two GEM GSM-19T base station magnetometers. They were operated at all times while airborne data were being collected. The base stations were located in an area with low magnetic gradient, away from electric power transmission lines and moving ferrous objects, such as motor vehicles, which could affect the survey data integrity.

The GEM GSM-19T magnetometer (Figure 14) with integrated GPS time synchronization uses proton precession technology with absolute accuracy of ±0.20 nT and sensitivity of 0.15 nT at 1

Hz. Base station magnetic data were recorded on internal solid-state memory and downloaded onto a field laptop computer using a serial cable and GEMt. Evansink 5.4 software. Profile plots of the base station readings were generated, updated, and reviewed at the end of each survey day.

Figure 14: GEM GSM-19T proton precession magnetometer.

3.2.8 Spectrometer

Gamma radiation data were collected by an Advanced Gamma Ray Spectrometer (AGRS) manufactured by Nuvia Dynamics. The AGRS is an intelligent, self-calibrating, fully integrated gamma detection system (Figure 15) containing two thallium-activated synthetic sodium iodide crystals; 8.4 litres (two crystals of 4.2 litres each) downward-looking, with user-selectable 256, 512, or 1024 channel output at 1 Hz sampling rate. The downward-looking crystals are designed to measure gamma rays from below the aircraft. The AGRS system is installed in the rear passenger cabin of the helicopter away from the fuel tank to minimize variable gamma attenuation from fluctuating fuel levels.

Figure 15: AGRS gamma spectrometer system with two downward detectors.

4.0 Survey Operations

The Mt. Evans geophysical survey was flown on March 5 and March 6, 2022 in winter conditions. The experience of the pilot ensured that data quality objectives were met, and that safety of the

flight crew was never compromised given the potential risks involved in airborne geophysical surveying. Field processing and quality control checks were performed daily.

4.1 Operations Base and Crew

The base of operation for the Mt. Evans survey was Cranbrook airport (CYXC), British Columbia, 35 km east of the survey block.

Precision's geophysical crew consisted of five members (Table 2):

Crew Member	Position
Harmen Keyser, P.Geo.	Helicopter pilot
Bruce Larsen	Helicopter co-pilot and geophysical operator
Michael Marriot, B.Sc.	Geophysical technician
Jenny Poon, B.Sc., P.Geo.	Geophysicist – data processor and reporting (off-site)
Shawn Walker, M.Sc., P.Geo.	Geophysicist – data processor and mapping (off-site)

Table 2: List of survey crew members.

4.2 Magnetic Base Station Specifications

Changes in the Earth's magnetic field over time, such as diurnal variations, magnetic pulsations, and geomagnetic storms, were measured and recorded by two stationary GEM GSM-19T proton precession magnetometers. The magnetic base stations were installed in a clearing beside a logging road north of the Mt. Evans survey block (Table 3; Figures 16 and 17) in an area away from sources of potential interference such as ferromagnetic objects, vehicles, and power lines that could affect the base station data and ultimately the survey data.

Station Name	Easting/Northing	Latitude/Longitude	Datum/Projection
GEM 4 S/N 2065370	548886 m E 5499822 m N	49° 38' 56.26" N 116° 19' 22.04" W	WGS 84, Zone 10N
GEM 5 S/N 1094678	548889 m E 5499833 m N	49° 38' 56.62" N 116° 19' 21.90" W	WGS 84, Zone 10N

Table 3: Magnetic base station locations.

Magnetic readings were reviewed at regular intervals to ensure that no airborne data were collected during periods of high magnetic activity (in excess of 10 nT from a linear chord length of two minutes).

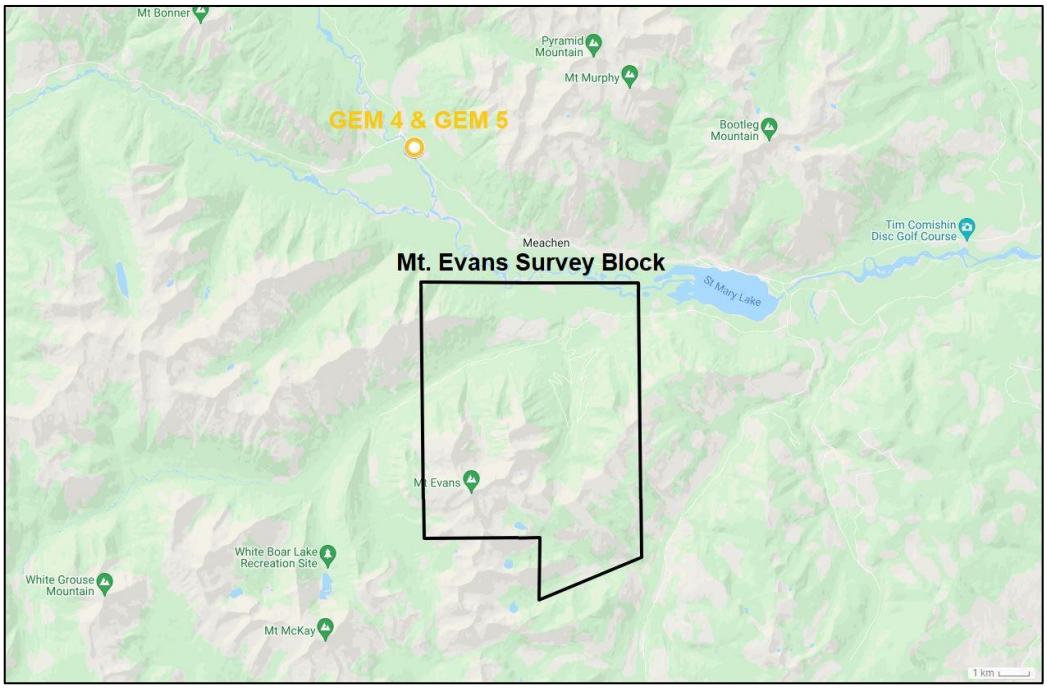

Figure 16: Location of GEM 4 and GEM 5 magnetic base stations in a clearing north of Mt. Evans survey block.

Figure 17: GEM 4 (L) and GEM 5 (R) magnetic base stations.

4.3 Field Processing and Quality Control

Survey data were transferred from the aircraft's data acquisition system onto a USB memory stick and copied onto a field data processing laptop computer on a flight-by-flight basis. The raw data files in PEI binary data format were converted into Geosoft GDB database format. Using Geosoft

Oasis Montaj 2021.2.1.11, the data were inspected to ensure compliance with contract specifications (Table 4; Figures 18 to 20).

Parameter	Specification	Tolerance
Position	Line Spacing	Flight line deviation within 8 m L/R from ideal flight path. No exceedance for more than 1 km.
	Height	Nominal flight height of 50 m above ground level (AGL) with tolerance of ±10 m. No exceedance for more than 1 km, provided deviation is not due to tall trees, topography, mitigation of wildlife/livestock harassment, cultural features, or other obstacles beyond the pilot's control.
	GPS	GPS signals from four or more satellites must be received at all times, except where signal loss is due to topography. No exceedance for more than 1 km.
Magnetics	Temporal/Diurnal Variations	Non-linear temporal magnetic variations within 10 nT of a linear chord of 2 minutes length.
	Normalized 4th Difference	Magnetic data within 0.02 nT peak to peak. No exceedance for distances greater than 1 km or more, provided noise is not due to geological or cultural features.
Radiometrics	Moisture Conditions	No delays shall be incurred due to unfavourable radiometric survey conditions.

Table 4: Contract survey specifications.

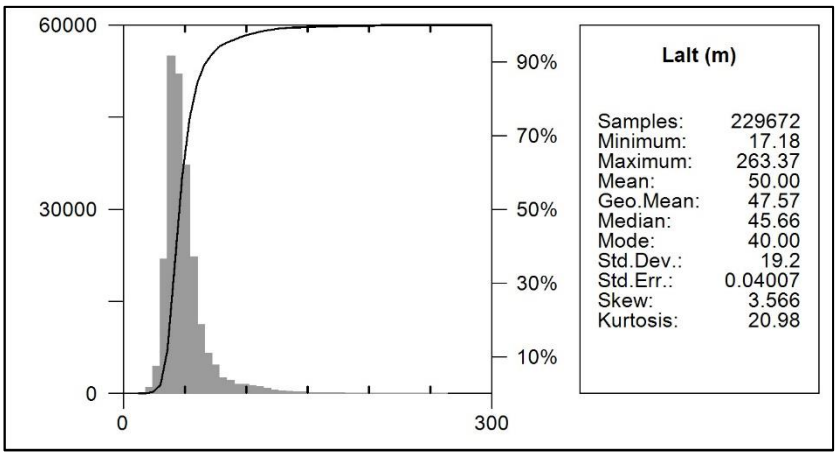

Figure 18: Histogram showing survey elevation vertically above ground.

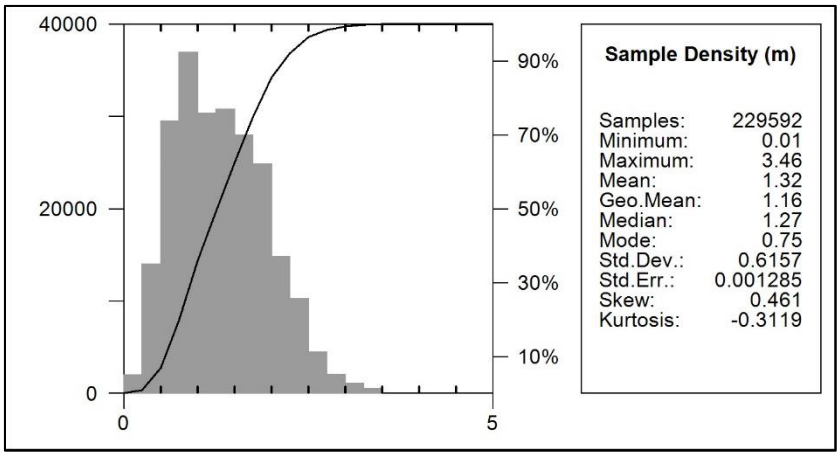

Figure 19: Histogram showing magnetic sample density. Horizontal distance in meters between adjacent measurement locations; magnetic sample frequency 20 Hz.

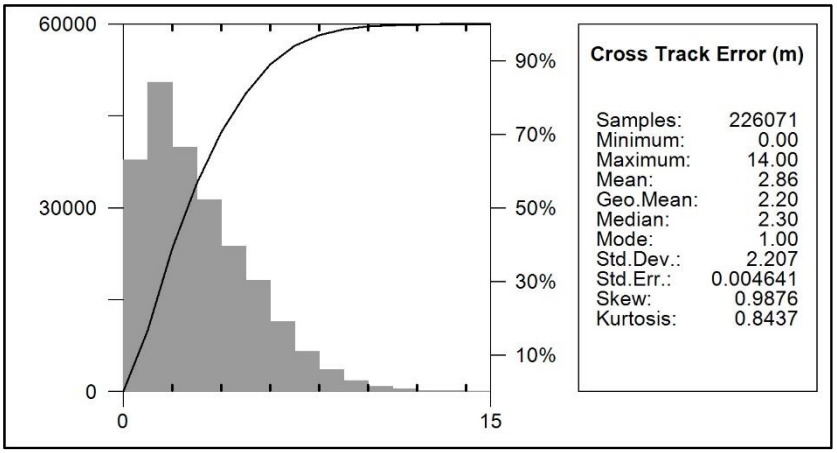

Figure 20: Histogram showing cross track error of survey helicopter.

5.0 Data Acquisition Equipment Checks

Equipment tests and calibrations were conducted for the laser altimeter, magnetometer, and spectrometer at the start of the survey to ensure compliance with contract specifications and to deliver high quality airborne geophysical data. A lag test was conducted for all sensors. For the airborne magnetometer, compensation and heading error test flights were flown. There were three tests conducted for the gamma spectrometer: calibration pad test, cosmic flight test, and altitude correction and sensitivity test.

5.1 Laser Altimeter Calibration

The Opti-Logic RS800 laser altimeter used on the survey helicopter was tested and calibrated in accordance with manufacturer's instructions prior to starting the survey. This ensured that heights reported by the laser were accurate within the normal survey operating range.

5.2 Lag Test

A lag test was performed to determine the difference in time the digital reading was recorded for the magnetometer, spectrometer, and laser altimeter with the position fix time that the fiducial of the reading was obtained by the GPS system resulting from a combination of system lag and different locations of the various sensors and the GPS antenna. The test was flown in reciprocal headings over identifiable features at survey speed and height to isolate position changes. The resulting data (Table 5) were used to correct for time and position.

Instrument	Source	Lag Fiducial	Correction (sec)
Magnetometer	Logging machinery	3	0.15
Laser	Sharp gully	20	1.00
Spectrometer	Lake edge	16	0.80

Table 5: Survey lag correction values. Magnetic data at 20 Hz; laser altimeter and spectrometer were resampled to 20 Hz.

5.3 Magnetometer Tests

The magnetometer was tested and calibrated with a series of dedicated flights specifically for removing instrument offset errors and undesired effects of aircraft movement, speed, and heading direction.

5.3.1 Compensation Flight Test

During aeromagnetic surveying, a small but significant amount of noise is introduced to the magnetic data by the aircraft itself, as the magnetometer is within the aircraft's magnetic field. Changes in aircraft attitude combined with the permanent magnetization of certain ferrous aircraft parts contribute to this noise. The aircraft was degaussed using proprietary technology prior to starting the survey and the remaining magnetic noise was removed by a process called magnetic compensation.

A magnetic compensation flight was completed for this survey. The process consists of a series of prescribed maneuvers (±10° roll, ±10° pitch, and ±10° yaw) where the aircraft flies in the four orthogonal headings required (089°/179°/269°/359° in the case of this survey) at a sufficient altitude (typically > 2,500 m AGL) in an area of low magnetic gradient where Earth's magnetic field becomes nearly uniform at the scale of the compensation flights. In each heading direction, three specified roll, pitch, and yaw maneuvers (total 36) are performed by the pilot at constant elevation so that any magnetic variation recorded by the airborne magnetometer can be attributed to aircraft movement. These maneuvers are determined by the airborne fluxgate magnetometer and provide the data that are required to calculate the necessary parameters for compensating the magnetic data to remove aircraft noise from survey data. Compensation flight test results are summarized in Table 6.

Pre-Compensation (nT)					Post-Compensation (nT)				
Heading	**Roll**	**Pitch**	**Yaw**	**Total**	**Heading**	**Roll**	**Pitch**	**Yaw**	**Total**
089°	1.0727	0.7727	0.6563	2.5017	089°	0.2090	0.2626	0.1732	0.6448
179°	0.8706	0.5650	0.5539	1.9895	179°	0.1924	0.2130	0.2125	0.6179
269°	1.0819	0.6940	0.5311	2.3070	269°	0.1825	0.2064	0.1820	0.5709
359°	1.6897	1.2403	1.4576	4.3876	359°	0.1504	0.1798	0.1685	0.4987
Figure of Merit = 11.1858					**Figure of Merit = 2.3323**				

Table 6: Results of compensation flight.

5.3.2 Heading Correction Test

To determine heading errors, a cloverleaf pattern flight test was conducted at high altitude to minimize the effect of natural magnetic gradient. The cloverleaf test was flown in the same orthogonal headings as the survey and tie lines (089°/179°/269°/359° in the case of this survey) at >2500 m AGL in an area with low magnetic gradient. For all four directions of the cloverleaf test the survey helicopter must pass over the same point, at the same elevation, with the aircraft in straight and level flight. The difference in magnetic values obtained in reciprocal headings is referred to as the heading error. Heading correction values derived from the test flight are summarized in Table 7.

Heading	Heading Correction (nT)
089°	-5.975
179°	-4.450
269°	3.975
359°	6.450
Total:	**0.0000**

Table 7: Magnetic sensor heading corrections.

5.4 Gamma-ray Spectrometer Tests and Calibrations

Calibration and testing of the AGRS-2 airborne gamma-ray spectrometry system was carried out prior to starting the survey. Spectrometer calibration involved three tests which enabled the conversion of airborne data to ground concentration of natural radioactive elements. These tests were the calibration pad test, cosmic flight test, and the altitude correction and sensitivity test. Procedures were generally in accordance with IAEA technical report series No. 323, *Airborne Gamma Ray Spectrometer Surveying*, and AGSO Record 1995/60, *A Guide to the Technical Specifications for Airborne Gamma-Ray Surveys*.

5.4.1 Calibration Pad Test

The calibration pad test was conducted using Geological Survey of Canada (GSC) portable calibration pads. The pads are slabs of concrete containing known concentrations of the natural radioelements K, Th, and U and are used to simulate ideal geological sources of radiation. The measurements collected from the calibration pad test were used to determine Compton scattering and Grasty backscatter (spectral overlap between element windows) coefficients.

5.4.2 Cosmic Flight Test

While the background source of gamma radiation from the aircraft itself is essentially constant, the amount of signal detected from ground sources varies with ground clearance. As the height of the aircraft increases, the distance between the ground and the spectrometer crystals increases, and the proportion of cosmic radiation in each spectral window increases exponentially. The cosmic flight test is conducted to determine the aircraft's background attenuation coefficients for the detector crystal packs and the cosmic coefficients. The pilot is required to fly over the same low gamma source location (such as a large lake) repeatedly at 4000, 5000, 6000, 7000, and 8000 feet (1220, 1520, 1830, 2130, and 2440 m) above ground, for approximately two minutes each, to collect gamma data used to determine the non-terrestrial component present in the total gamma signal.

5.4.3 Altitude Correction and Sensitivity Test

The altitude and sensitivity test is similar to the cosmic flight test but is conducted at lower elevations. The aircraft is required to fly over the same location at 30, 40, 50, 60, 70, 100, and 120 m above ground, for two minutes each. As the distance between the gamma detectors on the aircraft and the radioactive ground source increases, the source signature exponentially degrades. As a result, this test is used to determine the altitude attenuation coefficients and the radio-element sensitivity of the airborne spectrometer system.

6.0 Data Processing

After all data were collected, several procedures were undertaken to ensure that the data met a high standard of quality. Magnetic and radiometric data recorded by the AGIS were converted into Geosoft or ASCII file formats using Nuvia Dynamics software. Further processing (Figure 21) was carried out using Geosoft Oasis Montaj 2021.2.1.11 geophysical processing software along with proprietary processing algorithms.

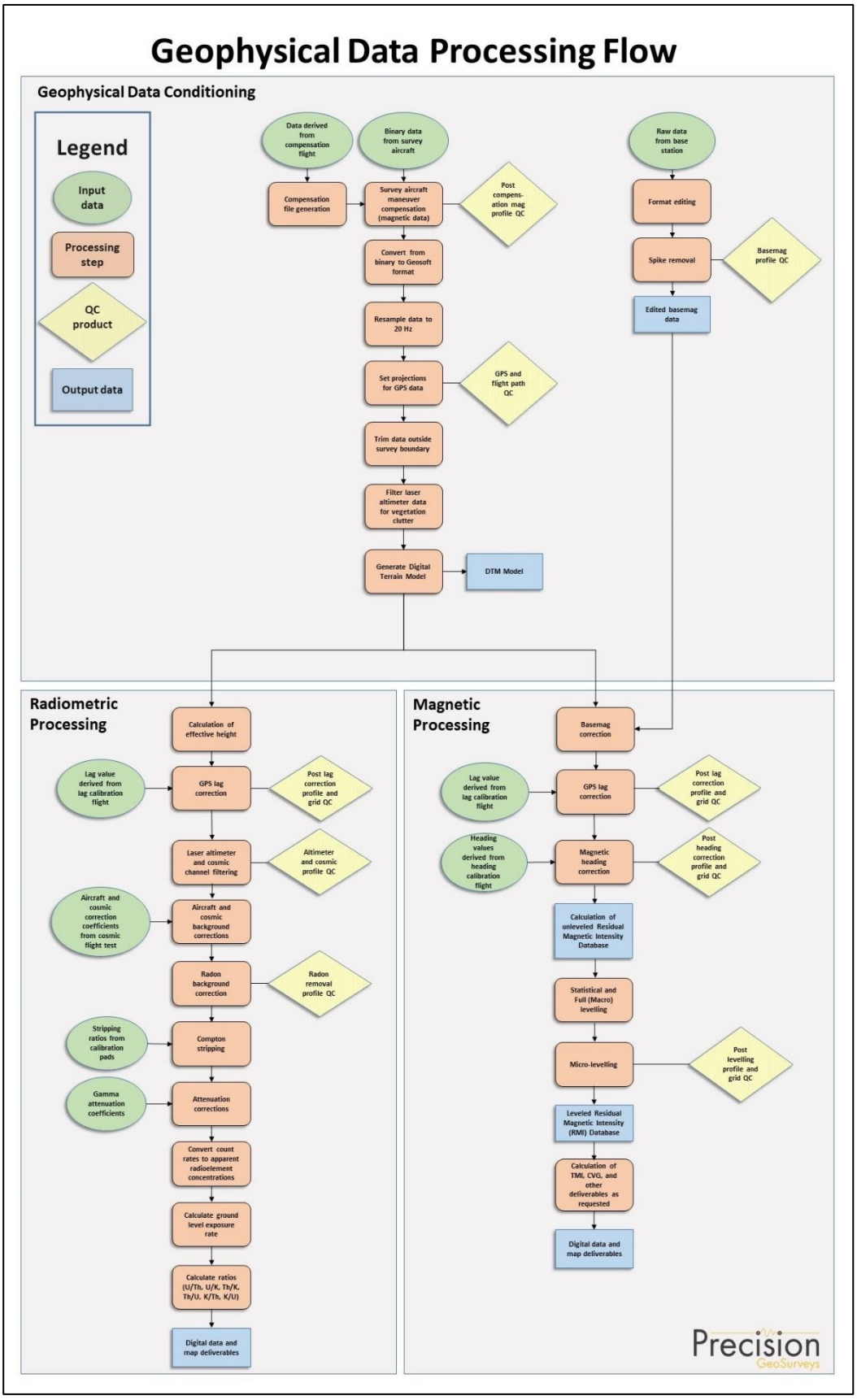

Figure 21: Magnetic and radiometric data processing flow.

6.1 Position Corrections

In order to collect high resolution geophysical data, the location at which the data were collected and recorded must be accurate.

6.1.1 Lag Correction

A correction for lag error was applied to the geophysical data recorded at each individual sensor to compensate for the combination of lag in the recording system and the sensing instrument flying in a different location from the GPS antenna, as determined during the lag test. Validity of the lag corrections was confirmed by the absence of grid corrugations in adjoining reciprocal lines.

6.2 Flight Height and Digital Terrain Model

Laser altimeters are unable to provide valid data over glassy water or fog which dissipate the laser so that a "zero" reading is obtained. In these cases, estimates of correct height are inserted manually. Dense vegetation generates high frequency variations from leaf and branch reflections. A Rolling Statistics filter is applied to the lag corrected (1 second lag) laser altimeter data to remove vegetation clutter followed by a Low Pass filter to smooth out the laser altimeter profile to eliminate isolated high frequency noise and generate a surface closely corresponding to the actual ground profile.

As the GPS antenna is on the tail of the helicopter, altitude data were corrected by subtracting 3.1 m to place measured heights in the same plane as the laser altimeter. A Digital Terrain Model (DTM) was determined by subtracting the laser altimeter data from the filtered GPS altimeter data defined by the WGS 84 ellipsoidal height. DTM accuracy is affected by the attitude of the aircraft, slope of the ground, sample density, and satellite geometry. Small inconsistencies in recorded flight height at the intersection points of survey lines and tie lines resulted in small spatial variabilities in the Digital Terrain Model (DTM). Conventional leveling and micro-leveling were applied to correct for these variations and a fully leveled DTM was generated.

6.3 Magnetic Processing

Magnetic data were compensated and then corrected for temporal variations (including diurnal), lag, and heading. The data were examined for magnetic noise and spikes, which were removed as required. The background magnetic field, International Geomagnetic Reference Field (IGRF) of the Earth, was removed and survey and tie line data of the resulting residual magnetic field were then leveled.

6.3.1 Flight Compensation

Data obtained from the compensation flight test were applied to the raw magnetic data as the first step of data processing. A computer program called MAGComp was used to create a model from the compensation flight test for each survey to remove the noise induced by the aircraft and its movement; this model was applied to data from each survey flight.

6.3.2 Temporal Variation Correction

The intensity of Earth's magnetic field varies with location and time. The time variable, known as diurnal or more accurately as temporal variation, is removed from the recorded airborne data to provide the desired magnetic field at a specified location. Magnetic data from base station GEM 4 were used for correcting the airborne magnetic survey data, and GEM 5 data were retained for backup. The data were edited, plotted, and merged into a Geosoft database (.GDB) on a daily basis. Base station measurements were averaged to establish a magnetic reference datum of 54670.37 nT. Magnetic deviations relative to the reference datum were used to calculate the observed variations of the Earth's magnetic field during the time it took to complete the survey. The airborne magnetic data were then corrected for temporal variations by subtracting the base station deviations from the data collected on the aircraft, effectively removing the effects of diurnal and other temporal variations.

6.3.3 Heading Correction

For each survey heading, changes in instrument magnetic fields along a survey flight line are detected and these systematic shifts are recorded. These values are used to construct a heading table (.TBL) file. An intersection table was created, containing all magnetic field values where tie lines intersected the survey lines, and the overall average magnetic field value was calculated. For each of the four headings, the averages were calculated and then compared to the overall average to determine four values which were used to correct heading and offset errors in each flight direction.

6.3.4 IGRF Removal

The International Geomagnetic Reference Field (IGRF) model is the empirical representation of Earth's dynamic magnetic field (main core field without external sources) collected and disseminated from satellite data and from magnetic observatories around the world. The IGRF has historically been revised and updated every five years by a group of modellers associated with the International Association of Geomagnetism and Aeronomy (IAGA).

The initial unleveled Residual Magnetic Intensity (RMI) was calculated by taking the difference between the 13th generation IGRF (IGRF-13, released in December 2019) and the non-leveled

Total Magnetic Intensity (TMI) to create a more valid model of individual near-surface magnetic anomalies. This model is independent of time to allow for other magnetic data (previous or future) to be more easily incorporated into each survey database.

6.3.5 Leveling and Micro-leveling

Small inconsistencies in flight height and line location result in variabilities in magnetic intensity measured at the intersection points of survey lines and tie lines. Using the initial Residual Magnetic Intensity (RMI) data (TMI with the IGRF removed), RMI data from survey and tie lines were leveled to each other. Two types of leveling were applied to the corrected data: conventional leveling and micro-leveling. There are two components to conventional leveling: statistical leveling to level tie lines and full leveling to level survey lines. The statistical leveling method corrected the SL/TL intersection errors that follow a specific pattern or trend. Through the error channel, an algorithm calculated a least-squares trend line and derived a trend error curve, which was then added to the channel to be leveled. The second component was full leveling. This adjusted the magnetic value of the survey lines so that all lines matched the trended tie lines at each intersection point.

Following statistical leveling, micro-leveling was applied to corrected conventional leveled data. This iterative grid-based process removed low amplitude components of flight line noise that still remained after tie line and survey line leveling, resulting in fully leveled RMI data. The IGRF was then added back onto the RMI to allow for the production of a leveled TMI grid and map.

6.3.6 Reduction to Magnetic Pole

Reduced to Magnetic Pole (RTP) data were determined from the leveled Residual Magnetic Intensity (RMI) data. The RTP filter was applied in the Fourier domain and rotates the observed magnetic inclination and declination field to what the field would look like at the north magnetic pole, to allow observation of magnetic trends and patterns independent of magnetic inclination and declination. Reducing the dipolar nature of magnetic anomalies is useful for interpretation because peak RTP magnetic values can be related to the centre of magnetic rock bodies and asymmetries in the RTP imagery closely reflect true dips and plunges.

Inclination and declination were calculated by using March 5, 2022, the first day of the survey. The derived values were used in the following formula:

$$RTP\ (\theta) = \frac{[\sin(I) - I\ \cdot \cos(I) \cdot \cos(D - \theta)]^2}{[\sin^2(I_a) + \cos^2(I_a) \cdot \cos^2(D - \theta)] \cdot [\sin^2(I) + \cos^2(I) \cdot \cos^2(D - \theta)]}$$

where: I is geomagnetic inclination in ° from horizontal
D is geomagnetic declination in ° azimuth from magnetic north

I_a is the inclination for amplitude correction (never less than I). Default is ± 20°. If $|I_a|$ is specified to be less than$|I|$, it is set to I

6.3.7 Horizontal Gradient

Calculated Horizontal Gradient (CHG) is the magnitude of the total horizontal gradient. It is used to estimate contact locations of magnetic bodies at shallow depths, reveal anomaly texture, and highlight anomaly-pattern discontinuities.

If M is the magnetic field, then the CHG is calculated as:

$$\mathrm{CHG}(x,y) = \sqrt{\left(\frac{\partial M}{\partial x}\right)^2 + \left(\frac{\partial M}{\partial y}\right)^2}$$

where: $\frac{\partial M}{\partial x}$ is the E-W gradient
$\frac{\partial M}{\partial y}$ is the N-S gradient

6.3.8 Calculation of Vertical Gradient

Calculated Vertical Gradient (CVG) is the first order vertical derivative of the leveled Residual Magnetic Intensity (RMI) data. It is the vertical rate of change in the magnetic field per unit distance. The vertical gradient is used to enhance shorter wavelength signals; therefore, edges of magnetic anomalies are highlighted, and deep geologic sources in the data are suppressed.

The filter, L, used to produce the nth vertical derivative is described by:

$$L(r) = r^n$$

where: r is the radial component in the wavenumber domain

6.3.9 Analytic Signal

Analytic Signal (AS) is the magnitude of the total magnetic gradient in three axes, determined as the square root of the sum of the squares of the horizontal gradients and vertical gradient. Analytic signal is useful in locating the edges of magnetic source bodies.

If M is the magnetic field, then Analytic Signal (AS) is calculated as:

$$\mathrm{AS}(x,y,z) = \sqrt{\left(\frac{\partial M}{\partial x}\right)^2 + \left(\frac{\partial M}{\partial y}\right)^2 + \left(\frac{\partial M}{\partial z}\right)^2}$$

where: $\frac{\partial M}{\partial x}$ is the E-W gradient
$\frac{\partial M}{\partial y}$ is the N-S gradient
$\frac{\partial M}{\partial z}$ is the vertical gradient

6.4 Radiometric Processing

Radiometric surveys map gamma rays from the concentration of radioelements present at or near the Earth surface; typically within 1 m of the surface. Before airborne radiometric data are processed, the spectrometer system is calibrated with the calibration pad test, cosmic flight test, and altitude correction and sensitivity test. Once calibration of the system was completed, radiometric data were processed by windowing the full 256 channel spectrum to create individual channels for U, Th, K, and total count (TC).

Potassium (^{40}K) is measured directly at 1.461 MeV and is reported as %K. Secular equilibrium in the decay chains of uranium (^{238}U determined from the radon daughter ^{214}Bi) and thorium (^{232}Th determined from ^{208}Tl) is assumed and the ground concentration results are reported as equivalent uranium (eU, ppm) and equivalent thorium (eTh, ppm). Total gamma count (TC) data (energy range from 0.41 to 2.81 MeV) is reported in dose rate (nGy/hr).

Radiometric processing generally followed the procedures provided by the International Atomic Energy Agency (IAEA) report 1363, *Guidelines for Radioelement Mapping using Gamma Ray Spectrometry Data*.

6.4.1 Calculation of Effective Height

Effective height (h_{ef}) in meters was determined using laser/radar altimeter, temperature, and pressure data, according to the formula below:

$$h_{ef} = h * \frac{273.15}{T + 273.15} * \frac{P}{1013.25}$$

where: h is measured laser/radar altitude in meters
T is measured air temperature in degrees Celsius
P is barometric pressure in millibars

6.4.2 Aircraft and Cosmic Background Corrections

Aircraft background and cosmic stripping corrections are applied to total gamma count and all three individual radioelements using the following formula:

$$C_{ac} = \mathrm{a}_c + b_c * Cos_f$$

where: C_{ac} is the background and cosmic corrected channel
a_c is the aircraft background for this channel
b_c is the cosmic stripping coefficient for this channel
Cos_f is the filtered cosmic channel

6.4.3 Radon Background Correction

Atmospheric radon can influence the gamma response of airborne radiometric data. The upward-looking detector provides directional sensitivity and the ability to discriminate between radiation from the atmosphere and radiation from the ground, to allow the removal of atmospheric radon effects from the downward-looking detectors.

Radon contribution to the uranium window of the "downward" uranium window is given by:

$$U_r = \frac{u - a_1 U - a_2 T + a_2 b_t - b_u}{a_u - a_1 - a_2 a_t}$$

where: U_r is radon background in the "downward" U window
u is count rate in the "upward" U window
U is count rate in the "downward" U window
T is count rate in the "downward" Th window
a_1, a_2, a_u, a_t, b_u, and b_t are constants derived by calibration

6.4.4 Compton Stripping

Spectral overlap corrections are applied to potassium, uranium, and thorium as part of the Compton stripping process. This is done by using the stripping ratios that have been calculated for the spectrometer by prior calibration.

For each of the stripping ratios α, β, and γ, height corrections at STP are made by using the following formulas:

$$\alpha_h = \alpha + h_{ef} * 0.00049$$

$$\beta_h = \beta + h_{ef} * 0.00065$$

$$\gamma_h = \gamma + h_{ef} * 0.00069$$

where: α, β, and γ are the Compton stripping coefficients
α_h, β_h, and γ_h are the height-corrected Compton stripping coefficients
h_{ef} is the effective height above ground in metres at STP

Stripping corrections are then carried out using the following formulas:

$$Th_c = Th_{bc}(1 - g\beta_h) + U_{bc}(b\gamma_h - a) + K_{bc}(ag - b)/A$$

$$U_c = Th_{bc}(g\beta_h - \alpha_h) + U_{bc}(1 - b\beta_h) + K_{bc}(b\alpha_h - g)/A$$

$$K_c = [Th_{bc}(\alpha_h\gamma_h - \beta_h) + U_{bc}(a\beta_h - \gamma_h) + K_{bc}(1 - a\alpha_h)]/A$$

where: U_c, Th_c, and K_c are stripping-corrected uranium, thorium, and potassium
α_h, β_h, and γ_h are height-corrected Compton stripping coefficients
U_{bc}, Th_{bc}, and K_{bc} are background corrected uranium, thorium, and potassium
a is the spectral ratio Th/U
b is the spectral ratio Th/K
g is the spectral ratio U/K
$A = 1 - g\gamma_h - (\alpha_h - g\beta_h) - b(\beta_h - \alpha_h\gamma_h)$ is the backscatter correction

6.4.5 Attenuation Corrections

Total count, potassium, uranium, and thorium data are then corrected to a nominal survey altitude (corrected to remove vegetation clutter from radar/laser altimeter data); in this case the nominal survey height was 50 m AGL. This is done according to the equation:

$$C_a = C * e^{\mu(h_{ef} - h_0)}$$

where: C_a is the output altitude-corrected channel
C is the input channel
μ is the attenuation correction for that channel
h_{ef} is the effective altitude
h_0 is the nominal survey altitude used as datum

6.4.6 Conversion to Apparent Radioelement Concentrations

With all corrections applied to the radiometric data, the final step is to convert the corrected potassium (^{40}K), uranium (from ^{214}Bi), and thorium (from ^{212}Tl) to apparent radioelement concentrations using the following formula:

$$eE = C_{cor}/S$$

where: eE is the element concentration of K (%) and equivalent element concentrations of U (ppm) & Th (ppm)
S is the experimentally determined sensitivity
C_{cor} is the fully corrected channel

Conversion of total count to natural exposure rate (Grasty et al, 1984) is determined by using the following formula:

$$\text{Natural Exposure} = [(1.505 * K) + (0.625 * eU) + (0.31 * eTh)]$$

where: Natural Exposure is in µR/hr
K is the concentration of potassium (%)
eU is the equivalent concentration of uranium (ppm)
eTh is the equivalent concentration of thorium (ppm)

6.4.7 Radiometric Ratios

Common radiometric ratios (U/Th, Th/K, U/K, and their inverses) were calculated using the guidelines of the IAEA. Due to statistical uncertainties in the individual radioelement measurements, care was taken during ratio calculation in order to obtain statistically significant values. The following guidelines were used to determine the ratios:

1. For each concentration, the lowest corrected count rate is determined.
2. Element concentrations of adjacent points on either side of each data point are summed until they exceed a pre-determined threshold value.
3. The ratios are calculated using the accumulated sums.

With these guidelines, errors associated with the calculated ratios are minimized and comparable for all data points.

6.4.8 Ternary Radioelement Image Map

Ternary images are a graphic representation of the relative proportion of the radioelement concentrations of %K, eTh, and eU components in proportion to the respective colours blue (cyan), red (magenta), and yellow. Since each distinct colour is used to represent each ternary ratio on the map, zones with similar ratios will be represented by a unique colour. This distinct relationship between colour and ternary ratio allows the map to show surficial radioelement concentration and distribution. Dark and light colours indicate high and low values for all three radionuclides, respectively. Areas of low radioactivity, and consequently low signal to noise ratios, can be masked and are shaded in white. Because the ternary image is a three-way ratio, topographic and

physiographic effects are suppressed and a visualization of the relative concentrations of the individual radioelements are presented to help discriminate between different zones of lithology and alteration.

7.0 Deliverables

Mt. Evans survey data are presented as digital databases, grids, maps, and a logistics report.

7.1 Digital Data

Digital files have been provided in three formats:

- GDB file for use in Geosoft Oasis Montaj,
- XYZ file,
- CSV Excel comma separated file.

Full descriptions of the digital data and contents are included in Appendix C.

7.1.1 Grids

Digital data were represented as grids as listed below:

- Digital Terrain Model (DTM)
- Total Magnetic Intensity (TMI)
- Residual Magnetic Intensity (RMI) – removal of IGRF from TMI
- Reduced to Magnetic Pole (RTP) – reduced to magnetic pole of RMI
- Calculated Horizontal Gradient (CHG) – total magnitude of the horizontal gradients of RMI
- Calculated Vertical Gradient (CVG) – first order vertical derivative of RMI
- Analytic Signal (AS) – analytic signal of RMI
- Potassium – Percentage (%K)
- Thorium – Equivalent Concentration (eTh)
- Uranium – Equivalent Concentration (eU)
- Total Count (TC)
- Total Count – Exposure Rate (TCexp)
- Potassium over Thorium Ratio (%K/eTh)
- Potassium over Uranium Ratio (%K/eU)
- Uranium over Thorium Ratio (eU/eTh)
- Uranium over Potassium Ratio (eU/%K)
- Thorium over Potassium Ratio (eTh/%K)
- Thorium over Uranium Ratio (eTh/eU)
- Ternary Image (TI)

Digital magnetic and radiometric data were gridded and displayed using the following Geosoft parameters:

- Gridding method: minimum curvature
- Grid cell size: 50 m
- Low-pass desampling factor: 2
- Tolerance: 0.001
- % pass tolerance: 99.99
- Maximum iterations: 100
- Shading effect: sun inclination at 45° and declination at 045°

All magnetic and radiometric grids were drawn with a conventional RGB colour shade. Descriptions of colour scales are presented in Appendix C.

7.2 KMZ

Gridded digital data were exported into .KMZ files which can be displayed using Google Earth. The grids can be draped onto topography and rendered to provide a 3D view.

7.3 Maps

The following digital map products were prepared for Mt. Evans:

Overview Maps (colour images with elevation contour lines):

- Actual flight lines, with topographic features
- DTM

Magnetic Maps (colour images with elevation contour lines):

- TMI, with actual flight lines and topographic features
- TMI
- RMI
- RTP
- CHG
- CVG
- AS

Radiometric Maps (colour images with elevation contour lines):

- %K – Percentage
- eTh – Equivalent Concentration
- eU – Equivalent Concentration
- TC
- TCexp – Exposure Rate
- %K/eTh Ratio
- %K/eU Ratio
- eU/eTh Ratio
- eU/%K Ratio
- eTh/%K Ratio
- eTh/eU Ratio
- Ternary Image

All survey maps were prepared in WGS 84 in UTM Zone 11N.

7.4 Report

A .PDF copy of the logistics report is included along with digital data and maps. The report provides information on acquisition, processing, and presentation of the Mt. Evans survey data.

8.0 Conclusions and Recommendations

The Mt. Evans survey collected 303 line km of high resolution magnetic and radiometric data over one survey block. The data have been processed and plotted on maps as a representation of the magnetic and radiometric features of the survey area.

Gamma ray energy is attenuated by snow, which was extensive and of variable depth on the Mt. Evans survey. Therefore, radiometric data have been compromised and should be used with discretion.

Geophysical data processing, particularly leveling and data interpolation routines, may tend to smooth the original data so that resolution is reduced. In addition, gridding algorithms are not always able to properly calculate grids where flight height between adjacent flight lines varied due to cultural obstacles or steep terrain, where geological structures are acute to flight lines, where line spacing exceeds the size of the causative anomaly, or near grid margins as in "edge effects." Therefore, subtle geophysical features observed near survey margins or in gridded and derivative-enhanced products must be evaluated with discretion.

The airborne geophysical data were acquired to map the magnetic and radiometric characteristics of the survey area, which are in turn related to the distribution of magnetic minerals and radioactive elements in the Earth. Magnetic patterns correspond to the concentration and distribution of magnetite and other magnetic minerals in the subsurface. Radiometric data are influenced by topographic features and surficial effects, and ratios can be used to evaluate the near-surface radioelement geochemistry of the survey area. When magnetic and radiometric data are integrated into a single-pass airborne survey, they provide complementary information that serve as a durable geophysical framework. Therefore, the geophysical data will be useful in mapping lithology, structure, and alteration, which will benefit mineral exploration initiatives and geological studies.

Geophysical data are rarely a direct indication of mineral deposits and therefore interpretation and careful integration with existing and new geological, geochemical, and other geophysical data are recommended to maximize value from the survey investment.

Respectfully submitted,
Precision GeoSurveys Inc.

Jenny Poon, P.Geo.
March 2022

Appendix A

Polygon Coordinates

Mt. Evans Survey Block – WGS 84 Zone 11N

Latitude (deg N)	Longitude (deg W)	Easting (m)	Northing (m)
49.61240	116.32004	549121	5495759
49.61226	116.22902	555697	5495807
49.53794	116.22784	555867	5487545
49.52625	116.27061	552785	5486215
49.54316	116.27045	552778	5488095
49.54308	116.31888	549275	5488053

Appendix B

Equipment Specifications

- GEM GSM-19T Proton Precession Magnetometer (Magnetic Base Station)
- Hemisphere R330 GPS Receiver
- Opti-Logic RS800 Rangefinder Laser Altimeter
- Geometrics G-822A Magnetometer
- Billingsley TFM100G2 Ultra Miniature Triaxial Fluxgate Magnetometer
- Setra Model 276 Barometric Pressure Sensor
- Rotronic HygroClip HC-S3 Relative Humidity and Temperature Probe
- Nuvia Dynamics Advanced Gamma-Ray Spectrometer (AGRS-2)
- Nuvia Dynamics IMPAC data recorder system (for navigation and geophysical data acquisition)

GEM GSM-19T Proton Precession Magnetometer (Magnetic Base Station)

Sensitivity	0.15 nT @ 1 Hz
Resolution	0.01 nT (gamma), magnetic field and gradient
Absolute Accuracy	±0.2 nT @ 1 Hz
Operating Range	20,000 nT to 120,000 nT
Gradient Tolerance	Over 7,000 nT/m
Operating Ranges	Temperature: -40°C to +50°C Battery Voltage: 10.0 V minimum to 15 V maximum Humidity: up to 90% relative, non-condensing
Storage Temperature	-50°C to +50°C
Dimensions	Console: 223 x 69 x 40 mm Sensor Staff: 4 x 450 mm sections Sensor: 170 x 71 mm dia. Weight: console 2.1 kg, sensor and staff assembly 2.2 kg
Integrated GPS	Yes

Hemisphere R330 GPS Receiver

GPS Sensor	Receiver Type	L1 and L2 RTK with carrier phase	
	Channels	12 L1CA GPS 12 L1P GPS 12 L2P GPS 12 L2C GPS 12 L1 GLONASS (with subscription code) 12 L2 GLONASS (with subscription code) 3 SBAS or 3 additional L1CA GPS	
	Update Rate	10 Hz standard, 20 Hz available	
	Cold Start Time	<60 s	
	Warm Start Time 1	30 s (valid ephemeris)	
	Warm Start Time 2	30 s (almanac and RTC)	
	Hot Start Time	10 s typical (valid ephemeris and RTC)	
	Reacquisition	<1 s	
	Differential Options	SBAS, Autonomous, External RTCM, RTK, OmniSTAR (HP/XP)	
Horizontal Accuracy		RMS (67%)	2DRMS (95%)
	RTK [1, 2]	10 mm + 1 ppm	20 mm + 2 ppm
	OmniSTAR HP [1, 3]	0.1 m	0.2 m
	SBAS (WAAS) [1]	0.3 m	0.6 m
	Autonomous, no SA [1]	1.2 m	2.5 m
L-Band Sensor	Channel	Single channel	
	Frequency Range	1530 MHz to 1560 MHz	
	Satellite Selection	Manual or Automatic (based on location)	
	Startup and Satellite Reacquisition Time	15 seconds typical	
Communications	Serial Ports	2 full duplex RS232	
	Baud Rates	4800 – 115200	
	USB Ports	1 Communications, 1 Flash Drive data storage	
	Correction I/O Protocol	Hemisphere GPS proprietary, RTCM v2.3 (DGPS), RTCM v3 (RTK), CMR, CMR+NMEA 0183, Hemisphere GPS binary	
	Timing Output	1 PPS (HCMOS, active high, rising edge sync, 10 kΩ, 10 pF load)	
	Event Marker Input	HCMOS, active low, falling edge sync, 10 kΩ	
Environmental	Operating Temperature	-40°C to +70°C	
	Storage Temperature	-40°C to +85°C	
	Humidity	95% non-condensing	
Power GPS Sensor	Input Voltage Range	8 to 36 VDC	
	Consumption, RTK	<3.5 W (0.30 A @ 12 VDC typical)	
	Consumption, OmniSTAR	<4.3 W (0.36 A @ 12 VDC typical)	

[1]Depends on multipath environment, number of satellites in view, satellite geometry and ionospheric activity.
[2] Depends also on baseline length.
[3] Requires a subscription from OmniSTAR.

Opti-Logic RS800 Rangefinder Laser Altimeter

Accuracy	±1 m on 1x1 m^2 diffuse target with 50% reflectivity, up to 700 m
Resolution	0.2 m
Communication Protocol	RS232-8, N, 1 ASCII characters
Baud Rate	19200
Data Raw Counts	~200 Hz
Data Calibrated Range	~10 Hz
Data Rate	~200 Hz raw counts for un-calibrated operation; ~10 Hz for calibrated operation (averaging algorithm seeks 8 good readings)
Calibrated Range Units	Feet, Meters, Yards
Laser	Class I (eye-safe), 905 nm ± 10 nm
Power	7 - 9 VDC conditioned required, current draw at full power (~ 1.8 W)
Laser Wavelength	RS100 905 nm ± 10 nm
Laser Divergence	Vertical axis – 3.5 mrad half-angle divergence; Horizontal axis – 1 mrad half-angle divergence; (approximate beam “footprint” at 100 m is 35 cm x 5 cm)
Dimensions	32 x 78 x 84 mm (lens face cross section is 32 x 78 mm)
Weight	<227 g (8 oz)
Casing	RS100/RS400/RS800 units are supplied as OEM modules consisting of an open chassis containing optics and circuit boards. Custom housings can be designed and built on request.

Geometrics G-822A Magnetometer

Operating Principal	Self-oscillating split-beam Cesium Vapor (non-radioactive ^{133}Cs)
Operating Range	20,000 nT to 100,000 nT
Operating Zones	Earth's field vector should be at an angle greater than 6° from the sensor's equator and greater than 6° away from the sensor's long axis.
Hemisphere Switching	Automatic
Sensitivity	<0.0005 nT/√Hz rms.
Noise Envelope	Typically 0.002 nT peak to peak at a 0.1 second sample rate (90% of all readings falling within the peak to peak envelope) using a 822A super-counter
Heading Error	<0.15 nT over entire 360° polar and equatorial spin
Absolute Accuracy	Better than 3 nT throughout range
Output	Cycle of Larmor frequency = 3.498572 Hz/nT, RS-232 data at 9600 baud, concatenated data streams from up to 6 sensors
Sensor Head	Diameter: 60.32 mm (2.375") Length: 158.75 mm (6.25") Weight: 680 g (24 oz)
Sensor Electronics	Diameter: 63.5 mm (2.5") Length: 279.4 mm (11") Weight: 680 g (24 oz)
Cable, Sensor to Electronics	Standard: 2.77 m (109") Cable length can be increased by 1.10 m (43") for a total length of 3.87 m (152")
Cable, Sensor Electronics to Counter	Standard: 10 m (33') Cable length can be increased up to 50 m (164')
Operating Temperature	-35°C to +50°C (-30°F to +122°F)
Storage Temperature	-45°C to +70°C (-48°F to +158°F)
Altitude	Up to 9,000 m (30,000 ft)
Water Tight	Sealed for up to 0.9 m (2 ft) water depth
Supply Power	24 to 35 VDC, 0.75 amp at turn-on and 0.5 amp thereafter

Billingsley TFM100G2 Ultra Miniature Triaxial Fluxgate Magnetometer

Axial Alignment	Orthogonality better than ±1°
Input Voltage Options	15 to 34 VDC @ 30 mA
Field Measurement Range Options	±100 µT = ±10 V
Accuracy	±0.75% of full scale (0.5% typical)
Linearity	±0.015% of full scale
Sensitivity	100 µV/nT
Scale Factor Temperature Shift	0.007% full scale/°C
Noise	≤12 pT rms/√Hz @ 1 Hz
Output Ripple	3 mV peak to peak @ 2^{nd} harmonic
Analog Output at Zero Field	±0.025 V
Zero Shift with Temperature	±0.6 nT/°C
Susceptibility to Perming	±8 nT shift with ± 5 Gs applied
Output Impedance	332 Ω ± 5%
Frequency Response	3 dB @ >500 Hz (to >4 kHz wide band)
Over Load Recovery	±5 Gs slew <2 ms
Random Vibration	>20 G rms 20 Hz to 2 kHz
Temperature Range	-55°C to +85°C
Acceleration	>60 G
Weight	100 g
Size	3.51 cm x 3.23 cm x 8.26 cm
Connector	Chassis mounted 9 pin male "D" type

Setra Model 276 Barometric Pressure Sensor

Performance	Accuracy RSS[1] (at constant temp)	±0.25% FS[2]
	Non-Linearity (BSFL)	±0.22% FS
	Hysteresis	0.05% FS
	Non-Repeatability	0.05% FS
	Thermal Effects[3]	Compensated range: 0°C to +55°C (+30°F to +130°F) Zero shift (over compensated range): 1% FS Span shift (over compensated range): 1% FS
	Resolution	Infinite, limited only by output noise level (0.0005% FS)
	Time Constant	10 msecs to reach 90% final output with step function pressure input
	Long Term Stability	0.25% FS / 6 months
Environmental	Temperature	Operating[4]: -18°C to +79°C (0°F to +175°F) Storage: -55°C to +121°C (-65°F to +250°F)
	Vibration	2 g from 5 Hz to 500 Hz
	Shock	50 g (Operating, 1/2 sine 10 ms)
	Acceleration	10 g
Electrical	Circuit	3-Wire[5] (Exc, Out, Com)
	Power Consumption	0.20 W (24 VDC)
	Output Impedance	5 Ω
	Output Noise	<200 µV RMS (0 to 100 Hz)

[1] RSS of non-linearity, hysteresis, and non-repeatability.
[2] FS = 300 mb for 800 – 1100 mb range; 500 for 600 – 1100 mb range; and 20 PSI for 0 to 20 PSIA.
[3] Units calibrated at nominal 70°F. Maximum thermal error computed from this datum.
[4] Operating temperature limits of the electronics only. Pressure media temperatures may be considerable higher or lower.
[5] The separate leads for +EXC, -EXC, +Out, -Out are commoned internally. The shield is connected to the case. For best performance, either the -Exc or -Out should be connected to the case. Unit is calibrated at the factory with -Exc connected to the case. The insulation resistance between all signal leads are tied together and case ground is 100 Ω minimum at 25 VDC.

Rotronic HygroClip HC-S3 Relative Humidity and Temperature Probe

Relative Humidity	Operating Range	0 to 100% RH
	Accuracy at 23°C	±1.5% RH
	Output	0 – 1 VDC
	Typical Long-Term Stability	Better than ±1% RH per year
Temperature	Measurement Range	-40°C to +60°C
	Temperature Accuracy	-30°C to +60°C ±0.2°C -50°C to +60°C ±0.6°C (worst case)
	Output	0 – 1 VDC
Power	Supply Voltage	3.5 to 50 VDC (typically powered by data logger's 12 VDC supply)
	Current Consumption	<4 mA
Dimensions	Diameter	1.53 cm (0.60")
	Length	16.8 cm (6.6")
	Housing Material	Polycarbonate

Nuvia Dynamics Advanced Gamma-Ray Spectrometer (AGRS-2)

Crystal Volume	Two 4.2 L NaI(Tl) synthetic downward-looking. Total volume of 8.4 L
Resolution	256/512/1024 channels
Data Handling	Individual detector processing and calibration
Energy Resolution	< 9% (@ 662 keV)
Differential Non-linearity	< 0.1%
Integral Non-linearity	< 0.01%
Gain Stabilization	Automatic multi-peak on natural radioisotopes
Calibration	Automatic using natural background radiation
Dynamic Input Range	250,000 cps (counts/sec) per detector
Baseline Restoration	Digital Individual Pulse Baseline Restoration (IPBR). The baseline is established for each individual pulse for maximum pulse height accuracy
Sampling Rate	0.1 – 10 secs user defined
Pulse Shaping	Digital Pulse Shaping
Power	9 to 40 VDC, 15 W
Detector Power	3 W per detector
Operating Temperature	-20°C up to +50°C
Upward Shielding	RayShield® non-radioactive shielding on downward-looking crystals
Spectra	20 keV to 3 MeV (plus cosmic)
System Stabilization	Cold start-up: less than 40 secs on the ground
GPS Connectivity	Time and position synchronization; additional add-on
Weight	~115 kg

Nuvia Dynamics IMPAC data recorder system

(for navigation and geophysical data acquisition)

Functions	Integrated Multi-Parameter Airborne Console (IMPAC) with integrated dual Global Positioning System Receiver (GPS) and all necessary navigation guidance software. Inputs for geophysical sensors - portable gamma ray spectrometer GRS-10/AGRS, MMS4/MMS8 Magnetometer, Herz Totem-2A EM, A/D converter, temperature/humidity probe, barometric pressure probe, and laser/radar altimeter. Output for the multi-parameter PGU (Pilot Guidance Unit)
Display	Monitor display 600 x 800 pixels; customized keypad and operator keyboard. Multi-screen options for real-time viewing of all data inputs, fiducial points, flight line tracking, and GPS channels by operator
Navigation	Pilot/operator navigation guidance. Software supports preplanned survey flight plan, along survey lines, way-points, preplanned drape profile surfaces
Data Sampling	Sensor dependent
Data Synchronization	Synchronized to GPS position. Supports dual GPS
Data File	PEI Binary data format
Storage	80 GB
Software	DataView: Allows fast data verification and conversion of PEI binary data to Geosoft GBN or ASCII formats MAGConv: For survey preparation, calibration and conversion of maps, and survey plot after data acquisition MAGComp: For calculation of magnetic compensation coefficients AGRS/GRS10 Calibration: High voltage adjustment, linearity correction coefficients calculation, and communication test support AGIS: Real time data acquisition and navigation system. Displays chart/spectrum view in real-time for fast data Quality Control (QC)
Electrical	Multiple ethernet connections, RS232 serial ports, USB ports, and 16-bit differential analog input channels. It can support up to 4 magnetometer sensors
Power Requirement	24 VDC

Appendix C

Digital File Descriptions

- Magnetic Database
- Radiometric Database
- Geosoft Grids
- Maps

Magnetic Database:

Abbreviations used in the GDB/XYZ/CSV files are listed below:

CHANNEL	UNITS	DESCRIPTION
X_WGS84	m	UTM Easting – WGS84 Zone 11N
Y_WGS84	m	UTM Northing – WGS84 Zone 11N
Lat_deg	Decimal degree	Latitude – WGS84
Lon_deg	Decimal degree	Longitude – WGS84
Date	yyyy/mm/dd	Dates of the survey flight(s) – Local
FLT		Flight number(s)
LineNo		Line numbers
STL		Number of satellite(s)
GPSfix		1 = non-differential 2 = WAAS/SBAS differential
Heading	degree	Heading of the aircraft
GPStime	HH:MM:SS	GPS time (UTC)
Geos_m	m	Geoidal separation
XTE_m	m	Cross track error
Galt	m	GPS height – WGS84 Zone 11N (ASL)
Lalt	m	Laser altimeter readings (AGL)
DTM	m	Digital Terrain Model
Sample_Density	m	Horizontal distance in meters between adjacent measurement locations; sample frequency is 20 Hz
Speed_km_hr	km/hr	Ground speed of aircraft in km/hr
basemag	nT	Base station temporal variation data
IGRF	nT	International Geomagnetic Reference Field, IGRF-13
Declin	Decimal degree	Calculated declination of magnetic field
Inclin	Decimal degree	Calculated inclination of magnetic field
XFg_Step	step	X - fluxgate
YFg_Step	step	Y - fluxgate
ZFg_Step	step	Z - fluxgate
Mag_Head	nT	Diurnal, lag, and heading corrected
TMI	nT	Total Magnetic Intensity
RMI	nT	Residual Magnetic Intensity

Radiometric Database:

Abbreviations used in the GDB/XYZ/CSV files are listed below:

CHANNEL	UNITS	DESCRIPTION
X_WGS84	m	UTM Easting – WGS84 Zone 11N
Y_WGS84	m	UTM Northing – WGS84 Zone 11N
Lat_deg	Decimal degree	Latitude – WGS84
Lon_deg	Decimal degree	Longitude – WGS84
Date	yyyy/mm/dd	Date of the survey flight(s) – Local
FLT		Flight number(s)
LineNo		Line numbers
STL		Number of satellite(s)
GPStime	HH:MM:SS	GPS time (UTC)
Geos_m	m	Geoidal separation
GPSFix		1 = non-differential 2 = WAAS/SBAS differential
Heading	degree	Heading of the aircraft
XTE_m	m	Cross track error
Galt	m	GPS height – WGS84 Zone 11N (ASL)
Lalt	m	Laser altimeter height (AGL)
DTM	m	Digital Terrain Model
Sample_Density	m	Horizontal distance in metres between adjacent measurement locations; sample frequency is 20 Hz
Speed_km_hr	km/hr	Ground speed of aircraft in km/hr
BaroSTP_kPa	kPa	Barometric altitude (pressure and temperature corrected)
Temp_degC	°C	Air temperature
Press_kPa	kPa	Atmospheric pressure
COSFILT	counts/sec	Spectrometer – Filtered Cosmic
Kcor	%	Concentration in Percentage - Potassium
Thcor	ppm	Equivalent Concentration - Thorium
Ucor	ppm	Equivalent Concentration - Uranium
TCcor	nGy/hour	Total Count
TCexp	µR/hour	Exposure Rate
KThratio		Spectrometer –%K/eTh ratio
KUratio		Spectrometer –%K/eU ratio
ThKratio		Spectrometer – eTh/%K ratio
ThUratio		Spectrometer – eTh/eU ratio
UKratio		Spectrometer – eU/%K ratio
UThratio		Spectrometer – eU/eTh ratio

Grids:

Mt. Evans, WGS 84 Zone 11N, sun inclination at 45° and declination at 045°

File Name	Description	Cell Size (m)
22130_MtEvans_DTM_50m.grd	Digital Terrain Model	50
22130_MtEvans_TMI_50m.grd	Total Magnetic Intensity	50
22130_MtEvans_RMI_50m.grd	Residual Magnetic Intensity	50
22130_MtEvans_RTP_50m.grd	Reduced to Magnetic Pole of RMI	50
22130_MtEvans_CHG_50m.grd	Calculated Horizontal Gradient of RMI	50
22130_MtEvans_CVG_50m.grd	Calculated Vertical Gradient of RMI	50
22130_MtEvans_AS_50m.grd	Analytic Signal of RMI	50
22130_MtEvans_K_50m.grd	Potassium (%K) – in percentage	50
22130_MtEvans_eTh_50m.grd	Thorium (eTh) – equivalent concentration	50
22130_MtEvans_eU_50m.grd	Uranium (eU) – equivalent concentration	50
22130_MtEvans_TC_50m.grd	Total Count (TC)	50
22130_MtEvans_TCexp_50m.grd	Total Count (TCexp) – exposure rate	50
22130_MtEvans_KThRatio_50m.grd	Potassium over Thorium ratio (%K/eTh)	50
22130_MtEvans_KURatio_50m.grd	Potassium over Uranium ratio (%K/eU)	50
22130_MtEvans_UThRatio_50m.grd	Uranium over Thorium ratio (eU/eTh)	50
22130_MtEvans_UKRatio_50m.grd	Uranium over Potassium ratio (eU/%K)	50
22130_MtEvans_ThKRatio_50m.grd	Thorium over Potassium ratio (eTh/%K)	50
22130_MtEvans_ThURatio_50m.grd	Thorium over Uranium ratio (eTh/eU)	50

*CHG, CVG, and AS grids; sun inclination at 45° and declination at 315°

Maps:

Mt. Evans, WGS 84 Zone 11N, sun inclination at 45° and declination at 045° (JPEG, PDF, and georeferenced PDF)

Plate Num	Plate Name	File Name	Description	Cell Size (m)	Colour Scale	Colour Shade
1	FL	22130_MtEvans_ActualFlightLines	Plotted actual flown flight lines	NA	NA	NA
2	DTM	22130_MtEvans_DTM_50m	Digital Terrain Model	50	Linear	NA
3	TMI_wFL	22130_MtEvans_TMI_wFL_50m	Total Magnetic Intensity with actual flown flight lines	50	Histogram-equalized	RGB
4	TMI	22130_MtEvans_TMI_50m	Total Magnetic Intensity	50	Histogram-equalized	RGB
5	RMI	22130_MtEvans_RMI_50m	Residual Magnetic Intensity	50	Histogram-equalized	RGB
6	RTP	22130_MtEvans_RTP_50m	Reduced to Magnetic Pole of RMI	50	Histogram-equalized	RGB
7	CHG	22130_MtEvans_CHG_50m	Calculated Horizontal Gradient of RMI	50	Histogram-equalized	RGB
8	CVG	22130_MtEvans_CVG_50m	Calculated Vertical Gradient of RMI	50	Histogram-equalized	RGB
9	AS	22130_MtEvans_AS_50m	Analytic Signal of RMI	50	Histogram-equalized	RGB
10	%K	22130_MtEvans_K_50m	Potassium (%K) – in percentage	50	Histogram-equalized	RGB
11	eTh	22130_MtEvans_eTh_50m	Thorium (eTh) – equivalent concentration	50	Histogram-equalized	RGB
12	eU	22130_MtEvans_eU_50m	Uranium (eU) – equivalent concentration	50	Histogram-equalized	RGB
13	TC	22130_MtEvans_TC_50m	Total Count (TC)	50	Histogram-equalized	RGB
14	TCexp	22130_MtEvans_TCexp_50m	Total Count (TCexp) – exposure rate	50	Histogram-equalized	RGB
15	%K/eTh	22130_MtEvans_KThRatio_50m	Potassium over Thorium ratio (%K/eTh)	50	Histogram-equalized	RGB
16	%K/eU	22130_MtEvans_KURatio_50m	Potassium over Uranium ratio (%K/eU)	50	Histogram-equalized	RGB
17	eU/eTh	22130_MtEvans_UThRatio_50m	Uranium over Thorium ratio (eU/eTh)	50	Histogram-equalized	RGB
18	eU/%K	22130_MtEvans_UKRatio_50m	Uranium over Potassium ratio (eU/%K)	50	Histogram-equalized	RGB
19	eTh/%K	22130_MtEvans_ThKRatio_50m	Thorium over Potassium ratio (eTh/%K)	50	Histogram-equalized	RGB
20	eTh/eU	22130_MtEvans_ThURatio_50m	Thorium over Uranium ratio (eTh/eU)	50	Histogram-equalized	RGB
21	TI	22130_MtEvans_TernaryImage_50m	Ternary ratio of all three elements (%K, eTh, eU)	50	Histogram-equalized	RGB inverted

*Grids displayed on the maps are exported as GeoTIFFs (.tiff) and KMZs.
**CHG, CVG, and AS grids; sun inclination at 45° and declination at 315°

Plates

Mt. Evans Survey Block

- Plate 1: Mt. Evans – Actual Flight Lines (FL)
- Plate 2: Mt. Evans – Digital Terrain Model (DTM)
- Plate 3: Mt. Evans – Total Magnetic Intensity with Actual Flight Lines (TMI_wFL)
- Plate 4: Mt. Evans – Total Magnetic Intensity (TMI)
- Plate 5: Mt. Evans – Residual Magnetic Intensity (RMI)
- Plate 6: Mt. Evans – Reduced to Magnetic Pole (RTP) of RMI
- Plate 7: Mt. Evans – Calculated Horizontal Gradient (CHG) of RMI
- Plate 8: Mt. Evans – Calculated Vertical Gradient (CVG) of RMI
- Plate 9: Mt. Evans – Analytic Signal (AS) of RMI
- Plate 10: Mt. Evans – Potassium - Percentage (%K)
- Plate 11: Mt. Evans – Thorium - Equivalent Concentration (eTh)
- Plate 12: Mt. Evans – Uranium - Equivalent Concentration (eU)
- Plate 13: Mt. Evans – Total Count (TC)
- Plate 14: Mt. Evans – Total Count - Exposure Rate (TCexp)
- Plate 15: Mt. Evans – Potassium over Thorium Ratio (%K/eTh)
- Plate 16: Mt. Evans – Potassium over Uranium Ratio (%K/eU)
- Plate 17: Mt. Evans – Uranium over Thorium Ratio (eU/eTh)
- Plate 18: Mt. Evans – Uranium over Potassium Ratio (eU/%K)
- Plate 19: Mt. Evans – Thorium over Potassium Ratio (eTh/%K)
- Plate 20: Mt. Evans – Thorium over Uranium Ratio (eTh/eU)
- Plate 21: Mt. Evans – Ternary Image (TI)

Appendix 4. Mt. Evans 2022 Volterra TDEM Survey-Logistics Report.

Logistics Report Prepared

for

Amaroq Gold Corp.

Volterra-TDEM Survey

on the

Mt Evans Project

Kimberley, BC, Canada

Survey conducted by SJ Geophysics Ltd.
July 2022

Report prepared
September 2022

Table of Contents

Index of Figures

Index of Tables

1. Survey Summary

SJ Geophysics Ltd. was contracted by Amaroq Gold Corp. to acquire Volterra Time-Domain Electromagnetic (TDEM) data on the Mt Evans project. The Volterra-TDEM data was acquired with a fixed-loop configuration utilizing one large loop. Table 1 provides a brief summary of the project.

Client	Amaroq Gold Corp.
Project Name	Mt Evans
Project Number	SJ922
Location (approx. Tx site)	Latitude: 49º 33' 24" N Longitude: 116º 18' 51" 549600E 5489550N; WGS84 UTM Zone 11N
Survey Coverage	Number of loops : 1 Number of lines: 5 Total Line Kilometers: 9.55
Production Dates	July11 to July 22, 2022

Table 1: Survey summary

The geology in the area is Lower to Middle Aldrige sediments intermixed with long, thin layers of gabbro sills. The mineralization of interests is usually associated with the Middle lower Aldrige contact.

The objective of the Volterra TDEM survey was to image geologic structures that may indicate the possibility of a lead/zinc deposit similar to the Sullivan Mine.

2. Location and Access

The Mt Evans property is located approximately 30 km southwest of Kimberley, B.C. and approximately 6 km southwest of St. Mary Lake, in the Purcell Mountain Range as shown on Figure 1 and 2.

Figure 1: Overview map for the Mt Evans project

The project area was mainly accessed from Cranbrook by helicopter due to the very steep inaccessible terrain for the main part of the survey area.

The northern part of the loop was accessible by vehicle from Cranbrook by the following directions:

- Drive north along Highway 95A to Marysville.
- Turn left for about 30 km to the east end of St. Mary Lake.
- Turn left onto the active logging road that follows the south shore of the lake.
- Continue on the logging road to the Mt Evans property.

A map of the project area, along with road access, is shown in Figure 2.

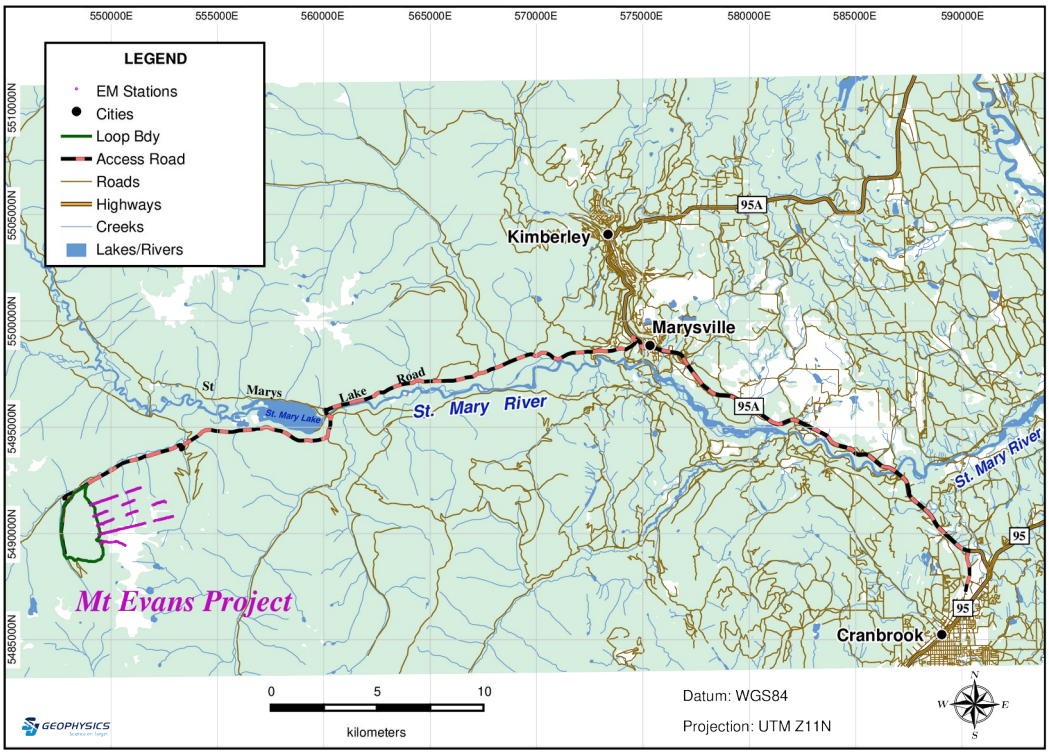

Figure 2: Location map for the Mt Evans project

3. Survey Grid

The Volterra-TDEM surface survey grid consisted of 5 lines and one large loop. The survey lines ranged in length from 1.5Km to 3.5Km with a station spacing of 50 m. No line or loop preparations were completed in advance of the survey. The loop setup and the data collection were conducted with the guidance of hand-held GPS units using predetermined points. The loop location was modified in the field and moved to where the terrain allowed. The lines and stations were also surveyed in section where terrain allowed. Stations were not flagged or marked. All survey stations were located in the field in real-time using hand-held GPS units. The EM loop parameters are summarized in Table 2 and displayed in the grid maps in Figures 3. Please refer to Appendix A for a detailed breakdown of the survey lines.

Loops	Dimensions approx. (m)	Base Frequency (Hz)	Loop Peak-Peak Current Approx. (A)
Loop 1	3500 by 1800	30.975	7.0

Table 2: EM loop parameters

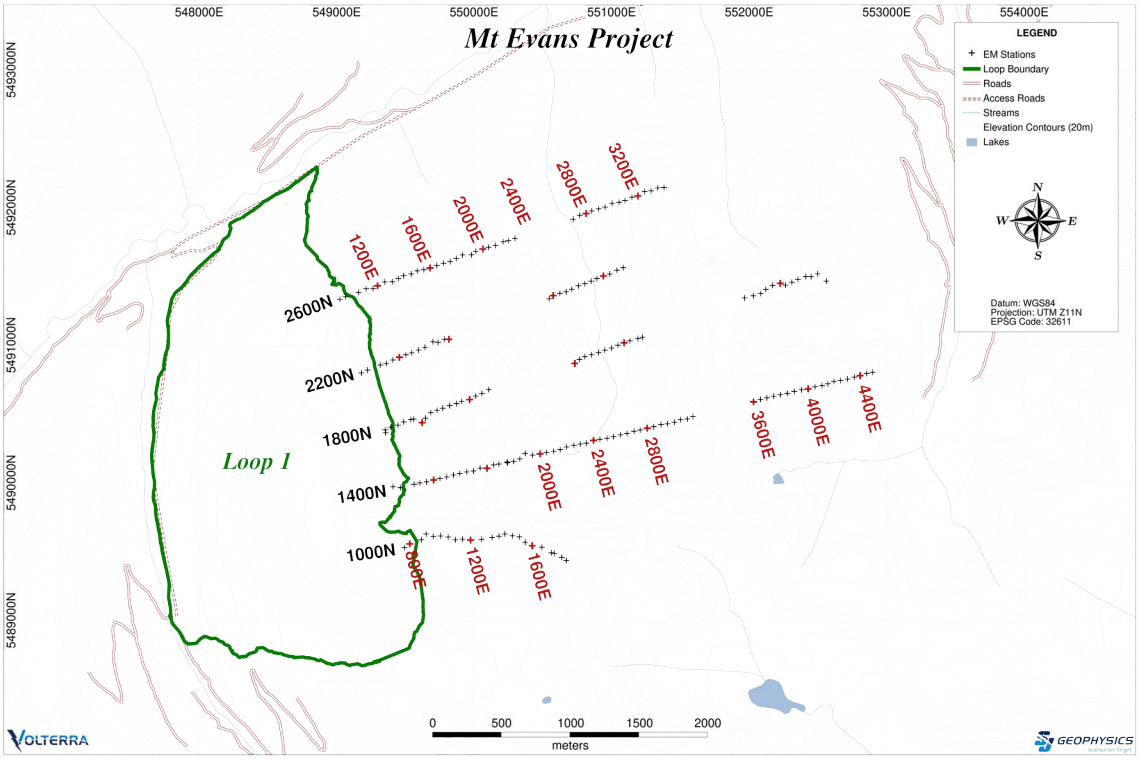

Figure 3: Grid map showing the Mt Evans grid

4. Survey Parameters and Instrumentation

4.1. Volterra-TDEM Survey Design

The Volterra Acquisition system was utilized to acquire the time-domain electromagnetic data. Each Volterra Acquisition unit records full-waveform data from attached sensors. The recorded data is then passed through proprietary signal processing software to calculate the geophysical response. Android tablets are used to view decimated raw data in real-time via a Bluetooth connection to the data acquisition unit. The signal (raw data) visible on the tablet enables the operators to verify the transmitter waveform and that the sensors are functioning correctly.

The TDEM survey utilized one, fixed transmitter loop. Data was acquired with a 50 m station spacing where terrain allowed along each survey line. At each measurement station, the vertical (Hz) and horizontal (Hx) components of the magnetic field was measured using induction magnetometers (B-field Coils) connected to a Volterra data acquisition unit. The induction magnetometers were leveled using a bubble level mounted on each coil and a tripod.

During the survey, calibration measurements inside and outside of the loop were collected with each coil used. Measurements were made with reading lengths of 90 and 120 seconds depending on distance from the loop.

The primary field was generated using a single transmitter connected to the fixed loop. The transmitter was an SJ Geophysics' EMTX 3000, which sent a square (100% duty cycle) waveform through the loop. The EMTX 3000 was powered by a 2200 W single phase Honda generator.

4.2. Volterra-TDEM Acquisition Parameters

The recording and transmitting parameters used for the survey are described in Table 3. The full instrument specifications are listed in Appendix B.

Survey Technique	Fixed-Loop Time Domain EM
EM Signal Recording	Volterra Data Acquisition Unit (8200 Series)
Sensor (B-Field)	ANT-23 Induction Magnetometer
Measured Component	X and Z component
Sample Rate	32,000 samples/second
Reading Length	90 and 120 seconds
EM Signal Processing	CSProc
EM Transmitter	EMTX 3000
Base frequency	Loop 1: 30.975 Hz
Waveform / Duty Cycle	Square / 100 %

Table 3: TDEM recording and transmitting parameters

4.3. Location Data

Location data was collected using Garmin handheld GPS units in the WGS 84 UTM Zone 11 N coordinate system. GPS points were acquired at each survey station where an induction magnetometer was set up. For the transmitter loop, GPS points were acquired approximately every 25 m along each the loop edge.

5. Field Logistics

The SJ Geophysics field crew consisted of one field technician and three or four clients provided assistants to perform the day-to-day operations of the survey. This team, with support by a senior geophysicist, a data processor at the SJ Geophysics' office, and local client representative oversaw all the operational aspects including field logistics, data acquisition and initial field data quality control. Tables 4 and 5 list the SJ Geophysics and client crew members on this project.

Crew Member Name	Role	Dates on Site
Justin Hall	Field Technician	July 11 – 22, 2022
Kalen Martens	Geophysical office support	
Syd (Sipke) Visser	Geophysical office support	

Table 4: Details of the SJ Geophysics crew

Crew Member Name	Role	Dates on Site
Paul Ransom	Client Field Rep.	July 11 – 22, 2022
Ben Rogers	Field Assistant	July 11 – 16, 2022
Logan Robison	Field Assistant	July 11 – 22, 2022
Megan Howe	Field Assistant	July 11 – 22, 2022
Joel Comely	Field Assistant	July 11 – 22, 2022

Table 5: Details of the client crew

The SJ Geophysics crew mobilized to Cranbrook from Delta, BC on July 10, 2022 and demobilized on July 23, 2022

On July 11, the crew met with the client field representative and the field assistants. Ransom and Robison provided an orientation for the survey area as well as a project safety meeting. Helicopter safety orientation was also conducted at Big Horn Helicopters base located in Cranbrook. During the course of the survey, the SJ Geophysics crew conducted daily safety tailgate meetings. At these meetings, personnel discussed issues related to weather conditions (including ramifications on the survey/personal safety), encounters with potentially problematic wildlife, efficient organization of daily tasks, and any other work-related questions or concerns.

The SJ Geophysics crew was accommodated at the Best Western motel in Cranbrook BC.

The hotel Wifi and cell phone reception in town were sufficient for good communication and data delivery. In the field, communication and safety check in with the office occurred by satellite phone. Dinners were purchased from local restaurants in town.

The crew laid out the transmitting loop between July 11 and 13, utilizing both truck and helicopter support. The loop location had to be sightly modified from the original planned loop due to extreme topography. The resistance of the loop was close to 80 ohm. Two transmitter power supplies were connected in series to increase the voltage and the current to about 7 Amps (Peak-to-peak). The transmitter was located near the south east corner of the loop mainly and accessed by helicopter.

Five lines were surveyed over a seven days period. To optimize stability of the coils, a tripod was used for the vertical Z component to level and keep the induction magnetometers stable. For the horizontal X component, the coils was laid flat on the surface of the ground. The orientation of the horizontal component was an issue and the data was not required for interpretation thus was not used.

Due to the extreme topography, all lines were adjusted for safety reason. Some lines were cut short while some lines had gaps. Not all planned lines were surveyed due to time and budget constrains.

All wires and equipment were picked up and removed from site on July 21 and 22.

6. Data Quality

6.1. Locations

The location data collected was of good quality with strong GPS signals observed across the survey area. The location data for each survey station was collected in the WGS84 UTM 11N coordinate system. The majority of the survey lines occurred in areas without significant forest canopy. GPS accuracy was excellent in these areas with errors of approximately ±3 metres. The GPS signals were less reliable in areas of thick forest canopy, where errors were up to ±12 metres.

6.2. Volterra-TDEM Data

The Vertical component EM data acquired was of good quality whereas the horizontal component was of very poor quality due to orientation errors. The site is a significant distance from anthropogenic sources of noise, allowing for very clean data.

7. Deliverables

This report, maps, and data are provided in digital format. A brief description of the provided data is below.

- Report as PDF
  - Grid maps in report
- Locations
  - Locations of survey stations and transmitter loops as csv files
- EM Data
  - Processed EM data as .TEM files
  - Profile plots as .png files

The processed EM data is provided in TEM file format. The TEM files contain column separated data with the instrument parameters stored in a header. The header describes the

instrument parameters, EM time gates, and loop locations. The EM data consists of the station label, UTM coordinates, loop label, and associated decay curve.

The processed EM data was divided into time gates using the "SQRT2" timing scheme. The timing scheme (ie. time gates) describes how the width of the time channels change with each subsequent channel, starting from late-time. The "SQRT2" scheme divides the previous channels width by a factor of $2^{1/2}$. The number of gates is chosen based on the minimum gate width (early time) and the sampling rate of the Volterra acquisition unit. The SQRT2 scheme for a 30.975 Hz base frequency provides 13 time gates. For Volterra-EM data, Channel 1 refers to the latest time gate, following the convention of the UTEM and UREM systems[1].

As the data is collected using a 100% duty cycle waveform, the results are a measurement of the total field. To obtain the secondary field, the primary field must be subtracted from the data in the direction of the sensor field. Handheld GPS units can be used to collect the location data, but are usually not of sufficient quality to accurately calculate the primary field for standard processing. To correct for the error in the calculation of the primary field, it can be assumed that the latest time gate (referred to as the reference time gate) is equal to the primary field and is subtracted from the total field to obtain the secondary field. The reference time gate itself is always reduced to the calculated primary field and will show any large very late-time responses.

The TEM data can be output three different ways to facilitate interpretation. The standard procedure is to deconvolve the EM data with the full-waveform transmitter current to obtain total field data with units of picoTesla per Amp. The total field data is then reduced to obtain secondary field data, which can be presented two ways. The first way is to reduce the total field data by the reference time gate or calculated primary field. Result is the secondary field presented in picoTesla per Amp. This is sometimes referred to as constant gain or point normalized measurements. The second way is to reduce the total field data by the reference time gate or calculated primary field and normalize by the calculated total primary field at that station then multiply by 100. Result is the secondary field expressed as a percentage of the total primary field. This is referred to as variable gain or continuously normalized measurements.

For the TDEM fixed-loop survey configuration, TEM files are provided for each survey line.

1 *UTEM: Lamontagne Geophysics Ltd.*
UREM: Vale Canada Ltd.

The data is provided in folders organized by survey line as described below.

- Loop/SurveyLine
  - Total-Field: Deconvolved to the current monitor. Units are pT/A.
  - CH1red: Total-Field data reduced to the reference time gate or calculated primary field. Units are pT/A.
  - CH1red-png: Images of the CH1 data in PNG format.
  - PercentPrimary: CH1red data normalized by calculated total primary field multiplied by 100. Units are percent of the primary field.
  - PercentPrimary-png: Images of the PercentPrimary data in PNG format.

Respectfully submitted,

Syd Visser, P.Geo

President & Senior Geophysicist

SJ Geophysics Ltd.

Statement of Qualifications

Syd Visser

I, Syd J. Visser, of 11966 – 95A Avenue, Delta, British Columbia, hereby certify that,

1) I am a graduate from the University of British Columbia, 1981, where I obtained a B.Sc. (Hon.) Degree in Geology and Geophysics.
2) I am a graduate from Haileybury School of Mines, 1971.
3) I have been engaged in mining exploration since 1968.
4) I am a professional Geoscientist registered in British Columbia.

Signed by: _____

Syd Visser, B.Sc., P.Geo.

Geophysicist/Geologist

Date: _____

Appendix A: Survey Details

Mt Evans Survey lines

Line	Series	Start Station	End Station	Survey Length (m)
1000	N	750	1850	1100
1400	N	900	3100	2200
		3600	4500	900
1800	N	900	1750	850
		2400	2950	550
		3750	4350	600
2200	N	900	1600	700
		2350	2950	600
2600	N	900	2250	1350
		2700	3400	700

Linear Meters: 9550

Appendix B: Instrument Specifications

Volterra Acquisition Unit (Dabtube 8200 Series)

Technical:

Input impedance:	20 MΩ/IP 1KΩ EM
Input overvoltage protection:	5.6 V
ADC bit resolution:	24-bit
Internal memory:	Storage Capacity 64 GB
Number of inputs:	4
Synchronization:	GPS
Selectable Sampling Rates (samples/second):	128000, 64000, 32000, 16000, 8000, 4000, 2000, 1000
Common mode rejection:	More than 80 dB (for Rs=0)
Voltage sensitivity:	Range: -5.0 to +5.0 V (24 bit)

General:

Dimensions:	Diameter: 43 mm, Length: 405 mm
Weight:	0.5 kg
Battery:	5.0 VDC nominal
Operating temperature range:	-40 ºC to 40 ºC

Surface Induction Magnetometer (ANT-23)

Sensor Serial Number	1323, 1923
Frequency Range:	1 Hz to 10,000 Hz
Sensitivity in Passband:	100 mV/nT
Sensor Serial Number	2923, 3423
Frequency Range:	0.1 Hz to 30,000 Hz
Sensitivity in Passband:	100 mV/nT

SJ Geophysics EM Transmitter (EMTX-3000 Series)

Transmitter Output Stage:

Input Voltage:	10 to 400 V DC
Output Voltage:	20 to 800 V, peak to peak
Output Current:	0 to 18 A, peak to peak
Frequency:	0.1 to 1 kHz, adjustable in 0.001 Hz
Duty Cycle:	10 to 100 %
Waveform:	Square
Features:	Output stages can be connected in parallel (up to 4 units) for a maximum of 72 A, peak-to-peak

Transmitter Controller:

Input Voltage:	7 – 20 V DC
Output Current:	0.4 – 2 A

Power Supply:

BK Precision 9116

Appendix C: Geophysical Techniques

Time Domain EM Method

The time domain EM technique energizes the ground with a variable magnetic field known as the primary field. A transmitter sends an alternating electric current through a loop of wire laid on the surface to create the primary field (Figure 4). Each time a variation occurs in the current (e.g. succession of on-time/off-time) and therefore in the primary field, induced voltage causes eddy currents to flow within underground conductors near the loop. Circulating about these currents is another magnetic field termed the "secondary" field. The magnitude and rate of decay of the eddy currents depend on the electrical conductivity and the geometry of the medium. As the secondary field is directly proportional to the eddy currents, recordings of the secondary field can be exploited to infer information about the conductivity structure of the subsurface. In resistive media eddy currents decay rapidly, whereas in conductive media the currents will decay more slowly.

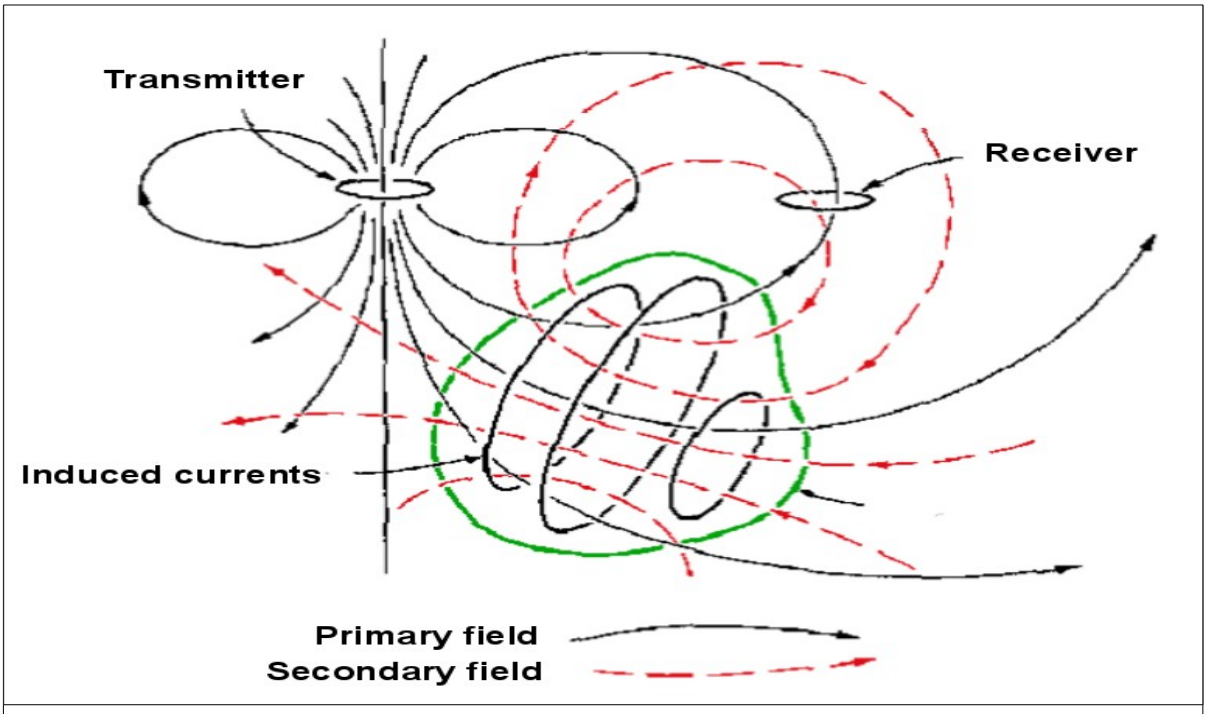

Figure 4: General Principles of TDEM (Grant & West, 1965).

Volterra-EM Method

The Volterra-EM system provides significantly more flexibility over traditional EM surveys (surface or downhole) through the use of SJ Geophysics' proprietary data acquisition units. Each data acquisition unit can be configured to record data from a unique sensor (B-field coil, dB/dt coil, fluxgate magnetometer, resistivity / IP sensors, etc.). The Volterra-EM system uses internal memory for data storage, is time synced using an onboard GPS sensor and high quality internal clock, and employs an inertial measurement unit. These advances eliminate the need for specialized receiver cables and a centralized receiver control station, making the system more portable, more versatile, and in the case of borehole surveys – much lighter. The Volterra-EM system takes advantage of SJ Geophysics' EMTX 3000 transmitter, capable of operating at variable duty cycle, although typically operated at 100% duty cycle. The SJ Geophysics' Volterra-EM system can be powered using standard batteries or a 2000 W generator, making the system that much more field ready.

A typical Volterra surface EM system will use sensitive induction magnetometer sensors connected to a data acquisition unit to measure the total magnetic field – the vector sum of the primary and secondary magnetic fields on the surface. The information carried by the secondary magnetic field will be extracted during a processing stage using filtering, modelling and normalization techniques. Downhole EM surveys will typically employ a highly sensitive induction magnetometer (B-field coil) and a three component fluxgate magnetometer, however this configuration can be altered depending on survey requirements.

Measurements are taken along a line or a borehole and can be outside, inside or crossing the transmitter loop. Moreover, two different loops using two different frequencies can stimulate the ground at the same time, and the secondary field related to each of them will be isolated in a processing stage. TDEM measurements are generally considered repeatable; however, changing field conditions such as variable water content can reduce the overall repeatability. Incorporating other data sets to assist in geological interpretation is prudent.

Appendix 5. Mt. Evans 2022 Volterra TDEM Station Coordinates

Line		Station	Easting	Northing	GPS Elev	
1000	N	750	549498	5489533	2329	
1000	N	800	549536	5489560	2353	
1000	N	850	549620	5489590	2383	
1000	N	900	549654	5489632	2397	
1000	N	950	549707	5489614	2416	
1000	N	1000	549759	5489618	2431	
1000	N	1050	549815	5489610	2447	
1000	N	1100	549867	5489589	2463	
1000	N	1150	549920	5489594	2473	
1000	N	1200	549978	5489588	2488	
1000	N	1250	550057	5489593	2504	
1000	N	1300	550134	5489607	2532	
1000	N	1350	550185	5489616	2545	
1000	N	1400	550227	5489632	2563	
1000	N	1450	550281	5489619	2585	
1000	N	1500	550332	5489611	2602	
1000	N	1550	550375	5489572	2608	
1000	N	1600	550426	5489546	2617	
1000	N	1650	550497	5489536	2632	
1000	N	1700	550565	5489495	2658	
1000	N	1750	550586	5489491	2675	
1000	N	1800	550640	5489463	2694	
1000	N	1850	550674	5489439	2714	
1400	N	900	549414	5489975	2032	
1400	N	950	549466	5489968	2040	
1400	N	1050	549567	5489993	2030	
1400	N	1100	549610	5490003	2044	
1400	N	1150	549658	5490011	2039	
1400	N	1200	549709	5490024	2050	
1400	N	1250	549756	5490035	2050	
1400	N	1300	549805	5490046	2064	
1400	N	1350	549854	5490061	2070	
1400	N	1400	549899	5490071	2073	
1400	N	1450	549950	5490083	2096	
1400	N	1500	549999	5490090	2131	
1400	N	1550	550047	5490111	2176	
1400	N	1600	550098	5490109	2222	
1400	N	1650	550145	5490134	2246	
1400	N	1700	550184	5490140	2264	
1400	N	1750	550246	5490149	2223	
1400	N	1750	550244	5490156	2223	
1400	N	1800	550291	5490159	2207	
1400	N	1850	550336	5490177	2173	
1400	N	1900	550375	5490217	2138	
1400	N	1950	550429	5490205	2080	
1400	N	2000	550483	5490214	2060	

Line		Station	Easting	Northing	GPS Elev	
1400	N	2050	550531	5490225	2030	
1400	N	2100	550582	5490233	2020	
1400	N	2150	550629	5490245	2011	
1400	N	2200	550677	5490264	2006	
1400	N	2250	550729	5490276	1996	
1400	N	2300	550775	5490286	1985	
1400	N	2350	550819	5490292	1960	
1400	N	2400	550872	5490312	1947	
1400	N	2450	550919	5490320	1929	
1400	N	2500	550970	5490327	1919	
1400	N	2550	551017	5490339	1919	
1400	N	2600	551067	5490352	1909	
1400	N	2650	551115	5490363	1898	
1400	N	2700	551167	5490378	1899	
1400	N	2750	551211	5490388	1897	
1400	N	2800	551262	5490401	1904	
1400	N	2850	551309	5490412	1922	
1400	N	2900	551362	5490428	1935	
1400	N	2950	551409	5490433	1959	
1400	N	3000	551460	5490444	1971	
1400	N	3050	551505	5490462	2004	
1400	N	3100	551553	5490468	2034	
1400	N	3150	551595	5490485	2067	
1400	N	3600	552035	5490592	2460	
1400	N	3650	552085	5490610	2442	
1400	N	3700	552132	5490621	2409	
1400	N	3750	552181	5490634	2389	
1400	N	3800	552230	5490644	2354	
1400	N	3850	552280	5490654	2332	
1400	N	3900	552331	5490667	2300	
1400	N	3950	552383	5490680	2276	
1400	N	4000	552432	5490686	2260	
1400	N	4050	552482	5490702	2241	
1400	N	4100	552533	5490711	2223	
1400	N	4150	552576	5490723	2210	
1400	N	4200	552620	5490740	2194	
1400	N	4250	552669	5490747	2174	
1400	N	4300	552719	5490758	2144	
1400	N	4350	552768	5490772	2126	
1400	N	4400	552810	5490783	2101	
1400	N	4450	552858	5490798	2056	
1400	N	4500	552902	5490807	2034	
1800	N	888	549360	5490367	1929	
1800	N	900	549357	5490389	1917	
1800	N	950	549398	5490408	1943	
1800	N	1000	549450	5490423	1972	

Line		Station	Easting	Northing	GPS Elev	
1800	N	1050	549492	5490446	2029	
1800	N	1100	549544	5490463	2062	
1800	N	1150	549565	5490467	2073	
1800	N	1200	549625	5490441	2105	
1800	N	1250	549650	5490473	2151	
1800	N	1300	549689	5490513	2188	
1800	N	1350	549734	5490531	2218	
1800	N	1400	549776	5490546	2249	
1800	N	1450	549826	5490565	2282	
1800	N	1500	549875	5490579	2298	
1800	N	1550	549912	5490596	2315	
1800	N	1600	549971	5490609	2345	
1800	N	1650	550016	5490634	2370	
1800	N	1700	550060	5490653	2395	
1800	N	1750	550110	5490680	2419	
1800	N	2400	550735	5490871	1887	
1800	N	2450	550771	5490901	1857	
1800	N	2500	550809	5490921	1820	
1800	N	2550	550858	5490934	1803	
1800	N	2600	550908	5490950	1775	
1800	N	2650	550954	5490968	1768	
1800	N	2700	551003	5490983	1768	
1800	N	2750	551049	5491004	1773	
1800	N	2750	551049	5491004	1773	
1800	N	2800	551094	5491021	1797	
1800	N	2800	551094	5491021	1797	
1800	N	2850	551137	5491036	1819	
1800	N	2900	551195	5491052	1858	
1800	N	2950	551228	5491062	1870	
1800	N	3750	551970	5491347	2331	
1800	N	3800	552033	5491363	2313	
1800	N	3850	552088	5491379	2312	
1800	N	3900	552124	5491410	2296	
1800	N	3950	552174	5491438	2271	
1800	N	4000	552229	5491453	2250	
1800	N	4050	552268	5491441	2238	
1800	N	4100	552314	5491462	2224	
1800	N	4150	552358	5491482	2200	
1800	N	4200	552415	5491502	2184	
1800	N	4250	552454	5491501	2162	
1800	N	4300	552501	5491523	2134	
1800	N	4350	552564	5491470	2097	
2200	N	900	549184	5490802	1932	
2200	N	950	549229	5490823	1966	
2200	N	1050	549321	5490860	2041	
2200	N	1100	549365	5490871	2064	

Line		Station	Easting	Northing	GPS Elev	
2200	N	1150	549413	5490896	2098	
2200	N	1200	549460	5490916	2116	
2200	N	1250	549508	5490934	2141	
2200	N	1300	549550	5490948	2167	
2200	N	1350	549600	5490969	2179	
2200	N	1400	549646	5490988	2198	
2200	N	1450	549704	5491028	2220	
2200	N	1500	549742	5491024	2236	
2200	N	1550	549787	5491047	2238	
2200	N	1600	549820	5491046	2236	
2200	N	2350	550549	5491341	1933	
2200	N	2400	550579	5491364	1913	
2200	N	2450	550627	5491381	1867	
2200	N	2500	550673	5491392	1820	
2200	N	2550	550714	5491410	1791	
2200	N	2600	550762	5491436	1767	
2200	N	2650	550809	5491451	1757	
2200	N	2700	550854	5491469	1749	
2200	N	2750	550897	5491488	1744	
2200	N	2800	550943	5491507	1749	
2200	N	2850	550990	5491521	1758	
2200	N	2900	551042	5491549	1785	
2200	N	2950	551088	5491567	1810	
2600	N	900	549028	5491337	1757	
2600	N	950	549069	5491355	1765	
2600	N	1050	549163	5491387	1792	
2600	N	1100	549218	5491414	1797	
2600	N	1150	549269	5491415	1817	
2600	N	1200	549302	5491436	1804	
2600	N	1250	549354	5491463	1807	
2600	N	1300	549408	5491465	1825	
2600	N	1350	549452	5491488	1828	
2600	N	1400	549492	5491509	1838	
2600	N	1450	549547	5491522	1847	
2600	N	1500	549590	5491544	1864	
2600	N	1550	549638	5491552	1871	
2600	N	1600	549683	5491565	1858	
2600	N	1650	549732	5491583	1829	
2600	N	1700	549782	5491599	1818	
2600	N	1750	549830	5491612	1792	
2600	N	1800	549874	5491634	1778	
2600	N	1850	549919	5491660	1765	
2600	N	1900	549984	5491661	1766	
2600	N	1950	550016	5491687	1755	
2600	N	2000	550067	5491703	1762	
2600	N	2050	550109	5491715	1775	

Line		Station	Easting	Northing	GPS Elev	
2600	N	2100	550159	5491729	1793	
2600	N	2150	550214	5491755	1839	
2600	N	2200	550252	5491763	1861	
2600	N	2250	550301	5491779	1887	
2600	N	2700	550724	5491919	1642	
2600	N	2750	550771	5491948	1652	
2600	N	2800	550818	5491961	1662	
2600	N	2850	550859	5491979	1693	
2600	N	2900	550909	5491994	1724	
2600	N	2950	550956	5492008	1772	
2600	N	3000	551006	5492036	1792	
2600	N	3050	551057	5492042	1832	
2600	N	3100	551101	5492055	1861	
2600	N	3150	551151	5492079	1885	
2600	N	3200	551194	5492088	1892	
2600	N	3250	551244	5492121	1918	
2600	N	3300	551291	5492125	1956	
2600	N	3350	551339	5492147	1981	
2600	N	3400	551384	5492150	1996	

Mt. Evans 2022 Volterra TDEM Loop1 Coordinates

UTMX	UTMY	GPS EL	UTMX	UTMY	GPS EL	UTMX	UTMY	GPS EL
548313	5491925	1293	548801	5492082	1362	548923	5491574	1591
548326	5491936	1303	548800	5492077	1372	548932	5491571	1608
548342	5491950	1298	548800	5492071	1372	548939	5491554	1608
548361	5491961	1302	548800	5492065	1372	548950	5491529	1632
548379	5491974	1301	548806	5492055	1381	548950	5491510	1632
548397	5491983	1291	548799	5492053	1381	548958	5491505	1632
548412	5491994	1295	548792	5492051	1381	548958	5491502	1632
548428	5492008	1288	548787	5492038	1387	548977	5491490	1650
548444	5492019	1296	548781	5492029	1387	548988	5491491	1657
548455	5492029	1285	548784	5492024	1387	548990	5491470	1670
548474	5492047	1289	548787	5492019	1387	548982	5491471	1663
548495	5492056	1297	548788	5492009	1387	548978	5491462	1663
548512	5492066	1286	548787	5492000	1397	548979	5491456	1663
548532	5492080	1296	548787	5491989	1397	548970	5491446	1677
548546	5492090	1290	548785	5491975	1407	548979	5491442	1677
548585	5492109	1291	548788	5491961	1416	548982	5491445	1677
548651	5492141	1294	548791	5491954	1420	548987	5491447	1683
548715	5492193	1295	548797	5491945	1420	548993	5491448	1683
548716	5492188	1295	548798	5491936	1428	549000	5491440	1683
548729	5492199	1284	548795	5491934	1428	549007	5491445	1697
548742	5492210	1288	548790	5491922	1436	549018	5491452	1697
548859	5492297	1282	548791	5491912	1436	549025	5491451	1705
548863	5492288	1292	548791	5491904	1444	549041	5491441	1705
548861	5492277	1292	548791	5491892	1444	549056	5491431	1723
548859	5492272	1303	548790	5491881	1444	549053	5491414	1732
548864	5492267	1303	548788	5491872	1444	549058	5491404	1732
548864	5492259	1303	548789	5491859	1452	549064	5491387	1755
548859	5492244	1303	548788	5491850	1447	549069	5491379	1755
548854	5492235	1314	548788	5491840	1461	549080	5491373	1755
548851	5492230	1314	548788	5491828	1455	549095	5491364	1762
548853	5492221	1314	548785	5491820	1464	549106	5491358	1769
548850	5492208	1325	548780	5491806	1473	549110	5491359	1769
548847	5492202	1325	548779	5491791	1473	549110	5491359	1769
548845	5492195	1332	548774	5491781	1482	549120	5491355	1785
548840	5492184	1332	548770	5491769	1482	549136	5491341	1785
548836	5492178	1332	548773	5491759	1482	549143	5491325	1807
548832	5492169	1342	548776	5491750	1482	549154	5491306	1818
548827	5492162	1342	548779	5491741	1490	549164	5491292	1836
548826	5492157	1345	548782	5491731	1490	549172	5491286	1836
548822	5492140	1345	548863	5491648	1560	549176	5491282	1836
548818	5492126	1345	548864	5491628	1560	549182	5491278	1853
548823	5492124	1345	548873	5491622	1566	549193	5491265	1853
548811	5492121	1345	548887	5491608	1578	549201	5491253	1876
548805	5492111	1352	548904	5491593	1578	549204	5491247	1876
548803	5492101	1352	548911	5491587	1591	549215	5491237	1876
548800	5492091	1362	548920	5491583	1591	549218	5491233	1876

UTMX	UTMY	GPS EL	UTMX	UTMY	GPS EL	UTMX	UTMY	GPS EL
549222	5491226	1883	549287	5490826	2011	549458	5490168	1935
549223	5491223	1883	549293	5490805	2004	549458	5490149	1941
549229	5491218	1895	549297	5490782	2008	549456	5490135	1947
549238	5491206	1902	549303	5490763	2001	549463	5490120	1955
549245	5491205	1902	549311	5490734	2001	549468	5490110	1955
549246	5491200	1915	549313	5490722	1996	549476	5490097	1955
549247	5491188	1915	549317	5490710	1999	549482	5490085	1966
549247	5491183	1915	549328	5490676	1992	549487	5490075	1966
549241	5491184	1915	549335	5490655	1985	549494	5490064	1980
549241	5491177	1928	549339	5490640	1987	549500	5490060	1980
549244	5491169	1928	549346	5490619	1978	549508	5490049	1980
549250	5491159	1938	549356	5490595	1988	549526	5490037	1997
549250	5491151	1938	549364	5490572	1978	549517	5490022	2011
549250	5491131	1949	549367	5490554	1968	549510	5490013	2007
549246	5491126	1949	549372	5490547	1968	549493	5490002	2021
549250	5491118	1949	549378	5490531	1966	549489	5489997	2020
549247	5491105	1949	549377	5490528	1966	549489	5489985	2020
549247	5491094	1968	549383	5490502	1959	549491	5489959	2037
549251	5491089	1968	549392	5490485	1959	549490	5489946	2061
549249	5491083	1986	549399	5490470	1960	549496	5489957	2037
549242	5491079	1986	549406	5490456	1955	549499	5489955	2037
549242	5491070	1986	549410	5490447	1955	549490	5489932	2061
549242	5491060	2001	549414	5490433	1956	549492	5489921	2085
549245	5491059	2001	549413	5490414	1943	549472	5489905	2122
549246	5491053	2001	549414	5490394	1941	549463	5489892	2126
549249	5491042	2007	549419	5490383	1941	549459	5489878	2152
549246	5491039	2007	549417	5490375	1932	549459	5489868	2152
549245	5491030	2007	549412	5490369	1926	549460	5489864	2152
549241	5491025	2007	549412	5490362	1926	549460	5489864	2152
549245	5491015	2007	549408	5490357	1926	549454	5489839	2176
549243	5491006	2007	549414	5490349	1932	549445	5489835	2179
549243	5491001	2007	549415	5490341	1932	549428	5489831	2195
549242	5490989	2007	549410	5490325	1920	549426	5489818	2195
549246	5490972	2007	549406	5490319	1915	549424	5489806	2213
549250	5490966	2006	549413	5490302	1915	549427	5489799	2213
549253	5490954	2006	549420	5490285	1917	549416	5489787	2233
549256	5490941	2003	549417	5490292	1917	549407	5489777	2236
549258	5490932	2013	549421	5490294	1917	549405	5489771	2257
549261	5490923	2010	549427	5490276	1917	549402	5489766	2257
549263	5490918	2010	549427	5490276	1917	549391	5489760	2265
549267	5490911	2010	549436	5490256	1923	549397	5489755	2257
549267	5490911	2010	549447	5490232	1923	549376	5489740	2285
549269	5490904	2006	549453	5490219	1927	549379	5489739	2285
549277	5490881	2023	549462	5490206	1927	549354	5489717	2289
549278	5490867	2023	549464	5490196	1930	549360	5489718	2287
549281	5490845	2018	549457	5490178	1935	549336	5489718	2289

UTMX	UTMY	GPS EL	UTMX	UTMY	GPS EL	UTMX	UTMY	GPS EL
549320	5489715	2300	549567	5488890	2070	548888	5488717	1853
549319	5489703	2300	549566	5488879	2070	548885	5488713	1851
549320	5489699	2300	549557	5488858	2059	548885	5488713	1851
549328	5489691	2301	549545	5488839	2053	548882	5488712	1851
549341	5489679	2308	549536	5488819	2046	548870	5488712	1851
549341	5489679	2308	549532	5488802	2040	548866	5488713	1849
549353	5489666	2309	549325	5488717	1959	548861	5488715	1849
549363	5489659	2313	549275	5488702	1939	548855	5488718	1849
549377	5489648	2316	549317	5488707	1959	548839	5488725	1844
549386	5489647	2316	549298	5488702	1954	548829	5488726	1844
549403	5489644	2325	549294	5488698	1944	548822	5488727	1841
549417	5489647	2329	549283	5488699	1944	548817	5488728	1841
549428	5489646	2329	549268	5488694	1939	548808	5488731	1841
549456	5489653	2340	549255	5488690	1933	548804	5488732	1838
549466	5489645	2340	549244	5488688	1933	548798	5488732	1838
549479	5489640	2343	549237	5488689	1925	548789	5488732	1838
549493	5489637	2346	549225	5488684	1925	548784	5488732	1835
549510	5489634	2346	549213	5488679	1920	548777	5488732	1835
549513	5489644	2351	549205	5488678	1920	548773	5488734	1835
549514	5489644	2351	549197	5488674	1913	548759	5488738	1830
549523	5489650	2351	549188	5488674	1913	548692	5488733	1819
549533	5489655	2361	549169	5488684	1903	548693	5488740	1818
549539	5489658	2354	549156	5488689	1897	548670	5488742	1812
549588	5489577	2363	549133	5488684	1891	548661	5488743	1812
549558	5489405	2327	549131	5488684	1891	548653	5488745	1812
549590	5489352	2329	549117	5488684	1886	548643	5488747	1808
549606	5489328	2322	549109	5488680	1886	548626	5488751	1800
549608	5489312	2314	549103	5488676	1884	548617	5488756	1800
549615	5489293	2317	549100	5488676	1878	548611	5488758	1795
549622	5489227	2286	549083	5488682	1879	548601	5488763	1795
549633	5489138	2237	549073	5488686	1877	548592	5488764	1790
549633	5489149	2251	549065	5488694	1877	548584	5488763	1790
549630	5489161	2251	549050	5488695	1874	548575	5488765	1790
549629	5489177	2266	549042	5488695	1870	548568	5488767	1779
549627	5489190	2273	549035	5488696	1870	548549	5488768	1774
549632	5489101	2223	549032	5488696	1870	548545	5488770	1774
549631	5489101	2223	549010	5488689	1868	548534	5488780	1768
549637	5489047	2185	548997	5488690	1866	548527	5488780	1768
549632	5489068	2200	548980	5488682	1864	548519	5488778	1768
549635	5489078	2212	548971	5488681	1864	548511	5488780	1757
549637	5489047	2185	548967	5488683	1864	548501	5488786	1757
549627	5488987	2143	548963	5488686	1861	548496	5488789	1757
549586	5488924	2097	548958	5488687	1861	548484	5488797	1750
549608	5488966	2125	548953	5488689	1861	548475	5488802	1743
549574	5488919	2097	548948	5488689	1861	548463	5488807	1743
549567	5488903	2081	548933	5488693	1859	548459	5488807	1743

UTMX	UTMY	GPS EL	UTMX	UTMY	GPS EL	UTMX	UTMY	GPS EL
548451	5488805	1736	548024	5488875	1571	547776	5489331	1516
548443	5488804	1736	548018	5488874	1570	547768	5489367	1512
548430	5488803	1720	548011	5488867	1570	547753	5489430	1505
548427	5488803	1720	548009	5488864	1570	547746	5489459	1505
548423	5488793	1720	547998	5488854	1563	547737	5489496	1503
548422	5488784	1720	547995	5488849	1563	547735	5489510	1503
548410	5488773	1708	547993	5488845	1563	547733	5489539	1499
548408	5488774	1708	547987	5488840	1559	547727	5489556	1499
548392	5488768	1701	547983	5488838	1559	547727	5489555	1499
548387	5488767	1701	547969	5488837	1559	547723	5489570	1498
548372	5488763	1687	547961	5488834	1549	547720	5489598	1498
548360	5488755	1684	547957	5488834	1549	547718	5489619	1498
548358	5488753	1678	547953	5488835	1549	547714	5489645	1493
548346	5488743	1678	547942	5488833	1545	547707	5489673	1493
548334	5488741	1672	547933	5488833	1545	547702	5489702	1493
548329	5488738	1668	547922	5488834	1542	547698	5489724	1493
548322	5488742	1672	547909	5488846	1537	547694	5489746	1488
548322	5488742	1672	547905	5488846	1537	547691	5489764	1489
548314	5488742	1666	547898	5488850	1537	547688	5489795	1491
548301	5488734	1656	547897	5488854	1537	547688	5489813	1490
548295	5488735	1650	547893	5488863	1535	547685	5489843	1490
548282	5488748	1655	547885	5488876	1533	547676	5489867	1489
548270	5488757	1649	547880	5488883	1533	547671	5489893	1478
548253	5488762	1648	547870	5488905	1530	547672	5489923	1476
548244	5488775	1648	547865	5488914	1530	547673	5489939	1474
548248	5488781	1653	547858	5488926	1529	547676	5489951	1483
548239	5488786	1640	547850	5488934	1527	547679	5489979	1481
548230	5488796	1640	547835	5488951	1527	547680	5490014	1478
548227	5488814	1640	547829	5488959	1525	547674	5490045	1466
548222	5488817	1645	547822	5488967	1525	547673	5490045	1466
548208	5488824	1638	547815	5488976	1523	547668	5490076	1470
548203	5488824	1638	547808	5488990	1524	547669	5490078	1470
548188	5488831	1631	547804	5489001	1522	547668	5490087	1470
548179	5488845	1622	547800	5489018	1520	547661	5490161	1469
548156	5488851	1616	547794	5489037	1519	547659	5490209	1467
548143	5488862	1612	547790	5489036	1518	547665	5490261	1464
548132	5488869	1612	547796	5489050	1519	547674	5490318	1461
548120	5488875	1607	547797	5489058	1519	547676	5490356	1466
548112	5488873	1607	547797	5489064	1519	547674	5490379	1458
548103	5488873	1596	547797	5489072	1519	547668	5490420	1452
548091	5488871	1596	547795	5489104	1519	547671	5490434	1452
548074	5488879	1592	547790	5489126	1517	547670	5490476	1450
548061	5488884	1587	547790	5489126	1517	547674	5490520	1443
548040	5488888	1576	547782	5489175	1517	547682	5490559	1442
548033	5488880	1576	547785	5489234	1516	547688	5490584	1442
548028	5488879	1576	547786	5489274	1515	547695	5490615	1441

UTMX	UTMY	GPS EL		UTMX	UTMY	GPS EL		UTMX	UTMY	GPS EL
547689	5490651	1430		547911	5491464	1379		548217	5491800	1325
547696	5490693	1432		547940	5491509	1372		548224	5491816	1322
547704	5490731	1430		548010	5491579	1372		548228	5491833	1314
547708	5490768	1432		548038	5491604	1366		548229	5491836	1314
547747	5490833	1432		548092	5491653	1348		548232	5491844	1314
547751	5490889	1419		548100	5491661	1348		548236	5491852	1305
547759	5490934	1415		548151	5491700	1347		548236	5491854	1305
547780	5490996	1419		548150	5491709	1337		548231	5491859	1305
547781	5491041	1414		548152	5491714	1337		548230	5491864	1305
547782	5491093	1408		548163	5491731	1330		548226	5491871	1296
547778	5491139	1403		548166	5491734	1332		548231	5491889	1286
547772	5491178	1395		548168	5491739	1332		548238	5491893	1286
547779	5491215	1399		548171	5491750	1325		548248	5491899	1288
547793	5491276	1394		548178	5491763	1325		548256	5491903	1288
547795	5491296	1390		548183	5491772	1322		548262	5491907	1285
547807	5491342	1383		548196	5491782	1322		548268	5491910	1285
547831	5491385	1381		548200	5491784	1322		548297	5491924	1289
547882	5491428	1378		548207	5491789	1325		548296	5491926	1289